

Hiroshima University Doctoral Thesis

**Development of a Two-Photon Responsive  
Chromophore, 2-(*p*-Aminophenyl)-5,6-dimethoxy-1-  
(hydroxyinden-3-yl)methyl Derivative, as  
Photoremovable Protecting Group**

(2光子応答性に優れた 2-(*p*-Aminophenyl)-5,6-  
dimethoxy-1-(hydroxyinden-3-yl)methyl 発色団の開発  
に関する研究)

2024

Department of Chemistry,  
Graduate School of Science,  
Hiroshima University

Nguyen Tuan Phong

# Contents

## **Chapter 1. General Introduction**

1.1 Photoremovable protecting group (PPGs).....	1
1.2 Two-photon excitation.....	4
1.3 References.....	8

## **Chapter 2. Development of a Two-Photon Responsive Chromophore, 2-(*p*-Aminophenyl)-5,6-dimethoxy-1-(hydroxyinden-3-yl)methyl Derivative, as Photoremovable Protecting Group**

2.1 Introduction.....	11
2.2 Result and discussion.....	13
2.3 Experiment section.....	31
2.4 Supplementary material.....	44
2.5 References.....	70

## **Chapter 3. Summary.....71**

## **Acknowledgement.....74**

## **List of publications.....76**



# **Chapter 1**

## General Introduction

## 1.1 Photoremovable protecting group (PPGs)

Photoremovable protecting groups (PPGs)<sup>1</sup> are powerful tools that are widely used to investigate biological events in cells.<sup>1,2</sup> As we known, one the research for investigating the mechanism of molecular function in life phenomena is use of temporal deactivation (caging) of bioactive substances with PPG and their activation substances such as Benzoic acid are temporary protected with PPG a renders inactive by irradiation compound with Light, uv-light and a biological reaction can be observed to conduct research on elucidation life phenomena. Figure 1 shows an overall mechanism diagram of one Photoremovable protecting groups (PPGs).<sup>1-5</sup>

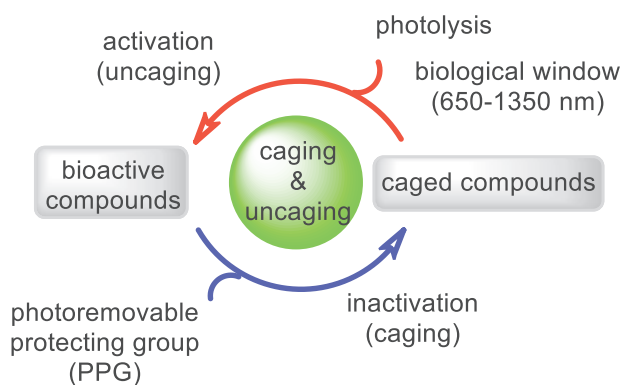


**Figure 1.** Caging and uncaging process of molecules containing bioactive group.

In 1989, J. H. Kaplan and A.P. Somlyo introduced flash photolysis of  $\text{Ca}^{2+}$  and  $\text{Mg}^{2+}$  caged compounds and properties of photolabile reagents.<sup>1,2</sup> In this report, they mentioned that useful photolabile compounds should have 4 properties. First, the biologically active should have no exists on caged compound precursor or at least the caged compound precursor less active than photoproduct.<sup>1,6</sup> Second, for high to yield the biologically effective concentration, the quantum efficiency QE (number of molecules photolysis per number of absorbed photons) and rate photolysis rate should be sufficiently fast. Third one. the side products of photolysis should be biologically inert. And last, the light source for irradiation for photoreaction should be more than 300 nm, that thing avoid of photodamage.<sup>6-11</sup>

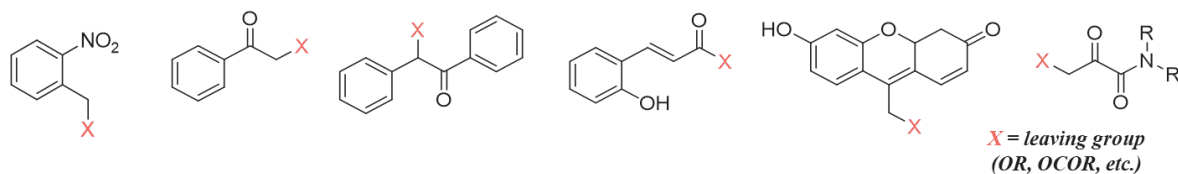


**Figure 2.** Examples of Photoremovable Protecting Groups (PPGs)

In recent years, PPGs aroused interest in applications to biological and materials science. Not only the protecting and release  $\text{Ca}^{2+}$  and  $\text{Mg}^{2+}$ , but also PPGs have liability release for biological group through irradiation photolysis, without chemical reagents.<sup>1,2</sup> Figure 2 shows some examples of the structure of PPGs containing leaving groups.<sup>1-3</sup> As mentioned above, the important thing of PPGs should have strong absorption at irradiation wavelengths (high quantum yield and conversion). Besides, the PPGs should be solved in the targeted media. Lastly, PPGs and photo byproducts should show no toxicity to living cells. For the application to the biological experiment, the source light for irradiation also needs to be avoided for tissue and cells. However, based on previous reports, UV-light was used for photoreaction. Therefore, developing visible (Vis) to near-infrared (NIR)-responsive PPG in the biological window (650–1350 nm) is crucial for these PPGs applications.<sup>12-17</sup>

Figure 3 shows the important photoreaction that led to liberation of a leaving group X of some structure of previous reports.<sup>2</sup>

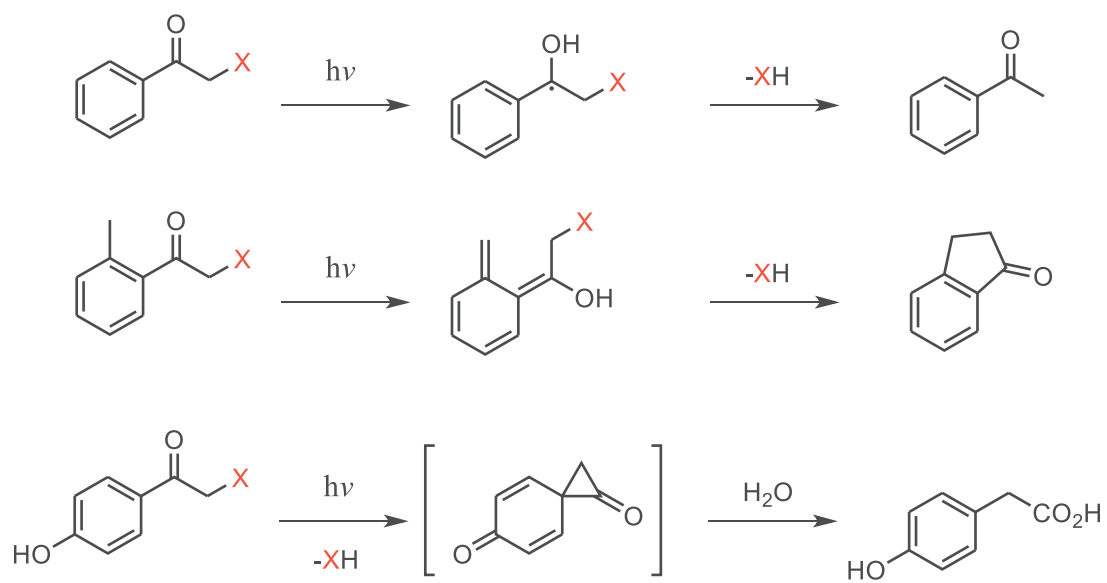


**Figure 3.** Photochemistry mechanism of release leaving group X of some structure.

## 1.2 Two-photon excitation

### a. Two-photon excitation

The first analysis theoretically of two photons absorption by the same molecule was reported by Goppert-Mayer in 1931, the unit of two photon (2TP) absorption cross-section is follow her named (GM).<sup>18,19</sup> However, after the exploration of the laser, W.Kaier and co-worker were proved 2TP by experiment first time in 1961. The Ti:sapphire laser appeared in the 1990s, which lead to investigation of two-photon absorption became easier.<sup>20</sup>

In recent times, two-photon absorption has been widely researched and applied to science, especially with biological experiments. This is because two-photon absorption (2PA) has more advantages than one-photon absorption (1PA). Normally, 2PA is only observed in intense laser beams (specially focused on pulsed lasers), which one create a high instantaneous photon density. This can be explained by 2PA involves the simultaneous interaction because of increases with the square of the light intensity; meanwhile, 1PA depends on linearly on the intensity (Figure 4).

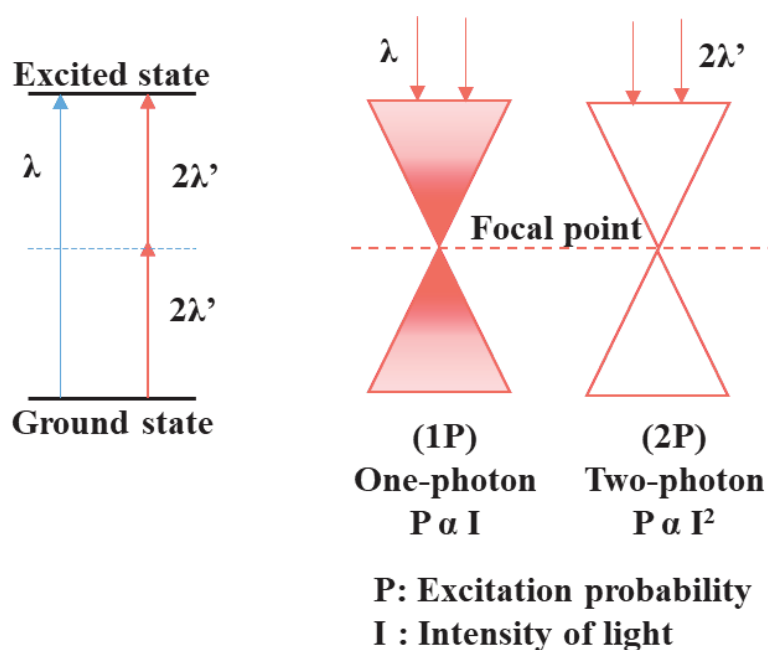


**Figure 4.** Excitation process of two-photon compare with one-photon.



Because two photon excitation (2PE) is observed only in a focus part of the lens , and it can activate molecules in three-dimensional space selectively, so, 2TP is possible for spatiotemporal release of bioactive compounds. Besides, 2PE can be deep penetration in living cell and tissues. Not only that, the wavelength for excitation of two photon is two time with one photon, that mean irradiation light at near IR region (650-900 nm),<sup>19,21</sup> which can be avoid damage to the living cells. With the above outstanding advantages, the application scope of 2PA is wide range in photodynamic therapy, three-dimensional data-storage, biological experiment and specially is delivery drug. Because of wide application range, recently, the design and synthesis of 2PA chromophore become prominent topic and high promising on science applications.<sup>19,22</sup>

For the identified the ability application for physiologist of 2PA chromophores, the photo uncaging efficiency value is needed to calculation. The photo uncaging efficiency ( $\delta_2 = \sigma_2 \times \Phi_u$ ) of the TPA process is calculated by product equation of quantum yield ( $\Phi_u$ ) of the 1TP corresponding uncaging reaction multiplied with TPA cross-section ( $\sigma_2$  in GM, 1 GM =  $10^{-50}$  cm<sup>4</sup> s photons<sup>-1</sup>).<sup>14,18,20</sup> And for applications to the biological experiments, the TPA cross-section ( $\sigma_2$ ) suggests that should be more than 0.5 GM.<sup>19,23</sup>

b. Some structures

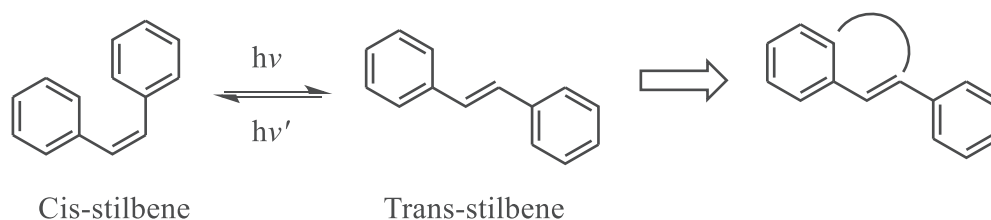


**Figure 5.** Cis-stilbene and Trans-stilbene structure

In 1979, Anderson, Hotton and coworker reported the first time with stilbene structures have good two-photon responsive,  $\sigma_2 = 12$  GM at 514 nm (Figure 5).<sup>18-20</sup> However, the stilbene

structure was unstable by irradiation process, the two isomers cis-stilbene and trans-stilbene convert to each other through photoreaction.<sup>11,12</sup> That thing lead to reducing quantum yield of uncaging. Besides, Marder and coworkers observed that trans-stilbene have good TP cross-section value more 10 times higher than unsubstituted stilbene. And to avoid cis-trans isomerization in stilbene structure moiety, we introduced a cyclized moiety (Figure 5).<sup>24,25</sup> The stability of stilbene structure by cyclizing has resulted in a high increase in the efficiency for the photo uncaging reaction. Not only that, the  $\pi$ -extended conjugated stilbene moieties also improve the  $\sigma_2$  value of TPA chromophores, some structures contain stilbene core in figure 6 was researched and reported.

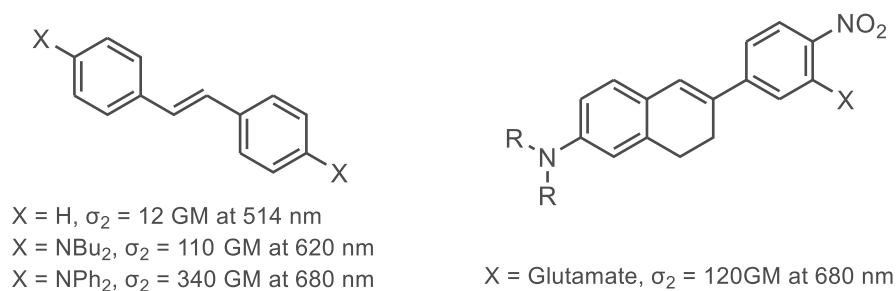


**Figure 6.** Some structures contain stilbene core after extended.

Besides cage compounds containing stilbene core, Nitroindoline (NI) chromophores and coumarin cages for two-photon uncaging were also widely developed and studied.<sup>5,18,19</sup> The NI compounds were introduced for the first time as photosensitive derivatives by Amit and coworkers in 1975. The advantage of NI chromophores is good stability at physiological pH, almost negligible hydrolysis in physiological conditions. That reason why, indole based caged derivatives were widely applied in biological (living cell, tissue...) and in vivo studies as caged neurotransmitters. However, the TP uncaging cross-section of NI chromophore is not so high. Some structures extended and using NI core showed in Figure 7.<sup>19</sup>

In 1984, Givens and Matuszewski were first reported about coumarin-4-ylmethyl and this molecular have become a new type of photolabile group.<sup>18</sup> Figure 8 shows some structure

containing coumarin was reported. Coumarin cage compounds have good TP cross-sections more than NI chromophores; but the uncaging reaction were not clean of di-substituted derivatives.<sup>18–20,26</sup>

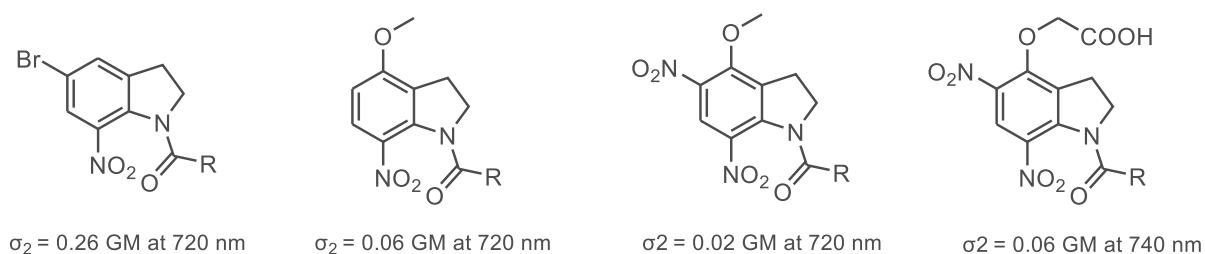


**Figure 7.** Nitroindoline (NI) chromophores for two photon uncaging.

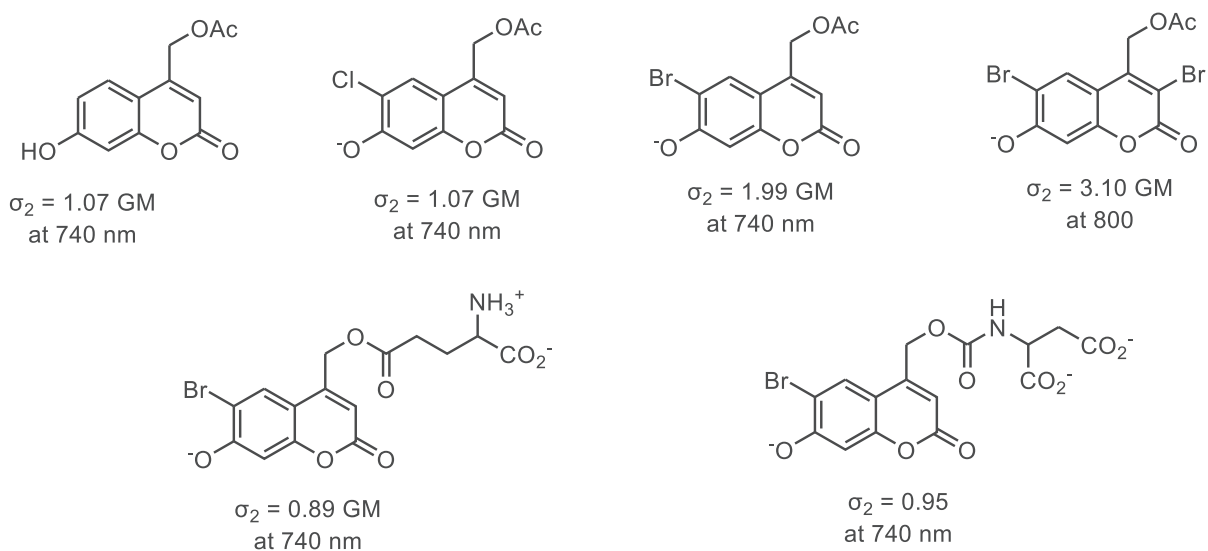


**Figure 8.** Coumarin cage compounds for two photon uncaging.

### 1.3. References

- (1) J. H. Kaplan; A. P. Somlyo. Flash Photolysis of Caged Compounds: New Tools for Cellular Physiology. *TECHNIQUES* **1989**, *12* (2), 54–59.
- (2) Bochet, C. G. Photolabile Protecting Groups and Linkers. *Journal of the Chemical Society. Perkin Transactions 1*. 2002, pp 125–142. <https://doi.org/10.1039/b009522m>.
- (3) Noguchi, J.; Nagaoka, A.; Watanabe, S.; Ellis-Davies, G. C. R.; Kitamura, K.; Kano, M.; Matsuzaki, M.; Kasai, H. In Vivo Two-Photon Uncaging of Glutamate Revealing the Structure-Function Relationships of Dendritic Spines in the Neocortex of Adult Mice. *Journal of Physiology* **2011**, *589* (10), 2447–2457.
- (4) Hayama, T.; Noguchi, J.; Watanabe, S.; Takahashi, N.; Hayashi-Takagi, A.; Ellis-Davies, G. C. R.; Matsuzaki, M.; Kasai, H. GABA Promotes the Competitive Selection of Dendritic Spines by Controlling Local Ca<sup>2+</sup> Signaling. *Nat Neurosci* **2013**, *16* (10), 1409–1416.
- (5) Maurice Goeldner; Richard Givens. Dynamic Studies in Biology: Phototriggers, Photoswitches and Caged Biomolecules. In *Dynamic Studies in Biology*; Wiley, 2005.
- (6) Armstrong, B. K.; Kricker, A. *The Epidemiology of UV Induced Skin Cancer*; 2001; Vol. 63.
- (7) Klán, P.; Šolomek, T.; Bochet, C. G.; Blanc, A.; Givens, R.; Rubina, M.; Popik, V.; Kostikov, A.; Wirz, J. Photoremovable Protecting Groups in Chemistry and Biology: Reaction Mechanisms and Efficacy. *Chemical Reviews*. January 9, 2013, pp 119–191.
- (8) Pham, T. T. T.; Jakkampudi, S.; Furukawa, K.; Cheng, F. Y.; Lin, T. C.; Nakamura, Y.; Morioka, N.; Abe, M. P-Nitroterphenyl Units for near-Infrared Two-Photon Uncaging of Calcium Ions. *J Photochem Photobiol A Chem* **2021**, 409.
- (9) Ellis-Davies, G. C. R. Chemist and Biologist Talk to Each Other about Caged Neurotransmitters. *Beilstein Journal of Organic Chemistry* **2013**, *9*, 64–73.
- (10) Yu, H.; Li, J.; Wu, D.; Qiu, Z.; Zhang, Y. Chemistry and Biological Applications of Photolabile Organic Molecules. *Chem Soc Rev* **2010**, *39* (2), 464–473.
- (11) Chitose, Y.; Abe, M.; Furukawa, K.; Katan, C. Design, Synthesis, and Reaction of  $\pi$ -Extended Coumarin-Based New Caged Compounds with Two-Photon Absorption Character in the near-IR Region. *Chem Lett* **2016**, *45* (10), 1186–1188.
- (12) Chitose, Y.; Abe, M.; Furukawa, K.; Lin, J. Y.; Lin, T. C.; Katan, C. Design and Synthesis of a Caged Carboxylic Acid with a Donor- $\pi$ -Donor Coumarin Structure: One-Photon and Two-Photon Uncaging Reactions Using Visible and Near-Infrared Lights. *Org Lett* **2017**, *19* (10), 2622–2625.
- (13) Klausen, M.; Blanchard-Desce, M. Two-Photon Uncaging of Bioactive Compounds: Starter Guide to an Efficient IR Light Switch. *Journal of Photochemistry and Photobiology C: Photochemistry Reviews*. Elsevier B.V. September 1, 2021.

- (14) Bort, G.; Gallavardin, T.; Ogden, D.; Dalko, P. I. From One-Photon to Two-Photon Probes: “Caged” Compounds, Actuators, and Photoswitches. *Angewandte Chemie - International Edition*. April 22, 2013, pp 4526–4537.
- (15) Palao, E.; Slanina, T.; Muchová, L.; Šolomek, T.; Vitek, L.; Klán, P. Transition-Metal-Free CO-Releasing BODIPY Derivatives Activatable by Visible to NIR Light as Promising Bioactive Molecules. *J Am Chem Soc* **2016**, *138* (1), 126–133.
- (16) Matsuzaki, M.; Ellis-Davies, G. C. R.; Kasai, H. Three-Dimensional Mapping of Unitary Synaptic Connections by Two-Photon Macro Photolysis of Caged Glutamate. *J Neurophysiol* **2008**, *99* (3), 1535–1544.
- (17) Sasaki, M.; Tran Bao Nguyen, L.; Yabumoto, S.; Nakagawa, T.; Abe, M. Structural Transformation of the 2-(p-Aminophenyl)-1-Hydroxyinden-3-Ylmethyl Chromophore as a Photoremovable Protecting Group. *ChemPhotoChem* **2020**, *4* (12), 5392–5398.
- (18) Pawlicki, M.; Collins, H. A.; Denning, R. G.; Anderson, H. L. Two-Photon Absorption and the Design of Two-Photon Dyes. *Angewandte Chemie - International Edition*. April 20, 2009, pp 3244–3266.
- (19) Jakkampudi, S.; Abe, M. Caged Compounds for Two-Photon Uncaging. In *Reference Module in Chemistry, Molecular Sciences and Chemical Engineering*; Elsevier, 2018.
- (20) Marius Albot; David Beljonne; Jean-Luc Bre, \*; Jeffrey E. Ehrlich; Jia-Ying Fu; Ahmed A. Heikal; Samuel E. Hess; Thierry Kogej; Michael D. Levin; Seth R. Marder, \*; Dianne McCord-Maughon; Joseph W. Perry, \*; Harald Rockel; Mariacristina Rumi; Girija Subramaniam; Watt W. Webb, \*; Xiang-Li Wu; Chris Xu. Design of Organic Molecules with Large Two-Photon Absorption Cross Sections. *Science (1979)* **1998**, *281* (5383), 1653–1656.
- (21) Yang, C. H.; Belawat, P.; Hafen, E.; Jan, L. Y.; Jan, Y. N. Drosophila Egg-Laying Site Selection as a System to Study Simple Decision-Making Processes. *Science (1979)* **2008**, *319* (5870), 1679–1683.
- (22) Santiko, E. B.; Babu, S. B.; Zhang, F.; Wu, C.-L.; Lin, T.-C.; Abe, M. Synthesis, Characterization, and Application of a Cyclic Stilbene Derivative with Simultaneous Two-Photon Absorption Character. *Chem Lett* **2023**.
- (23) Susumu, K.; Fisher, J. A. N.; Zheng, J.; Beratan, D. N.; Yodh, A. G.; Therien, M. J. Two-Photon Absorption Properties of Proquinoidal D-A-D and A-D-A Quadrupolar Chromophores. *Journal of Physical Chemistry A* **2011**, *115* (22), 5525–5539.
- (24) Nguyen, L. T. B.; Abe, M. Development of Photoremovable Protecting Groups Responsive to Near-Infrared Two-Photon Excitation and Their Application to Drug Delivery Research. *Bulletin of the Chemical Society of Japan*. Chemical Society of Japan September 1, 2023, pp 899–906.
- (25) M.M. Duvenhage; H.G. Visser; O.M. Ntwaeaborwa; H.C. Swart. The Effect of Electron Donating and Withdrawing Groups on the Morphology and Optical Properties of Alq3 , for EDGs. *Physica B: Condensed Matter* **2014**, *439*, 46–49.

- (26) Shaw, P. A.; Forsyth, E.; Haseeb, F.; Yang, S.; Bradley, M.; Klausen, M. Two-Photon Absorption: An Open Door to the NIR-II Biological Window? *Frontiers in Chemistry*. Frontiers Media S.A. June 24, 2022.

## Chapter 2

Development of a Two-Photon Responsive Chromophore,  
2-(*p*-Aminophenyl)-5,6-dimethoxy-1-(hydroxyinden-3-  
yl)methyl Derivative, as Photoremovable Protecting  
Group

## 2.1 Introduction

As mentioned in chapter 1, photoremovable protecting groups (PPGs) have 3 criteria. PPGs should have high efficiency in light absorption and be soluble in the targeted media. And for apply to biological experiments, the high excitation efficient, quickly release and avoid toxicity to living cells was necessary with a PPGs. However, the use of UV light to release bioactive molecules is harm and damage to living cells and tissues. The solution to this problem is to use light near-infrared ( NIR) for irradiation reaction and using two-photon excitation is good solution. Therefore, developing visible (Vis) to near-infrared (NIR)-responsive PPG in the biological window (650–1350 nm) is crucial for these applications.<sup>1-3</sup>

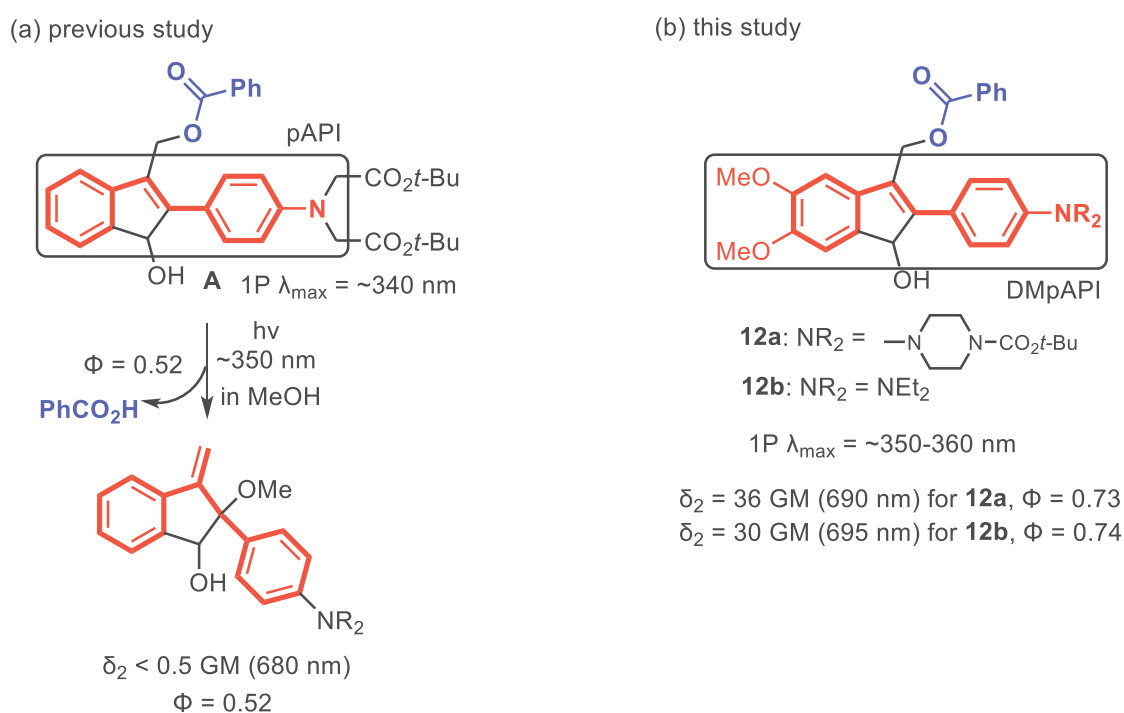


**Figure 1.** (a) previous study using 2-(p-aminophenyl)-1-(hydroxyinden-3-yl)methyl (pAPI) PPG; (b) this study using 2-(p-aminophenyl)-5,6-dimethoxy-1-(hydroxyinden-3-yl)methyl (DM-pAPI-PPG) for two photon (2P)-induced uncaging reaction.



On previous study, a chromophore was synthesis base on stilbene core as known as a 2-*p*-aminophenyl-1-(hydroxyinden-3-yl)methyl (pAPI) in caged benzoic **A** with high conversion of benzoic acid (**BA**). The  $\pi$ -conjugated stilbene system that determines the absorption spectra was designed to be changed to the less-conjugated styrene unit during the photoreaction (Figure 1a). In fact, on previous study, we observed the high release yield of BA of cage compound **A** (96%) with relatively high photochemical quantum yields in DMSO and MeOH ( $\Phi_u = 0.13$ ,  $\Phi_u = 0.52$ , respectively).<sup>4</sup> We can be seen the chromophore pAPI can be seen hopefully of potential. However, the problem of **A** is low two-photon (2P) absorption cross-section in near-infrared region with the uncaging efficiency of  $\delta_2 < 0.5$  GM at 680 nm, which could not application to biological experiments.<sup>1-3</sup> That reason above, in this study, we tried to design new caged compounds **12a** and **12b**, two methoxy groups such as EDG (electron-donating groups) was added at the C5 and C6 position of pAPI structure. We expected the two methoxy groups to the bath chromatically red-shift and 2P absorption band toward the biological window. Besides, for the future biological experiments, we added the piperazine moiety for increase the water solubility for biological experiments (Figure 1b).<sup>4-6</sup>

## 2.2. Results and discussion

Route of synthesis of caged benzoic acids **12a,b** and chromophore DM-pAPI-PPGs **13a,b** showed on scheme 1 and synthesis from commercially available chemicals.<sup>7-11</sup> Compounds **3**, **4a**, **5a**, **5b**, and **7** were prepared using methods reported in previous studies. The syntheses of compounds **8** and **12** were optimized, as described in the Experimental section, to obtain relatively high yields. Compounds **13a** and **13b** were prepared by the oxidation of **9a** and **b** using SeO<sub>2</sub>, respectively, followed by the reduction of the corresponding aldehydes by NaBH<sub>4</sub> as a reducing reagent at 0 °C. and **12a** at B3LYP/6-31G(d) level of theory.

**Scheme 1.** Synthesis of new caged compounds **12a** and **12b** and DM-pAPI-PPG **13a** and **13b**

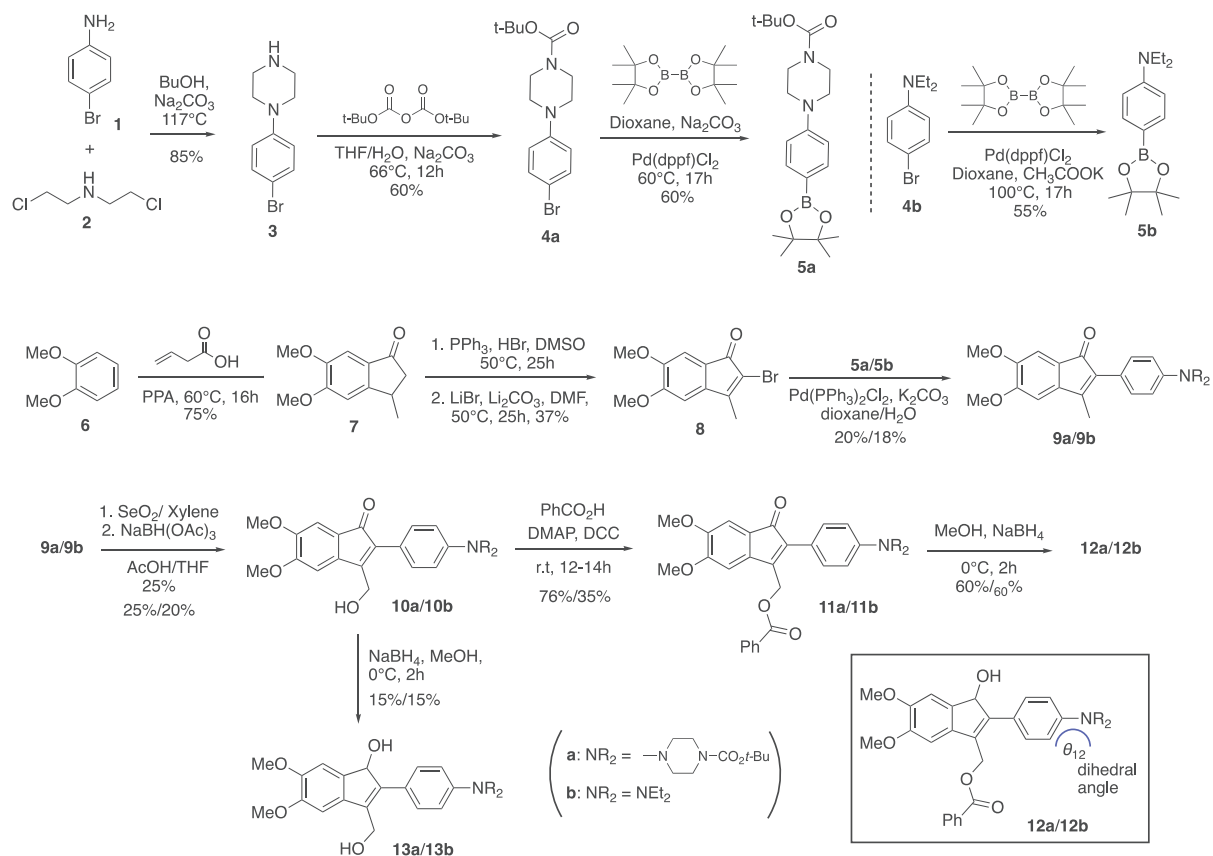


Table 1 shows photophysical properties, wavelength maximum absorption ( $\lambda_{\text{abs}}$ ), molar absorptivity ( $\epsilon$ ), wavelength maximum emission ( $\lambda_{\text{emission}}$ ), quantum yield fluorescence ( $\Phi_f$ ), fluorescence lifetime ( $\tau$ ) of **12a,b** and **13a,b** in various solvents in the direction of increasing polarization. As predicted, the one-photon (1P) absorption bands of **12a,b** measured in DMSO and MeOH were bathochromically shifted compared to that of compound A by 5-20 nm, respectively (Figure 2 and Table 2). From table 1, the increasing polarization is decreasing of UV absorption maximum wavelength of **12a,b**. We also observed a similar thing with chromophores **13a** and **13b**.

**Table 1: Photophysical properties, wavelength maximum absorption ( $\lambda_{\text{abs}}$ ), molar absorptivity ( $\epsilon$ ), wavelength maximum emission ( $\lambda_{\text{emission}}$ ), quantum yield fluorescence ( $\Phi_f$ ), fluorescence lifetime ( $\tau$ ) of compounds 12a,b and 13a,b**

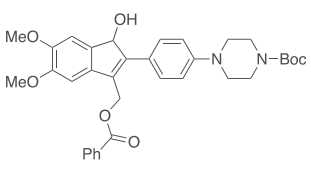
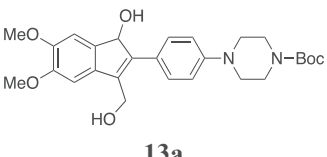
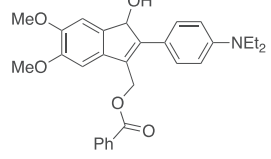
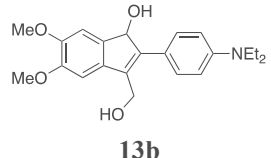
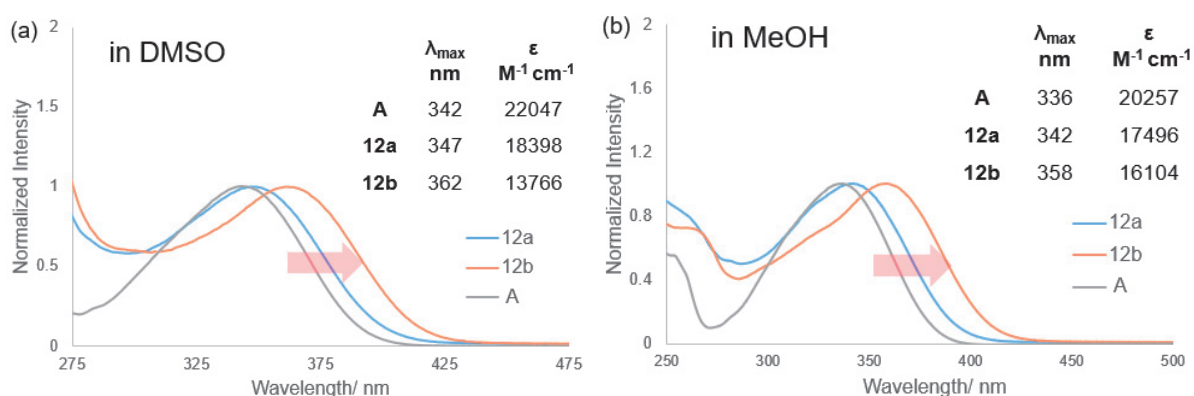
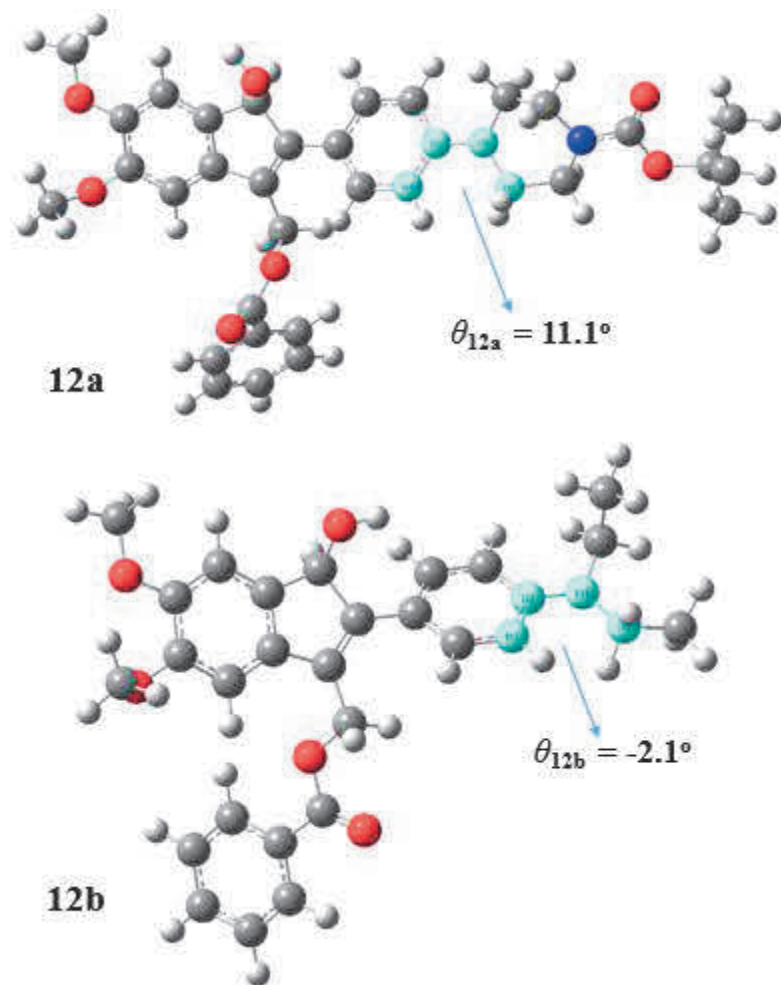
Entry	Compound	Solvent	$\lambda_{\text{abs}}$ nm	$\epsilon/ \text{M}^{-1} \text{cm}^{-1}$	$\lambda_{\text{emission}}$ nm	$\Phi_f$ at $\lambda_{\text{abs max}}$	$\tau/ \text{ns}$ at $\lambda_{\text{emi.max}}$
1	 <b>12a</b>	Toluene	352	16978 $\pm$ 446	453	0.008	1.2
2		$\text{CHCl}_3$	350	17979 $\pm$ 479	450	0.001	2.5
3		MeOH	342	17496 $\pm$ 461	428	0.007	1.8
4		$\text{CH}_3\text{CN}$	344	21596 $\pm$ 460	445	0.001	2.1
5		DMSO	347	18398 $\pm$ 488	444	0.004	2.4
6	 <b>13a</b>	Toluene	348	20758 $\pm$ 661	455	0.153	1.1
7		$\text{CHCl}_3$	349	13264 $\pm$ 422	456	0.011	1.6
8		MeOH	337	18968 $\pm$ 605	422	0.045	1.7
9		$\text{CH}_3\text{CN}$	340	12986 $\pm$ 413	450	0.049	1.8
10		DMSO	343	18994 $\pm$ 725	454	0.189	1.2
11	 <b>12b</b>	Toluene	365	21398 $\pm$ 462	456	0.001	1.5
12		$\text{CHCl}_3$	367	15347 $\pm$ 332	459	0.003	2.7
13		MeOH	358	16104 $\pm$ 348	448	0.002	1.8
14		$\text{CH}_3\text{CN}$	357	15847 $\pm$ 260	455	0.002	2.9
15		DMSO	362	13766 $\pm$ 341	456	0.004	6.7
16	 <b>13b</b>	Toluene	361	17069 $\pm$ 534	464	0.199	0.7
17		$\text{CHCl}_3$	364	15051 $\pm$ 514	463	0.015	2.0
18		MeOH	352	17813 $\pm$ 558	440	0.004	1.8
19		$\text{CH}_3\text{CN}$	354	21521 $\pm$ 624	465	0.049	1.4
20		DMSO	356	18297 $\pm$ 523	458	0.189	0.7

Figure 3 showed UV absorption of compounds **12a** and **12b** in DMSO and MeOH compared with compound **A** of previous report. In DMSO, the maximum absorption wavelength of compound **12a** (347 nm) is 5 nm higher than of compound **A** (342 nm) (table 2). Moreover, we observed the compound **12b** ( $\lambda_{\text{abs}} = 362$  nm) redder shift than compound **12a** ( $\lambda_{\text{abs}} = 347$  nm). We also observed a similar thing in MeOH. For explanation that thing, The more red-shifted absorption band of **12b** in comparison with that of **12a** could be explained by the smaller dihedral angle between diethyl amino moiety and the benzene ring ( $\theta_{12b}$ ) compared to that between piperazine moiety and the benzene ring ( $\theta_{12a}$ ), facilitating the charge transfer from the EDGs. Figure 4 showed dihedral angles  $\theta_{12b}$  and  $\theta_{12a}$  were calculated to be  $-2.1^\circ$  and  $11.1^\circ$ , respectively, in the optimized structures of **12b** and **12a** at B3LYP/6-31G(d) level of theory.



**Figure 3.** UV–Vis absorption spectra of compounds **A**, **12a** and **12b** in (a) DMSO and (b) MeOH



**Figure 4.** The angle between diethyl amino moiety and the benzene ring ( $\phi_1$ ) compared to that angle between piperazine moiety and the benzene ring ( $\phi_2$ ) B3LYP/6-31G(d) level of theory.

**Table 2.** Amino group effect on absorption spectra and photoreaction in DMSO

Entry	Caged compound	$\lambda_{\max}$ [nm]	$\epsilon$ [ $M^{-1} \text{ cm}^{-1}$ ]	Chemical yields of benzoic acid (%) <sup>[a]</sup>	Quantum yields <sup>[b]</sup>
1	A	342	22047	96	0.20
2	12a	347	18398	94	0.73
3	12b	362	13766	92	0.74

[a] Photoreaction of caged compounds were conducted using LED lamp at 365 nm and monitoring by  $^1\text{H-NMR}$ . [b] Quantum yields for the consumption of cage compounds were determined using HPLC and a ferrioxalate actinometer.

For the study about chemical yield of uncaging of benzoic acid (BA) of new cage compounds, photoreactions of **12a** and **12b** (5.43 mM) were examined in air-saturated *d*<sub>6</sub>-DMSO using a 365 nm LED lamp ( $\pm 20$  nm, 45 mW) as the light source at room temperature (approximately 25 °C). Figure 5 showed spectra during photolysis mixture at 365 nm in DMSO-*d*<sub>6</sub> under air at different time points of **12a** and **12b** compared with NMR spectra of authentic sample of benzoic acid (BA), and the time of consume compound **12b** (5 min) longer than compound **12a** (2 min). Benzoic acid (BA) was observed in the photoreactions of **12a** and **12b** with yields of 92% (entry 2 in Table 2) and 94% (entry 3). Notably, the photochemical quantum yields of decomposition of **12a** and **12b** were 0.73 and 0.74, respectively, which were significantly higher than those reported previously for caged compound **A** (entry 1 in Table 2). Products derived from the chromophore moiety were not identified because of the complex mixtures in *d*<sub>6</sub>-DMSO.

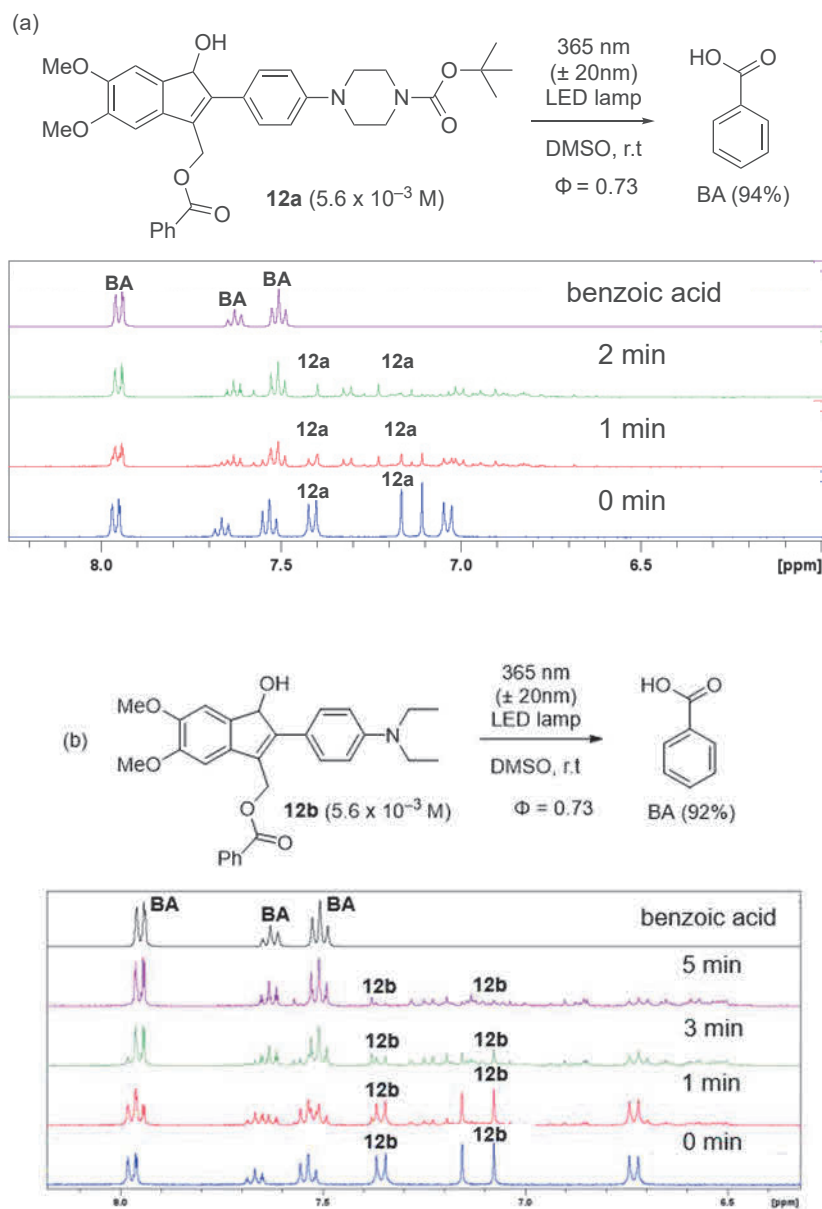


**Figure 5.**  $^1\text{H}$ -NMR spectra (6.5–8.2 ppm) during photolysis mixture at 365 nm in  $\text{DMSO-d}_6$  under air at different time points of **12a** [a] and **12b** [b] compare with NMR spectra of authentic sample of benzoic acid (BA). The chemical yields were determined by comparing the integration of triphenylmethane with those of BA.

Next experiment, the photoreaction of **12a** was performed in MeOH under air condition and LED lamp at 365 nm for irradiation (Figure 6) to identify the photoproducts derived from the chromophore and the intermediates generated in the photoreactions. The photoproducts were purified by column chromatography on silica gel (eluent: hexane: Hex/EtOAc = 5/1 v/v). Benzoic acid (BA) was isolated in 92% yield, similar to the yield observed in DMSO. Interestingly, cis- and trans-**14a** compounds, whose structures were determined by <sup>1</sup>H NMR and NOESY spectroscopy, were isolated as the primary photoproducts with chemical yields of 26% and 33%, respectively. The formation of two MeOH adducts provides strong evidence for the existence of **B2** (Scheme 2).

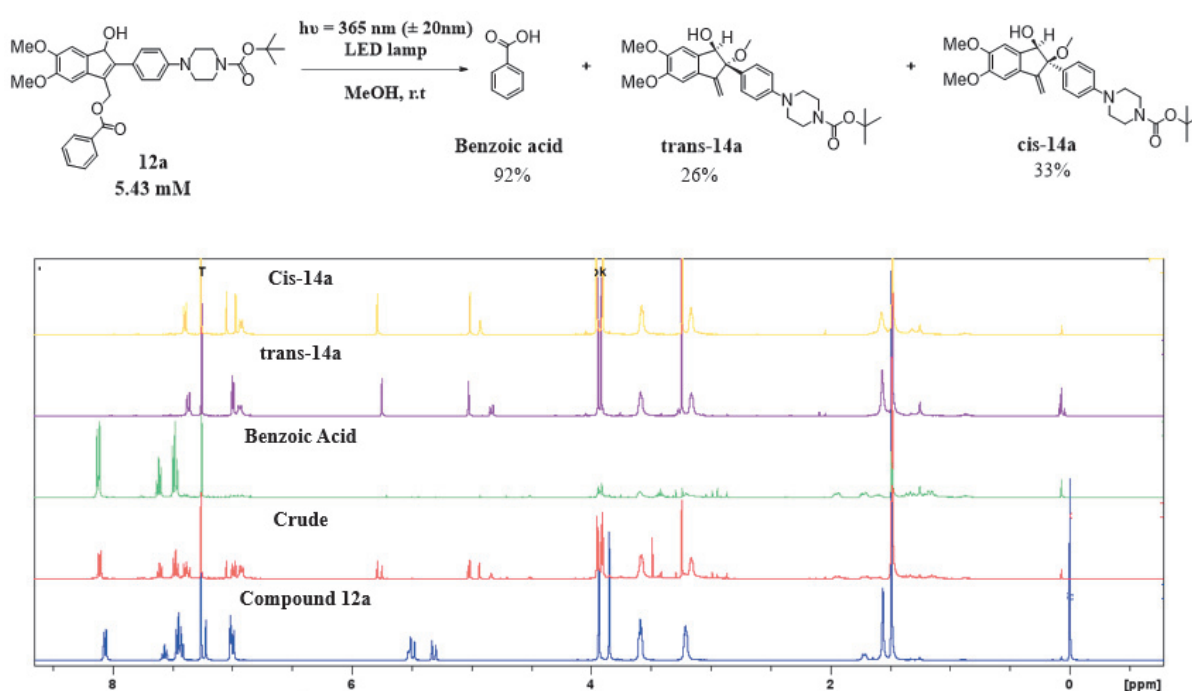
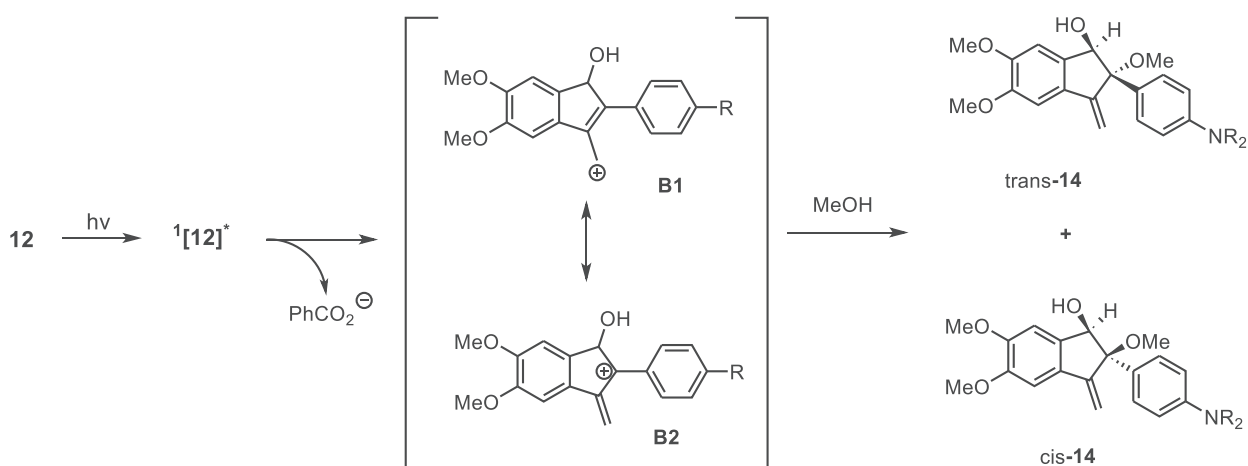


**Figure 6.** <sup>1</sup>H-NMR spectra of photoreaction of compound **12a** in MeOH and photo products BA, cis-**14a**, and trans-**14a** (400 MHz, CDCl<sub>3</sub>)



Based on product analysis, the mechanism of the photoreactions of **12a** and **12b** was proposed, as described in Scheme 2. Light irradiation generates cation **B1**, which is the resonant form of **B2**: DFT optimization of cation **B1** at the B3LYP/6-31G(d) level of theory showed that the atomic polar tensor positive charge was localized at the *p*-aminobenzyl moiety (Figure 7), which rationalized the experimental results that the MeOH-adduct product of **B2** was observed instead of the MeOH-adduct product of **B1**.

**Scheme 2.** Proposed mechanism for photoreactions of **12a** and **12b**



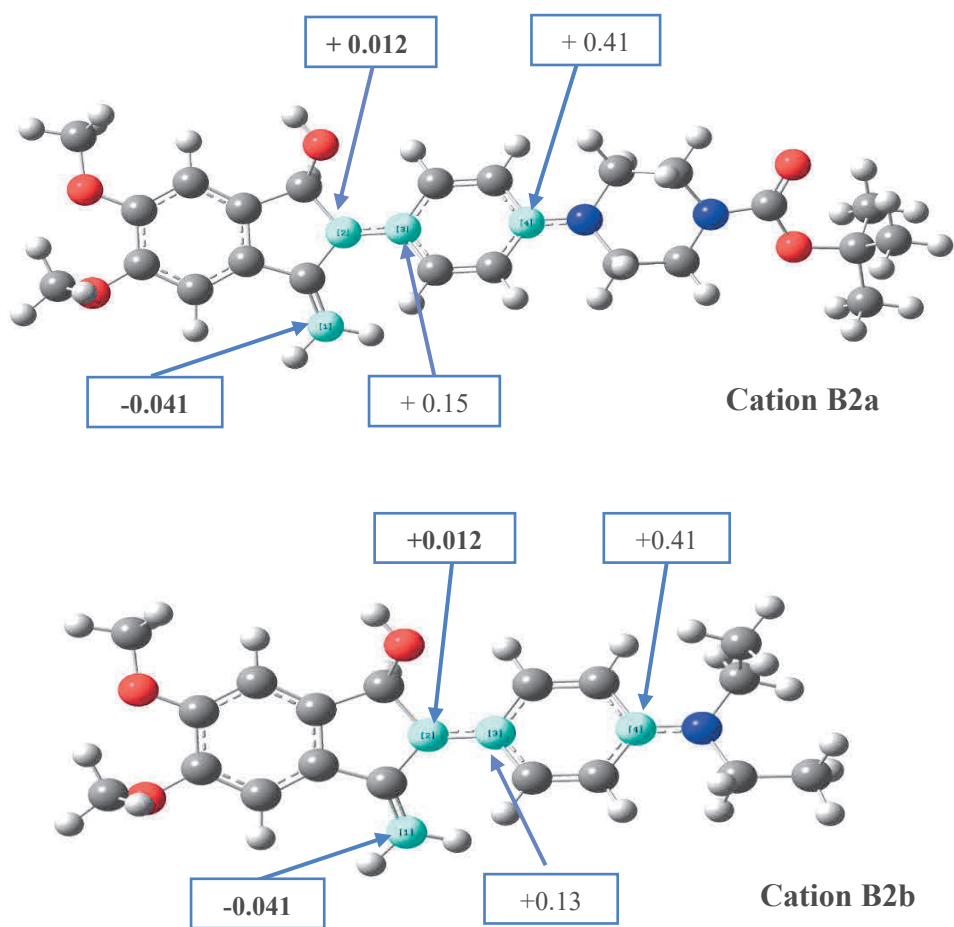


**Figure 7.** The optimization of charge distribution of cations **B2a** and **B2b** at B3LYP/6-31G(d) level of theory

**Transient absorption spectroscopy in photolysis of 12a,b.** Transient absorption spectroscopy with a laser flash photolysis method was performed using an Nd:YAG laser (355 nm, 4 ns pulse width, 4 mJ/pulse) to further investigate the mechanism of the photoreaction of **12a,b**. First able, the transient absorption band at 440 nm is consistent with the UV spectrum of cation **B2a** and **B2b** calculated at the B3LYP/6-31G(d) level of theory (Figure 8). Based on experimental and computational considerations ( at 400 nm ), we assigned an absorption band at 440 nm to cation **B2a** and **B2b**.

The transient absorption spectra of **12a** in argon (Ar)-saturated DMSO and air-saturated DMSO showed a negative band at 360 nm, corresponding to the photobleaching of **12a**, and a positive band at 440 nm (Figures 9a,b). The lifetime of  $\tau_{\text{DMSO,Ar}} = 0.31$  ms at 440 nm under Ar at 298 K was similar to that observed under air conditions,  $\tau_{\text{DMSO,air}} = 0.31$  ms (Figure 9c). We also observed transient absorption spectra of **12a** in MeOH under argon and air condition, the negative band showed at 360 nm. The lifetime of **12a** in MeOH under both conditions is similar (  $\tau_{\text{MeOH,Ar}} = 4.98$  ms,  $\tau_{\text{MeOH,air}} = 4.73$  ms), longer than in DMSO (Figure 9d-e).

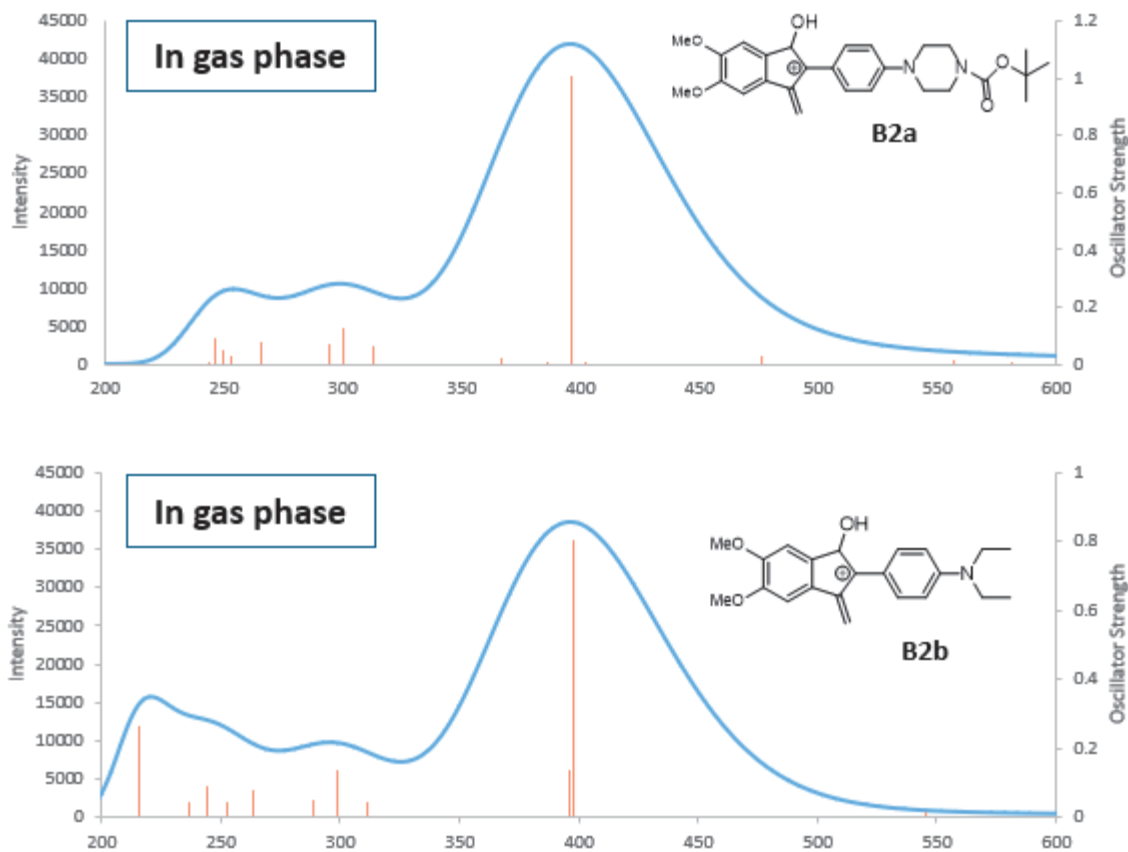


**Figure 8.** Computed UV-vis absorption spectra of cations **B2a** and **B2b** in gas phase at td-rb3lyp/6-31g (d) level of theory.

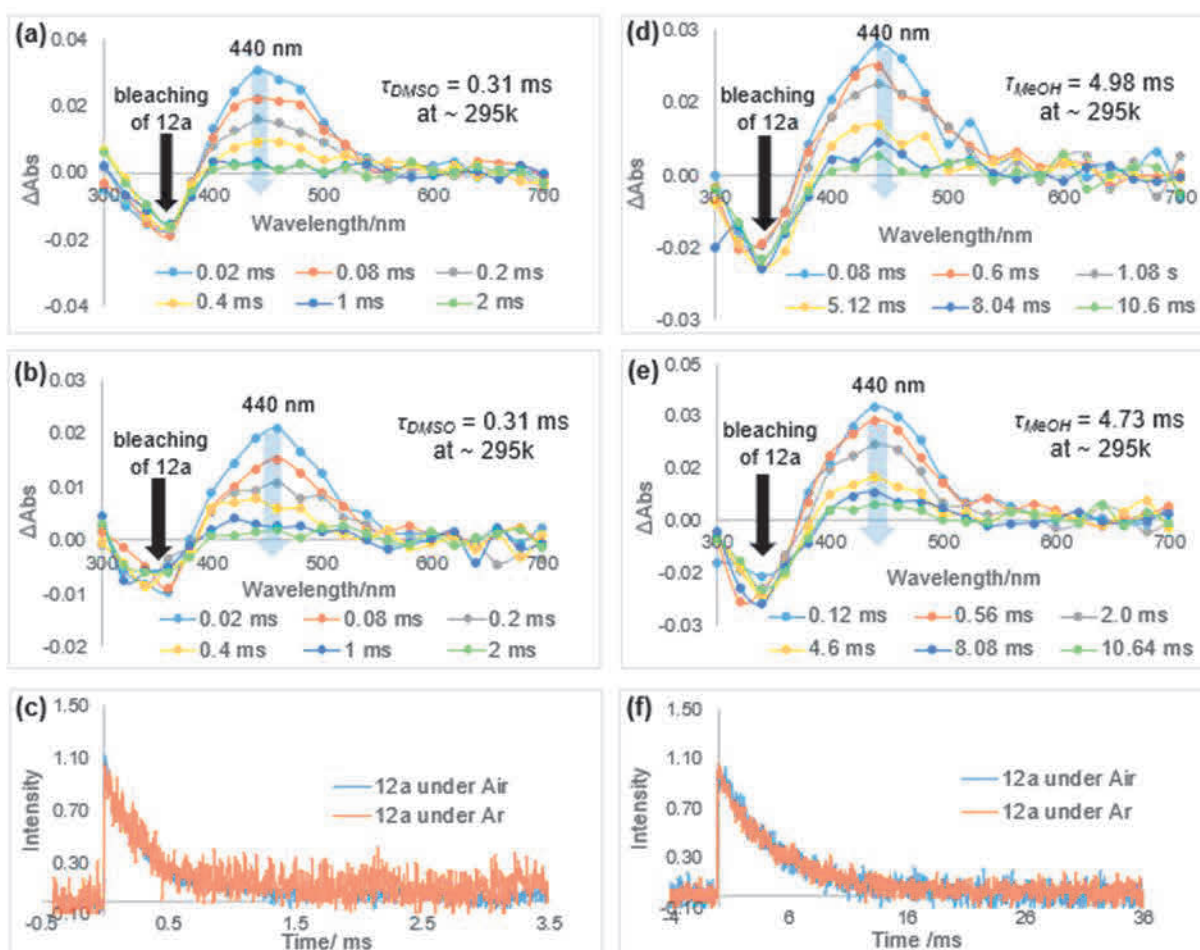


**Figure 9.** Sub-microsecond transient absorption spectroscopy of **12a** in DMSO and MeOH (51  $\mu\text{M}$ , Abs at 355 nm  $\sim 1.0$ ) using 355 nm Nd:YAG laser (4 ns pulse width, 4.2 mJ/pulse) at 298 K. (a) Transient absorption spectra after LFP under Air in DMSO. (b) Transient absorption spectra after LFP under Ar in DMSO. (c) time profile observed at 440 nm in DMSO. (d) Transient absorption spectra after LFP under Air in MeOH. (e) Transient absorption spectra after LFP under Ar in MeOH. (f) time profile observed at 440 nm in MeOH

Similarly, the transient absorption spectrum of **12b** showed a positive absorption band at 440 nm (Figure 10a–e), indicating that the cation **B2** formed under light irradiation. Moreover, the lifetimes of the decay curve monitored at 440 nm of **12b** ( $\tau_{\text{DMSO}} = 1.01$  ms,  $\tau_{\text{MeOH}} = 530$  ms) were considerably longer than those number of **12a** ( $\tau_{\text{DMSO}} = 0.31$  ms,  $\tau_{\text{MeOH}} = 4.98$  ms) measured in similar conditions, suggesting the stronger conjugation from the diethylamino group than that from the piperazine moiety.

As mentioned above, the lifetimes of the decay process of **12a** monitored at 440 nm measured in MeOH ( $\tau_{\text{MeOH,Air}} = 4.73$  ms;  $\tau_{\text{MeOH,Air}} = 4.98$  ms) were longer than those observed in DMSO. The similar thing also observed with **12b** (Figure 10). This result could be attributed to the higher donor number of DMSO ( $\text{DN}^{12} = 29.8$  kcal/mol) compared to that of MeOH ( $\text{DN}^{12} = 19$  kcal/mol), leading to faster quenching of **B2** by DMSO than MeOH, resulting in a longer lifetime of **B2** in MeOH.

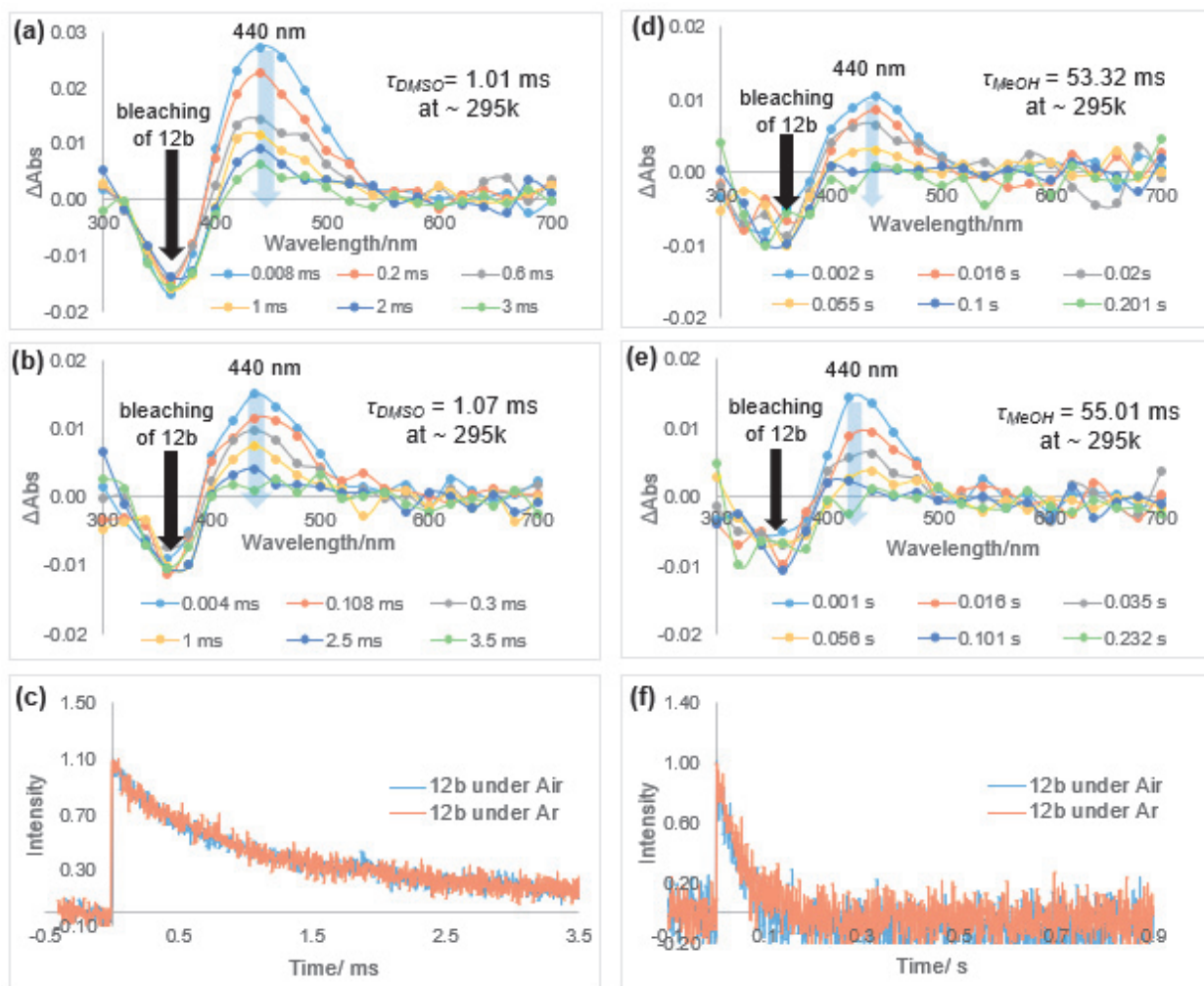


**Figure 10.** Sub-millisecond and second transient absorption spectroscopy of **12b** in DMSO and MeOH ( $32 \mu\text{m}$ , Abs at  $355 \text{ nm} \sim 1.0$ ) using  $355 \text{ nm}$  Nd:YAG laser ( $4 \text{ ns}$  pulse width,  $4.2 \text{ mJ/pulse}$ ) at  $298 \text{ K}$ . (a) Transient absorption spectra after LFP under Air in DMSO. (b) Transient absorption spectra after LFP under Ar in DMSO. (c) Time profile observed at  $440 \text{ nm}$  in DMSO. (d) Transient absorption spectra after LFP under Air in MeOH. (e) Transient absorption spectra after LFP under Ar in MeOH. (f) time profile observed at  $440 \text{ nm}$  in MeOH

**Simultaneous two-photon (2P) excitation reactions of 12a,b.** Finally, the photoreactions of **12a,b** in DMSO under 2P excitation were examined. A femtosecond Ti:sapphire laser (approximately 700 mW) was used as light source. The photoreactions were monitored by HPLC analysis. The standard compound, 2-(4-nitrophenyl)benzofuranbenzoate (NPBF-BA, Figure 11) (18 GM at 720 nm),<sup>27</sup> was used as a reference to determine the 2P cross section of compounds **12a,b**. Figures 12a and 12c show the time profiles of the photoreactions of **12a,b**, respectively, at wavelengths of 690–720 nm. The slopes of the fitted lines represent the decomposition rate constants. Based on these data, the 2P cross sections were calculated using the following equation:

$$\sigma_{12} = \sigma_{\text{NBPF}} \times \Phi_{\text{NBPF}} \times \frac{k_{\text{NBPF}}}{k_{12}} \times \frac{1}{\Phi_{12}}$$

where  $\sigma_{\text{NBPF}}$ ,  $\Phi_{\text{NBPF}}$ , and  $k_{\text{NBPF}}$  are the two-photon cross sections of NBPF at 720 nm, the decomposition quantum yield of NBPF-BA, and the rate constant of the decomposition of NBPF-BA under 720 nm light irradiation, respectively.

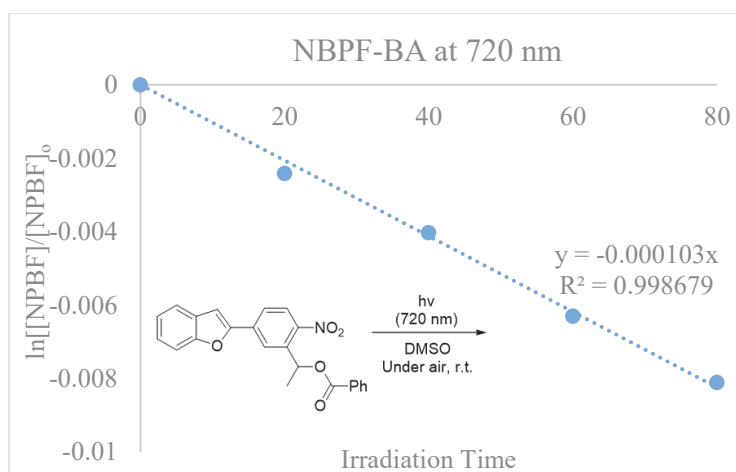


**Figure 11.** Two-photon Photolysis of NPBF-BA

$\sigma_{\text{NPBF-BA}}$  : 2PA cross-section of NPBF-BA at 720 nm (18 GM)

$\phi_{\text{NPBF-BA}}$  : quantum yield of NPBF-BA at 720 nm (0.09)

$k_{\text{NPBF-BA}}$  : rate constant of NPBF-BA at 720 nm (0.000103)



Two photon absorption spectra were obtained based on the calculated two-photon cross-sectional values, as shown in Figure 12b and 12d. As shown in Figure 12b, an absorption band with a maximum wavelength below 690 nm was observed in the absorption spectrum of **12a**. The 2P cross section and 2P efficiency at 690 nm were determined to be 49.5 and 36 GM, respectively, which are ideal values for biological experiments. In contrast, an absorption maximum is observed at 695 nm in the 2P absorption spectrum of **12b** (Figure 12b), indicating a bathochromic shift in the 2P absorption band of **12b** compared to that of **12a**. This result followed the same trend as that of the 1P absorption spectra of **12a** and **12b**, which originated from the stronger electron donation from the diethyl amino group to the benzene ring compared to the piperazine moiety. The 2P cross section and 2P uncaging efficiency measured at 695 nm for **12b** were 40.7 and 30 GM, respectively, implying that chromophores **13a,b** are also promising PPGs for application in biological studies, which is the next target of our research.

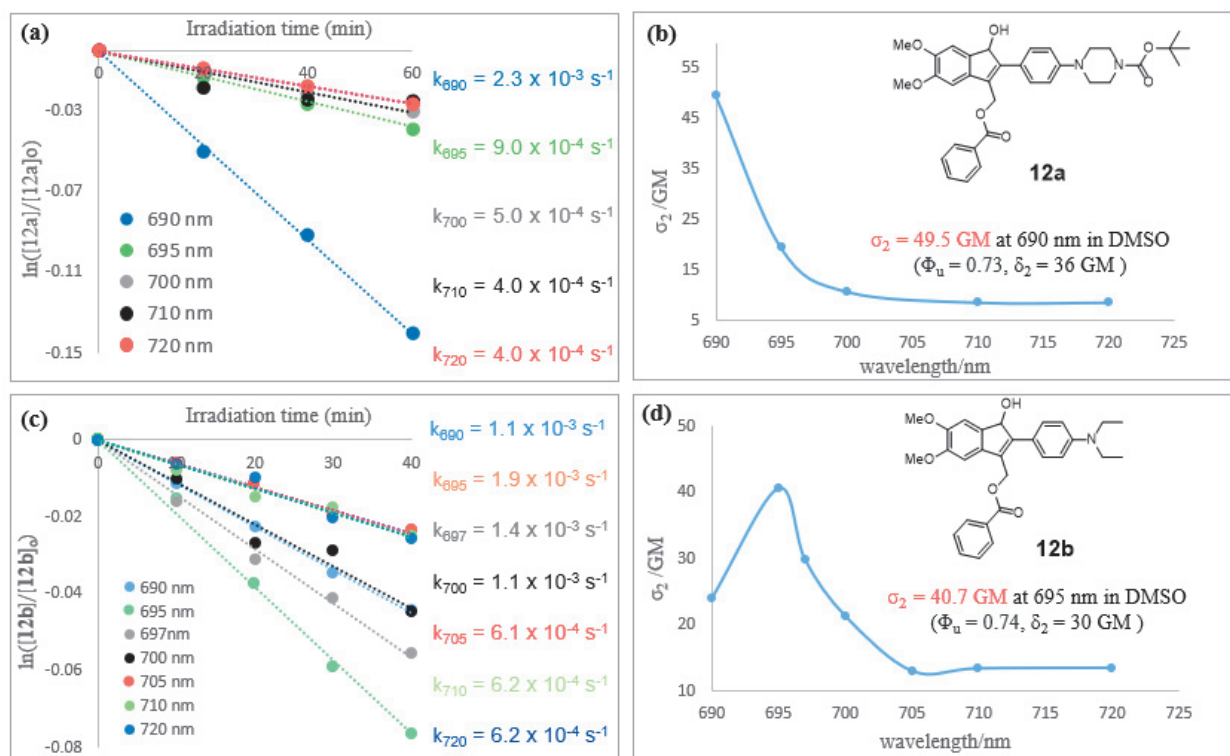


**Figure 12.** (a) Time profiles of 2P photolysis of **12a** in DMSO, depicted as a function of  $\ln([\mathbf{12a}]/[\mathbf{12a}]_0)$  with irradiation time at 690–720 nm, (c) Time profiles of 2P photolysis of **12b** in DMSO, depicted as a function of  $\ln([\mathbf{12b}]/[\mathbf{12b}]_0)$  with irradiation time at 690–720 nm. (b) 2PA spectra of **12a** in DMSO. (d) 2PA spectra of **12b** in DMSO

## 2.3 Experimental section

### General Information.

All reactions were performed under nitrogen atmosphere in flame-dry glassware with stirring magnetic and the temperature is controlled by an oil stove. Reagents were used as obtained from commercial suppliers without further purification. Silica Gel 60 N (spherical, neutral) 63–210  $\mu\text{m}$  was purchased from Kanto Chemical CO., Inc. to use silica gel column chromatography. Preparatory TLC (prep TLC) was conducted using Merck F<sub>254</sub> Prep-20  $\times$  20 cm TLC plates. <sup>1</sup>H-NMR and <sup>13</sup>C-NMR spectra were recorded on a Bruker ASCENDTM 400 (1H, 400 MHz, 13C, 100 MHz). Signal positions were given in parts per million (ppm) from tetramethylsilane ( $\delta$  0.00) and measured relative to the signal of the solvent (CDCl<sub>3</sub>:  $\delta$  7.26, 1H NMR;  $\delta$  77.16, 13C NMR). Data are reported as follows: chemical shift, multiplicity (s=singlet, d= doublet, dd=doublet of doublets, t=triplet, q=quartet, dq= doublet of quartets, br=broad signal, m=multiplet), coupling constant (Hz), and integration. UV-vis spectra were recorded on a SHIMADZU UV-3600 Plus spectrophotometer. Mass-spectrometric data were measured by Mass Spectrometric Thermo Fisher Scientific LTQ Orbitrap XL, whose measurements were supported by National Science Centre for Basic Research and Development (N-BARD), Hiroshima Univ.

### Laser flash photolysis (LFP) measurements

Transient absorption spectroscopy with a laser flash photolysis method was performed using an Nd:YAG laser at 355 nm, 4 ns pulse width, 4 mJ/pulse.

### Computational method

B3LYP/6-31G(d) level of theory of reaction profiles and geometry optimization were using for calculated and using the Gaussian suite programming.

## Synthesis

Synthesis of compounds **3**, **4a**, **5a**, **5b**, and **7** were prepared using methods reported in previous studies and confirmed by  $^1\text{H-NMR}$  spectra.<sup>28-32</sup>

*1-(4-bromophenyl)piperazine (3)*.  $^1\text{H NMR}$  (400 MHz,  $\text{CD}_3\text{OD}$ ),  $\delta$  (ppm) 7.40 (d,  $J = 9.0$  Hz 2H), 6.95 (d,  $J = 9.0$  Hz 2H), 3.41-3.33 (m, 8H).

*tert-butyl 4-(4-bromophenyl)piperazine-1-carboxylate (4a)*.  $^1\text{H NMR}$  (400 MHz,  $\text{CDCl}_3$ ),  $\delta$  (ppm) 7.35 (d,  $J = 8.8$  Hz 2H), 6.78 (d,  $J = 8.8$  Hz 2H), 3.56 (t,  $J = 7.2$  Hz 4H), 3.09 (d,  $J = 7.2$  Hz 4H), 1.47 (s, 9H).

*tert-butyl 4-(4-(4,4,5,5-tetramethyl-1,3,2-dioxaborolan-2-yl)phenyl)piperazine-1-carboxylate (5a)*.  $^1\text{H NMR}$  (400 MHz,  $\text{CDCl}_3$ ),  $\delta$  (ppm) ) 7.36 (d,  $J = 8.8$  Hz 2H), 6.90 (d,  $J = 8.8$  Hz 2H), 3.58 (t,  $J = 7.04$  Hz 4H), 3.24 (d,  $J = 7.04$  Hz 4H), 1.49 (s, 9H), 1.34(s, 12H).

*N,N-diethyl-4-(4,4,5,5-tetramethyl-1,3,2-dioxaborolan-2-yl)aniline (5b)*.  $^1\text{H NMR}$  (400 MHz,  $\text{CDCl}_3$ ),  $\delta$  (ppm) 7.65 (d,  $J = 8.8$  Hz 2H), 6.63 (d,  $J = 8.8$  Hz 2H), 3.37 (q,  $J = 7.04$  Hz 4H), 1.16 (t,  $J = 7.04$  Hz 6H).

*5,6-dimethoxy-3-methyl-2,3-dihydro-1H-inden-1-one (7)*.  $^1\text{H NMR}$  (400 MHz,  $\text{CDCl}_3$ ),  $\delta$  (ppm) 7.15 (s, 1H), 6.88 (d, 1H), 3.98 (t, 3H), 3.90 (d, 3H), 3.40-3.31 (m, 1H), 2.90 (dd,  $J = 7.04$  Hz 1H), 2.16 (dd,  $J = 3.1$  Hz 1H), 1.37 (d,  $J = 7.04$  Hz 3H).

*2,2-Dibromo-5,6-dimethoxy-3-methyl-2,3-dihydro-1H-inden-1-one (8)*.  $\text{PPh}_3 \cdot \text{HBr}$  (7.35 g, 21.43 mmol) was taken in a flask and DMSO dry (60 ml) was added dropwise under nitrogen atmosphere. Compound **7** (2.2 g, 10.68 mmol) was added into the reaction mixture at r.t and the mixture of reaction was stirred over  $50^\circ\text{C}$  in oil bath for 24 h. After finished reaction, the reaction mixture was quenched by saturated  $\text{NH}_4\text{Cl}$  and extracted with EtOAc. The organic

phase was dried with Na<sub>2</sub>SO<sub>4</sub>, filtered, concentrated under reduced pressure, and was quickly subjected to a short column chromatography to afford 1.45 g (3.98 mmol) of the dibromide. The dibromide, Li<sub>2</sub>CO<sub>3</sub> (1.03 g, 11.94 mmol) and LiBr (882.4 mg, 11.94 mmol) was added in a flask and degassed by Nitrogen. After that, 16.5 mL of DMF was added to the mixture reaction under nitrogen atmosphere and stirred at 50°C by oil bath over 24 h. After 24 h, the mixture was extracted with EtOAc. The organic phase was dried by Na<sub>2</sub>SO<sub>4</sub>, filtered and the organic solvent evaporated. The products were purified by column chromatography with Hexane/EtOAc = 3/1, v/v to afford compound **8** (1.2 g, 37%) with red solid. <sup>1</sup>H NMR (400 MHz, CDCl<sub>3</sub>), δ (ppm) 7.09 (s, 1H), 6.66 (s, 1H), 3.95 (s, 3H), 3.88 (s, 3H), 2.18 (s, 3H); <sup>13</sup>C {<sup>1</sup>H} NMR (100 MHz, CDCl<sub>3</sub>), δ (ppm) 189.2, 155.9, 153.1, 148.85, 139.3, 121.9, 116.6, 107.9, 104.3, 56.5, 56.4, 13.2; IR (KBr, cm<sup>-1</sup>), 2988, 2937, 1710, 1611, 1582, 1465, 1406, 1347, 1312, 1254, 1024. HRMS (ESI) m/z: [M + Na]<sup>+</sup> calcd for C<sub>12</sub>H<sub>11</sub>BrO<sub>3</sub>Na, 304.9789; found, 304.9786. Mp: 135-146 °C.

*tert*-Butyl 4-(4-(5,6-dimethoxy-3-methyl-1-oxo-1H-inden-2-yl)phenyl)piperazine-1-carboxylate (**9a**). Compound **8** (1.12 g, 3.98 mmol), compound **5a** (1.7 g, 4.38 mmol), NaHCO<sub>3</sub> (1.05 g, 17.5 mmol) and PdCl<sub>2</sub>(PPh<sub>3</sub>)<sub>2</sub> (176 mg, 0.25 mmol) were mixed in dioxane/H<sub>2</sub>O (5:2, 90 ml). The reaction mixture was stirred at 70 °C (using oil bath) for 16h under nitrogen. After the reaction was completed, the mixture was diluted with H<sub>2</sub>O and extracted with CH<sub>2</sub>Cl<sub>2</sub>. The organic layers were dried over Na<sub>2</sub>SO<sub>4</sub>, filtered and concentrated. The products were separated using column chromatography on silica gel with Hex/ EtOAc = 2:1, v/v as an eluent and obtained **9a** with red solid (370 mg, 20%). <sup>1</sup>H NMR (400 MHz, CDCl<sub>3</sub>), δ (ppm) 7.35 (d, *J* = 8.8 Hz 2H), 7.11 (s, 1H), 6.97 (d, *J* = 8.8 Hz 2H), 6.72 (s, 1H), 3.98 (s, 3H), 3.91 (s, 3H), 3.59 (t, *J* = 5.3 Hz 4H), 3.18 (t, *J* = 5.3 Hz 4H), 2.27 (s, 3H), 1.49 (s, 9H); <sup>13</sup>C {<sup>1</sup>H} NMR (100 MHz, CDCl<sub>3</sub>), δ (ppm) 197.0, 152.9, 149.4, 148.4, 147.0, 141.2, 132.2, 130.5, 122.9, 118.2, 111.3, 107.0, 103.8, 56.4, 56.3, 44.3, 12.67, 12.61. IR (KBr, cm<sup>-1</sup>), 2982, 2935, 1700, 1596, 1493, 1416,

1234, 1171, 1121, 1034; HRMS (ESI)  $m/z$ :  $[M + Na]^+$   $C_{27}H_{32}N_2O_5Na$ , 487.2203; found 487.2202. Mp: 170-176 °C .

*2-(4-(Diethylamino)phenyl)-5,6-dimethoxy-3-methyl-1H-inden-1-one (9b)*. Compound **8** (1.05 g, 3.74 mmol), compound **5b** (1.2 g, 4.1 mmol),  $K_2CO_3$  (2.26 g, 16.4 mmol) and  $PdCl(PPh_3)_2$  (166 mg, 0.24 mmol) were mixed in dioxane/ $H_2O$  (5:2, 85 mL). The reaction is carried out similar to that of synthesis compound **9a**. The crude was separated using column chromatography on silica gel with Hex/ EtOAc = 2:1, v/v as an eluent and obtained **9b** with dark red solid (230 mg, 18%).  $^1H$  NMR (400 MHz,  $CDCl_3$ ),  $\delta$  (ppm) 7.31 (d,  $J = 8.8$  Hz, 2H), 7.09 (s, 1H), 6.71 (d,  $J = 8.8$  Hz, 2H), 6.69 (s, 1H), 3.97 (s, 3H), 3.90 (s, 3H), 3.43 (q,  $J = 7.04$  Hz, 4H), , 2.27 (s, 3H), 1.18 (t,  $J = 7.04$  Hz, 4H);  $^{13}C\{^1H\}$  NMR (100 MHz,  $CDCl_3$ ),  $\delta$ (ppm) 197.2, 153.1, 149.5, 148.6, 147.2, 141.4, 130.6, 123.1, 118.4, 111.4, 107.2, 103.9, 77.3, 56.58, 56.53, 44.5, 12.8; IR (KBr,  $cm^{-1}$ ), 3012, 2989, 2915, 1694, 1592, 1516, 1490, 1351, 1293, 1210, 1121, 1092, 1038; HRMS (ESI)  $m/z$ :  $[M + H]^+$   $C_{22}H_{26}ON_3$ , 352.1907; found, 352.1911. Mp: 200-207 °C .

*tert-Butyl 4-(4-(3-(hydroxymethyl)-5,6-dimethoxy-1-oxo-1H-inden-2-yl)phenyl)piperazine-1-carboxylate (10a)*. Compound **9a** (200 mg, 0.43 mmol) and  $SeO_2$  (71.1 mg, 0.65 mmol) were dissolved in 12.3 ml xylene and stirred by oil bath at 130 °C for 20 h. The suspension was filtrated (without cooling to rt) and residue was washed with EtOAc and evaporated crude of product for the next step. The mixture of  $NaBH_4$  (122.5 mg, 3.23 mmol) in 13.1 mL of benzene and  $CH_3COOH$  (1.5 mL) in 5 mL benzene was prepared and refluxed over 80 °C in 30 min. The mixture was transferred to a solution of crude product in dry benzene (2.05 mL). This solution was heated to 80°C in 2 h. After 2h of stirring, the solution was extracted with DCM, dried with  $Na_2SO_4$ , and evaporated. The crude product was purified by silica gel column chromatography (hexane/EtOAc=2/1, v/v) to give **10a** as a red solid (46 mg, 25%).  $^1H$  NMR (400 MHz,  $CDCl_3$ ),  $\delta$ (ppm) 7.30 (d,  $J = 8.8$  Hz 2H), 7.13 (s, 1H), 7.05 (s, 1H), 6.96 (d,  $J = 8.9$  Hz 2H), 4.81 (d,  $J = 5.6$  Hz 2H), 3.97 (s, 3H), 3.91 (s, 3H), 3.59 (t,  $J = 5.2$  Hz 4H), 3.20 (t,

$J = 5.0$  4H), 1.49 (s, 9H);  $^{13}\text{C}\{^1\text{H}\}$  NMR (100 MHz,  $\text{CDCl}_3$ ),  $\delta(\text{ppm})$  196.7, 154.8, 153.4, 151.0, 150.4, 148.8, 139.5, 132.9, 131.0, 130.6, 128.9, 122.7, 121.9, 116.0, 107.6, 106.1, 80.1, 58.0, 56.57, 56.52, 48.8, 28.5. IR (KBr,  $\text{cm}^{-1}$ ), 3362, 2971, 2933, 1697, 1592, 1460, 1352, 1234, 1171, 1030; HRMS-ESI  $m/z$ :  $[\text{M} + \text{Na}]^+$  calcd for  $\text{C}_{27}\text{H}_{32}\text{N}_2\text{O}_6\text{Na}$ , 503.2152; found 503.2152. Mp: 130-136 °C.

*2-(4-(diethylamino)phenyl)-3-(hydroxymethyl)-5,6-dimethoxy-1H-inden-1-one* (**10b**).

Compound **9b** (200 mg, 0.57 mmol) and  $\text{SeO}_2$  (124.5 mg, 1.14 mmol) were mixed on reaction flask in 16.2 ml xylene and stirred at 130°C by oil bath over 16h. A mixture of  $\text{NaBH}_4$  and  $\text{CH}_3\text{COOH}$  was prepared in the same way as for **9a** and performed similar to the synthesis of compound **9a**. Compound **10b** was obtained as a dark red solid (40 mg, 20%).  $^1\text{H}$  NMR (400 MHz,  $\text{CDCl}_3$ ),  $\delta(\text{ppm})$  7.30 (d,  $J = 8.8$  Hz 2H), 7.15 (s, 1H), 7.04 (s, 1H), 6.73 (d,  $J = 8.8$  Hz 2H), 4.85 (d,  $J = 5.8$  Hz 2H), 3.99 (s, 3H), 3.92 (s 3H), 3.41 (q,  $H = 7.2$  Hz, 4H), 1.21 (t,  $H = 7.1$  Hz 6H);  $^{13}\text{C}\{^1\text{H}\}$  NMR (100 MHz,  $\text{CDCl}_3$ ), 197.2, 153.4, 148.5, 148.4, 147.7, 140.1, 133.5, 130.8, 122.8, 117.2, 111.4, 107.6, 105.7, 58.1, 56.5, 56.5, 44.5, 12.7. IR (KBr,  $\text{cm}^{-1}$ ), 3493, 2988, 1736, 1701, 1606, 1587, 1491, 1462, 1301, 1295, 1087. HRMS (ESI)  $m/z$ :  $[\text{M} + \text{H}]^+$   $\text{C}_{22}\text{H}_{26}\text{NO}_4$ , 368.1857; found, 368.1857. Mp: 158-165 °C.

*General Procedure for the synthesis of 11a-b.* Benzoic acid (16 mg, 0.131 mmol, 1.4 eq) in dry  $\text{CH}_2\text{Cl}_2$  was added DMAP (4.1 mg, 0.033 mmol, 0.351 eq) and this mixture was stirred at room temperature for 10 min under nitrogen atmosphere. Subsequently,  $\text{N,N}'$ -Dicyclohexylcarbodiimide (24.3 mg, 0.118 mmol, 1.25 eq) was added, and the mixture was stirred at room temperature for 12-14h. The reaction mixture was poured into water and extracted with DCM. The organic layer was dried over  $\text{Na}_2\text{SO}_4$ , filtered, evaporated under reduced pressure, and separated via column chromatography (hexane/EtOAc = 4/1, v/v) to obtain the product.

**(11a)** *Tert-butyl 4-(4-(3-((benzyloxy)methyl)-5,6-dimethoxy-1-oxo-1H-inden-2-yl)phenyl)piperazine-1-carboxylate*. The synthesis of **10a** (45 mg, 0.094 mmol, 1 eq) in 10 ml CH<sub>2</sub>Cl<sub>2</sub> at r.t. afforded compound **11a** as a white solid (42 mg, 76%). <sup>1</sup>H NMR (400 MHz, CDCl<sub>3</sub>), δ (ppm) 8.05 (d, *J* = 8.4 Hz 2H), 7.62-7.37 (m, 5H), 7.15 (s, 1H), 6.97 (d, *J* = 8.8 Hz 2H), 6.91 (s, 1H), 5.44 (s, 2H), 3.9 (s, 3H), 3.85 (s, 3H), 3.58 (t, *J* = 5.3 Hz 4H), 3.20 (t, *J* = 5.2 Hz 4H), 1.48 (s, 9H).; <sup>13</sup>C{<sup>1</sup>H} NMR (100 MHz, CDCl<sub>3</sub>), δ (ppm) 196.2, 166.3, 154.8, 153.5, 151.1, 148.9, 145.9, 139.3, 135.1, 133.6, 130.7, 129.8, 129.7, 128.7, 122.6, 121.6, 116.0, 107.8, 105.5, 80.1, 77.8, 59.5, 56.5, 56.4, 48.7, 28.5.; IR (KBr, cm<sup>-1</sup>), 3412, 3069, 2932, 1701, 1493, 1351, 1267, 1234, 1171, 1029. HRMS-ESI m/z: [M + Na]<sup>+</sup> calcd for C<sub>34</sub>H<sub>36</sub>N<sub>2</sub>O<sub>7</sub>Na, 607.2421; found 607.2418. Mp: 155-162 °C.

**(11b)** *(2-(4-(Diethylamino)phenyl)-5,6-dimethoxy-1-oxo-1H-inden-3-yl)methyl benzoate*. Compound **10b** (34.31 mg, 0.094 mmol, 1eq) in 10 ml CH<sub>2</sub>Cl<sub>2</sub> at r.t. Compound **11b** was a white solid (18 mg, 35%). <sup>1</sup>H NMR (400 MHz, CDCl<sub>3</sub>), δ (ppm), 8.07 (d, *J* = 7.6 Hz 2H), 7.62 – 7.39 (m, 5H), 7.14 (s, 1H), 6.88 (s, 1H), 6.72 (d, *J* = 7.4 Hz 2H), 5.45 (s, 2H), 3.90 (s, 3H), 3.85 (s, 3H), 3.39 (q, *J* = 7.2 Hz, 4H), 1.18 (t, *J* = 7.1 Hz 6H). <sup>13</sup>C{<sup>1</sup>H} NMR (100 MHz, CDCl<sub>3</sub>), δ (ppm) 196.7, 166.3, 153.4, 148.4, 147.8, 143.5, 139.7, 133.3, 130.7, 129.75, 129.72, 128.57, 128.54, 126.6, 122.4, 116.8, 111.3, 107.6, 105.1, 59.5, 56.4, 56.2, 44.3, 12.6. IR (KBr, cm<sup>-1</sup>), 3348, 3015, 2925, 1698, 1524, 1500, 1350, 1262, 1209, 1029. HRMS (ESI) m/z: [M + H]<sup>+</sup> C<sub>29</sub>H<sub>29</sub>NO<sub>5</sub>, 472.2119; found, 472.2116. Mp: 195-201 °C.

*General Procedure for the synthesis of 12a-b.* Solvent for reaction used methanol and cooled to 0 °C, NaBH<sub>4</sub> ( 6 eq) was added slowly in portion over 30 min. The mixture was stirred at 0 °C in 2 h. The mixture was then treated with diluted HCl 1N, extracted with EtOAc, washed with NaHCO<sub>3</sub> and dried with Na<sub>2</sub>SO<sub>4</sub>. After filtration, the organic layer was concentrated under vacuum. The crude product was purified by column chromatography using a Hex: EtOAc = 2:1.



*Tert-butyl 4-(4-(3-((benzoyloxy)methyl)-1-hydroxy-5,6-dimethoxy-1H-inden-2-yl)phenyl)piperazine-1-carboxylate (12a)*. Prepared from **11a** (42 mg, 0.07 mmol, 1eq) in 1.55 ml MeOH. After purification, **12a** was obtained as a white solid (25 mg, 60% yield). <sup>1</sup>H NMR (400 MHz, CDCl<sub>3</sub>), δ (ppm) 8.06 (d, *J* = 8.3 Hz 2H), 7.59 - 7.40 (m, 5H), 7.22 (s, 1H), 7.04 - 6.95 (m, 3H), 5.49 (d, *J* = 12.7 Hz 2H), 5.31 (d, *J* = 12.5 Hz 1H), 3.93 (s, 3H), 3.85 (s, 3H), 3.59 (t, *J* = 5.3 Hz 4H), 3.21 (s, *J* = 5.3 Hz 4H), 1.49 (s, 9H).; <sup>13</sup>C{<sup>1</sup>H} NMR (100 MHz, CDCl<sub>3</sub>) δ (ppm) 166.7, 154.8, 150.9, 149.9, 148.1, 136.3, 135.4, 133.3, 131.2, 130.13, 130.10, 129.8, 128.6, 116.4, 108.1, 104.2, 80.1, 77.6, 59.7, 56.5, 56.3, 48.8, 28.6. IR (KBr, cm<sup>-1</sup>), 3451, 3072, 2978, 2925, 1692, 1606, 1491, 1415, 1268, 1239, 1161, 1063. HRMS-ESI *m/z*: [M + Na]<sup>+</sup> calcd for C<sub>34</sub>H<sub>38</sub>N<sub>2</sub>O<sub>7</sub>Na, 609.2571; found 609.2580. Mp: 96-101 °C.

*(2-(4-(diethylamino)phenyl)-1-hydroxy-5,6-dimethoxy-1H-inden-3-yl)methyl benzoate (12b)*. Prepared from **11b** (33.46 mg, 0.07 mmol, 1eq) in 1.55 ml MeOH. Compound **12b** was obtained as a white solid in 60% yield (20 mg). <sup>1</sup>H NMR (400 MHz, CDCl<sub>3</sub>), δ(ppm) 8.08 (d, *H* = 8.0 Hz, 2H), 7.58-7.40 (m, 5H), 7.22 (s, 1H), 6.99 (s, 1H), 8.76 (d, *J* = 8.8 Hz), 5.54 – 5.31 (m, 3H), 3.93 (s, 3H), 3.85 (s, 3H), 3.39 (q, *J* = 7.2 Hz 4H), 1.19 (t, *J* = 7.04 Hz 6H); <sup>13</sup>C{<sup>1</sup>H} NMR (100 MHz, CDCl<sub>3</sub>) δ (ppm) 147.7, 136.1, 133.2, 130.4, 130.3, 129.9, 128.6, 111.8, 111.5, 108.2, 103.9, 77.8, 77.3, 59.9, 56.5, 56.3, 56.3, 44.5, 12.8. IR (KBr, cm<sup>-1</sup>), 3464, 3079, 2982, 1716, 1600, 1520, 1491, 1352, 1268, 1211, 1067. HRMS (ESI) *m/z*: [M + H]<sup>+</sup> C<sub>29</sub>H<sub>32</sub>NO<sub>5</sub>, 474.2275; found, 474.2278. Mp: 78-84 °C.

*General Procedure for the synthesis of 13a-b*. Reagent for reaction was using SeO<sub>2</sub> (17.8 mg, 0.16 mmol, 1.5 eq). The mixture was heated under reflux for 24 h in xylene (3.0 ml). After the reaction was complete, the reaction mixture was extracted with EtOAc and evaporated, and the crude product was used for the next step. MeOH (7 ml) and cooled to 0 °C. After that, the NaBH<sub>4</sub> (13.62 mg, 0.36 mmol, 3 eq) was added slowly over 30 min and the mixture was stirred at 0 °C in 2 h. The reaction mixture was diluted by HCL 2N, extracted with EtOAc, and washed

with salt. NaHCO<sub>3</sub> and dried over Na<sub>2</sub>SO<sub>4</sub>. After filtration and evaporation, the crude product was purified by column chromatography using Hex: EtOAc = 1:1

*tert*-Butyl 4-(4-(1-hydroxy-3-(hydroxymethyl)-5,6-dimethoxy-1*H*-inden-2-yl)phenyl)piperazine-1-carboxylate (**13a**). Synthesis of **9a** (50 mg, 0.107 mmol, 1 equiv.) in 3.0 ml Xylene. Compound **13a** was obtained as a white solid (7.5 mg). <sup>1</sup>H NMR (400 MHz, CDCl<sub>3</sub>), δ (ppm) 7.44 (d, *J* = 8.8 Hz 2H), 7.23 (s, 1H), 7.09 (s, 1H), 7.01 (d, *J* = 8.8 Hz 2H), 5.49 (d, *J* = 6.6 Hz, 1H), 4.82-4.69 (m, 2H), 3.97 (s, 3H), 3.96 (s, 3H), 3.62 (t, *J* = 5.3 Hz 4H), 3.23 (t, *J* = 5.3 Hz, 4H), 1.51 (s, 9H); <sup>13</sup>C{<sup>1</sup>H} NMR (100 MHz, CDCl<sub>3</sub>) δ (ppm) 154.7, 149.8, 148.0, 145.6, 36.5, 135.4, 135.2, 135.0, 129.9, 125.3, 116.2, 108.1, 104.1, 80.0, 77.2, 57.4, 56.34, 56.31, 48.8, 43.3, 28.4. IR (KBr, cm<sup>-1</sup>), 3401, 2973, 1704, 1602, 1498, 1460, 1420, 1240, 1141, 1062. HRMS-ESI *m/z*: [M + Na]<sup>+</sup> calcd for C<sub>27</sub>H<sub>34</sub>N<sub>2</sub>O<sub>6</sub>Na, 505.2309; found 505.2308. Mp: 145-151 °C.

2-(4-(diethylamino)phenyl)-3-(hydroxymethyl)-5,6-dimethoxy-1*H*-inden-1-ol (**13b**). Compound **13b** was prepared from **9b** (37.6 mg, 0.107 mmol, 1 equiv). Compound **13b** was obtained as a white solid (6.0 mg). <sup>1</sup>H NMR (400 MHz, CDCl<sub>3</sub>), δ (ppm) 7.04 (d, *J* = 8.9 Hz 2H), 7.23 (s, 1H), 7.07 (s, 1H), 6.77 (d, *J* = 8.9 Hz 2H), 5.50 (d, *J* = 8.3 Hz 1H), 4.85-4.69 (m, 2H), 3.97 (s, 3H), 3.95 (s, 3H), 3.43 (q, *J* = 7.0 Hz 4H), 1.22 (t, *J* = 7.4 Hz); <sup>13</sup>C{<sup>1</sup>H} NMR (100 MHz, CDCl<sub>3</sub>), δ (ppm) 149.7, 147.6, 147.4, 146.4, 136.2, 135.9, 133.3, 130.2, 120.3, 111.6, 108.1, 103.8, 77.2, 57.6, 56.3, 56.2, 44.3, 12.6. IR (KBr, cm<sup>-1</sup>), 3488, 2975, 2892, 1732, 1611, 1514, 1501, 1461, 1456, 1268, 1204, 1096. HRMS (ESI) *m/z*: [M + H]<sup>+</sup> C<sub>22</sub>H<sub>28</sub>NO<sub>4</sub>, 370.2013; found, 370.2016. Mp: 160-168 °C.

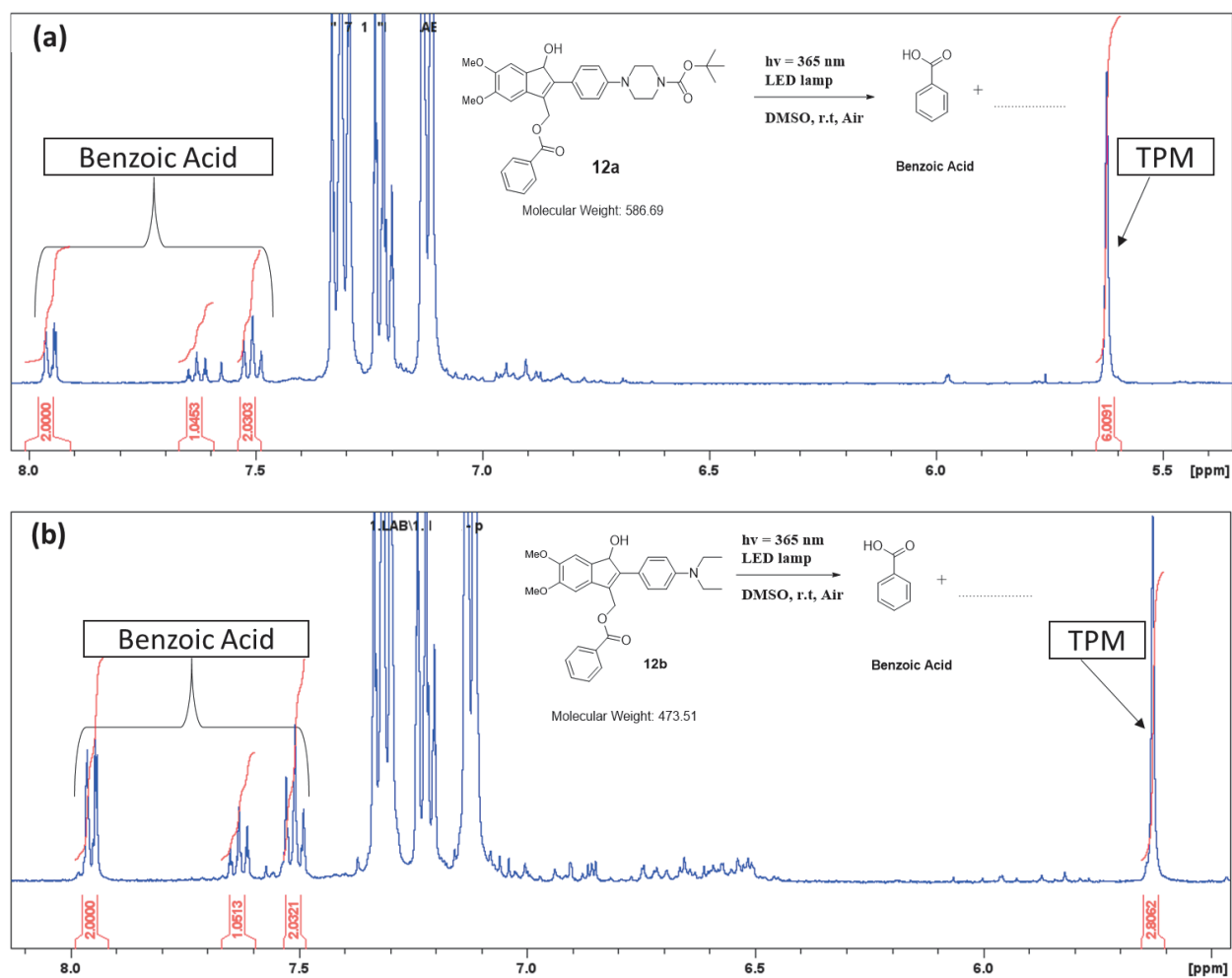
**Photolysis of compound 12a in MeOH.** The photolysis of **12a** (16 mg, 5.43 mM) was conducted in 5 ml MeOH at r.t and using LED lamp at 365 nm for irradiation . The

photo by products **trans-14a** (3.2 mg) and **cis-14a** (4.5 mg) were isolated by silica-gel column chromatography (Hex/EtOAc = 3/1 v/v).

*tert-butyl 4-(4-((1R,2R)-1-hydroxy-2,5,6-trimethoxy-3-methylene-2,3-dihydro-1H-inden-2-yl)phenyl)piperazine-1-carboxylate (trans-14a)*. <sup>1</sup>H NMR (400 MHz, CDCl<sub>3</sub>), δ(ppm) 7.37 (d, *J* = 8.7 Hz, 2H), 7.00 (s, 1H), 6.99 (s, 1H), 6.94 (d, *J* = 8.3 Hz 2H), 5.75 (s, 1H), 5.02 (s, 1H), 4.83 (d, *J* = 10.1 Hz 1H), 3.94 (s, 3H), 3.91 (s, 3H), 3.58 (t, *J* = 4.9 Hz 4H), 3.24 (s, 3H), 3.16 (t, *J* = 4.9 Hz 4H), 1.48 (s, 9H); <sup>13</sup>C{<sup>1</sup>H} NMR (100 MHz, CDCl<sub>3</sub>), δ(ppm) 154.9, 151.4, 150.2, 146.1, 137.0, 130.5, 128.4, 116.2, 111.0, 107.9, 107.0, 103.3, 87.9, 83.2, 80.1, 56.2, 52.1, 49.4, 43.7, 28.5. IR (KBr, cm<sup>-1</sup>),. HRMS (ESI) *m/z*: [M + Na]<sup>+</sup> C<sub>28</sub>H<sub>36</sub>N<sub>2</sub>O<sub>6</sub>Na, 519.2465; found, 519.2468. Mp: 148-156 °C.

*tert-butyl 4-(4-((1R,2S)-1-hydroxy-2,5,6-trimethoxy-3-methylene-2,3-dihydro-1H-inden-2-yl)phenyl)piperazine-1-carboxylate (cis - 14a)*. <sup>1</sup>H NMR (400 MHz, CDCl<sub>3</sub>), δ(ppm) 7.39 (d, *J* = 8.7 Hz, 2H), 7.04 (s, 1H), 6.97 (s, 1H), 6.92 (d, *J* = 8.7 Hz 2H), 5.78 (s, 1H), 5.01 (s, 1H), 4.92 (s, 1H), 3.95 (s, 3H), 3.90 (s, 3H), 3.57 (t, *J* = 4.8 Hz 4H), 3.24 (s, 3H), 3.16 (t, *J* = 4.8 Hz 4H), 1.48 (s, 9H); <sup>13</sup>C{<sup>1</sup>H} NMR (100 MHz, CDCl<sub>3</sub>), δ(ppm) 154.8, 151.3, 150.7, 146.8, 136.2, 132.6, 129.5, 129.3, 115.9, 108.0, 107.8, 107.5 103.3, 92.5, 80.3, 80.1, 56.2, 51.7, 49.1, 43.5, 28.5. IR (KBr, cm<sup>-1</sup>), HRMS (ESI) *m/z*: [M + Na]<sup>+</sup> C<sub>28</sub>H<sub>36</sub>N<sub>2</sub>O<sub>6</sub>Na, 519.2465; found, 519.2471. Mp: 148-156 °C.

## Chemical yield of benzoic acid



**Figure 13.** (a) <sup>1</sup>H-NMR spectra 5.5-8.0 ppm of 4.0 mg (0.0164 mmol) TPM was added for calculated benzoic acid (BA) chemical yield after irradiation compound **12a**; (b) <sup>1</sup>H-NMR spectra 5.5-8.0 ppm of 2.0 mg (0.0082 mmol) TPM was added for calculated benzoic acid (BA) chemical yield after irradiation compound **12b**.

## Quantum yield measurement

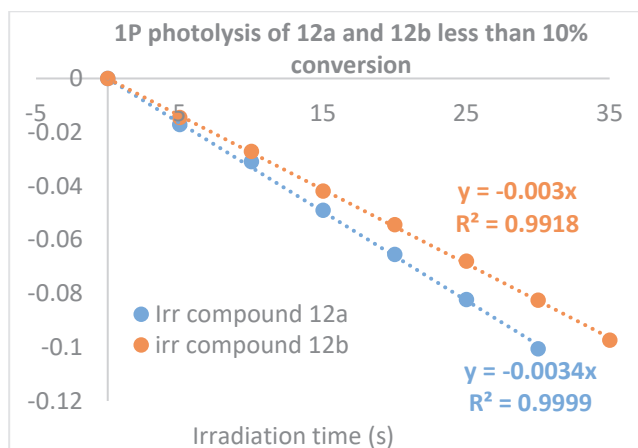
### Measurement method and preparation of sample

One photon (1P) photolysis of **12a** in DMSO. A solution of compound **12a** in DMSO ( $Abs_{405} = 5$ ,  $Conc = 2.65 \times 10^{-4}$ ) was prepared in cuvette 1cm. Light irradiation was using Xe-lamp at 365 nm, and 10  $\mu$ L of the solution after irradiation at 5s, 10s, 15s, 20s, 25s, 30s, 60s, 120s, 240s and 300s was injected into the HPLC (Column ODS-3, detector at 370 nm, flow rate is 1.0 mL/min) and analyzed with mobile phase ACN/H<sub>2</sub>O 6/1 v/v.

1P photolysis of **12b** in DMSO. A solution of compound **12b** in DMSO ( $Abs_{405} = 5$ ,  $Conc = 3.2 \times 10^{-4}$ ) was prepared in cuvette 1cm. Light irradiation was using Xe-lamp at 365 nm, and 10  $\mu$ L of the solution after irradiation at 5s, 10s, 15s, 20s, 25s, 30s, 35s, 70s, 130s, 190s was injected into the HPLC (Column ODS-3, detector at 370 nm, flow rate is 1.0 mL/min and analyzed with mobile phase ACN/H<sub>2</sub>O 3.5/1 v/v.

Chemical Actinometer for Quantum Yield Measurement (Xe lamp 365 nm). First, 291.7 mg K<sub>3</sub>[Fe(C<sub>2</sub>O<sub>4</sub>)]. H<sub>2</sub>O was dissolved in 50 ml 0.05M H<sub>2</sub>SO<sub>4</sub> (solution 1) and 10.2 mg of 1,10-phenanthroline monohydrate and 2.25-gram CH<sub>3</sub>COONa.3H<sub>2</sub>O were dissolved in 10 ml H<sub>2</sub>SO<sub>4</sub> 0.5 M (solution 2). After that, take 3 ml of solution 1 was irradiated at 400 nm for 0, 10, 20, 30s in cuvette. And then, 0.5 ml of solution 2 was added each time after irradiated and the mix solution measured UV absorption spectra at 510 nm. Change of absorbance with respect to irradiation time was used to calculate the light amount and quantum yield of **12a** and **12b** are calculated according to the following formula:

$$\text{Quantum yield} = \frac{\text{number of reacted molecules (mol)}}{\text{number of photon (mol/min)} \times \text{reaction time (min)}}$$



Time irr (s)	I (mol/s)	I <sub>average</sub> (mol/s)
10	$3.559 \times 10^{-9}$	
20	$3.386 \times 10^{-9}$	$3.477 \times 10^{-9}$
30	$3.487 \times 10^{-9}$	

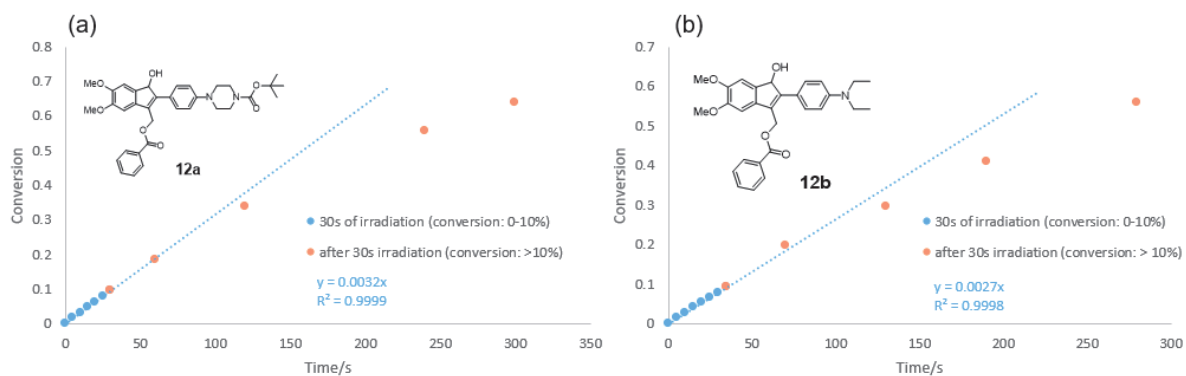
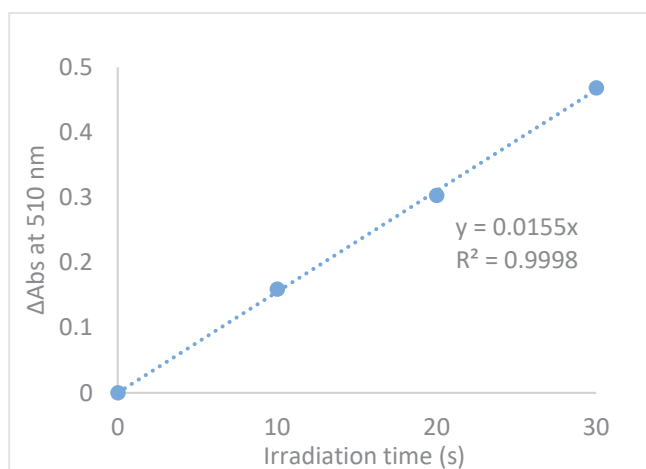


**Figure 14.** (a) One photon photolysis of **12a** and **12b** in DMSO less than 10% conversion, monitoring by HPLC; (b) Absorbance change with irradiation time at 510 nm. (c) Time profile of photoreaction of **12a** in DMSO monitored by HPLC; (d) Time profile of photoreaction of **12b** in DMSO monitored by HPLC.

## LFP measurements

The solutions of **12a** and **12b** in DMSO were prepared ( $C_{12a} = 5.1 \times 10^{-5}$  M;  $C_{12b} = 6.3 \times 10^{-5}$  M). Approx of 3.0 mL of the solution was transferred into a 1.0 cm cuvette. The measurements were performed under Air and Ar (by bubbling for 15 min). The temperature was controlled at 20°C. (Condition of experiment:  $\lambda_{\text{pump}} = 355$  nm, time scale = 4 ms, laser power = 4.3 mJ, number of shots = 2 shots). Make the same in MeOH, the solutions of **12a** and **12b** in MeOH were prepared ( $C_{12a} = 2.6 \times 10^{-5}$  M;  $C_{12b} = 3.2 \times 10^{-5}$  M). (Condition of experiment:  $\lambda_{\text{pump}} = 355$  nm, time scale of **12a** = 40 ms, time scale of **12b** = 1s, laser power = 4.2 mJ, number of shots = 2 shots).

**Table 3.** Lifetime of **12a** and **12b** in DMSO at difference wavelength after fitting

12a In DMSO	Under Air	380 nm	400 nm	420 nm	440 nm	460 nm	480 nm	500 nm	520 nm	540 nm	560 nm
	$\tau_1$ (ms)	-	0.32	0.31	0.31	0.33	0.29	0.33	0.33	-	-
	Under Ar	380 nm	400 nm	420 nm	440 nm	460 nm	480 nm	500 nm	520 nm	540 nm	560 nm
	$\tau_1$ (ms)	-	0.33	0.28	0.31	0.29	0.30	0.28	0.28	-	-
12b In DMSO	Under Air	380 nm	400 nm	420 nm	440 nm	460 nm	480 nm	500 nm	520 nm	540 nm	560 nm
	$\tau_1$ (ms)	-	1.43	1.02	1.01	0.98	0.81	1.07	-	-	-
	Under Ar	380 nm	400 nm	420 nm	440 nm	460 nm	480 nm	500 nm	520 nm	540 nm	560 nm
	$\tau_1$ (ms)	-	1.42	1.01	1.07	1.05	1.12	0.78	-	-	-

**Table 4.** Lifetime of **12a** and **12b** in MeOH at difference wavelength after fitting

12a In MeOH	Under Air	380 nm	400 nm	420 nm	440 nm	460 nm	480 nm	500 nm	520 nm
	$\tau_1$ (ms)	-	4.62	5.15	4.98	4.70	5.55	5.29	-
	Under Ar	380 nm	400 nm	420 nm	440 nm	460 nm	480 nm	500 nm	520 nm
	$\tau_1$ (ms)	-	4.40	4.85	4.73	5.17	5.00	4.35	-
12b In MeOH	Under Air	380 nm	400 nm	420 nm	440 nm	460 nm	480 nm	500 nm	520 nm
	$\tau_1$ (s)	-	0.053	0.052	0.053	0.056	0.053	-	-
	Under Ar	380 nm	400 nm	420 nm	440 nm	460 nm	480 nm	500 nm	520 nm
	$\tau_1$ (s)	-	0.059	0.050	0.055	0.052	0.053	-	-

## Two-photon measurement.

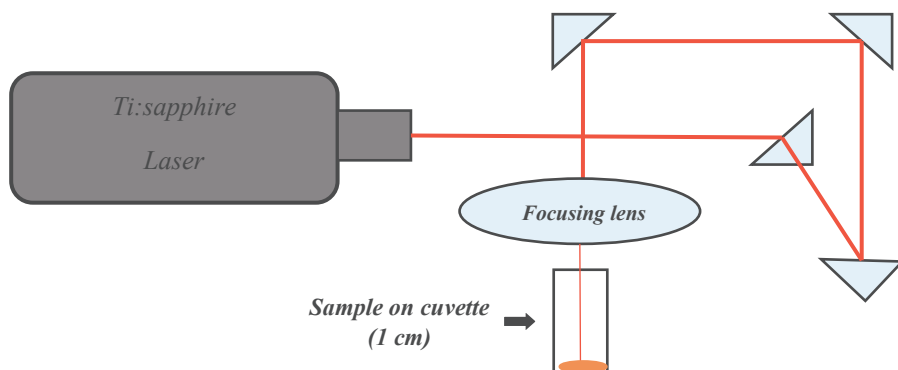


**Figure 15.** Measurement system diagram with Ti:sapphire Laser for 2P photolysis experiment for compound **12a** and **12b** in DMSO under Air.

A solution of compound **12a** in DMSO ( $C_{12a} = 5.1 \times 10^{-5}$ ) was prepared. Light irradiation was carried out using Ti:sapphire laser ( $\sim 700$  mW at  $\sim 25^\circ\text{C}$ ), and  $10 \mu\text{L}$  of the solution after irradiation at 0 min, 20 min, 40 min, and 60 min was injected into the HPLC (Column ODS-3, detector at 370 nm, flow rate is 1.0 mL/min) and analyzed with mobile phase ACN/H<sub>2</sub>O 6/1 v/v.

Similar with **12a**, solution of compound **12b** in DMSO ( $C_{12a} = 5.1 \times 10^{-5}$ ) was also prepared. Light irradiation was carried out using Ti:sapphire laser ( $\sim 700$  mW at  $\sim 25^\circ\text{C}$ ), and  $10 \mu\text{L}$  of the solution after irradiation at 0 min, 10 min, 20 min, 30 min and 40 min was injected into the HPLC (Column ODS-3, detector at 370 nm, flow rate is 1.0 mL/min) and analyzed with mobile phase ACN/H<sub>2</sub>O 3.5/1 v/v.

For measurement of NPBF-BA. The solution of NPBF-BA in DMSO ( $C_{\text{NPBF-BA}} = 5.12 \times 10^{-5} \text{M}$ ) was prepared and irradiated by using Ti:sapphire laser ( $\sim 700$  mW at  $\sim 25^\circ\text{C}$ ). And then,  $10 \mu\text{L}$  of the solution after irradiation at 720 nm at 0 min, 20 min, 40 min, 60 min, 80 min was injected HPLC (Column ODS-3, detector at 270 nm, flow rate is 1.0 mL/min) and analyzed with mobile phase ACN/H<sub>2</sub>O/TFA 90/10/0.1 v/v/v.



## 2.4 Supplementary materials

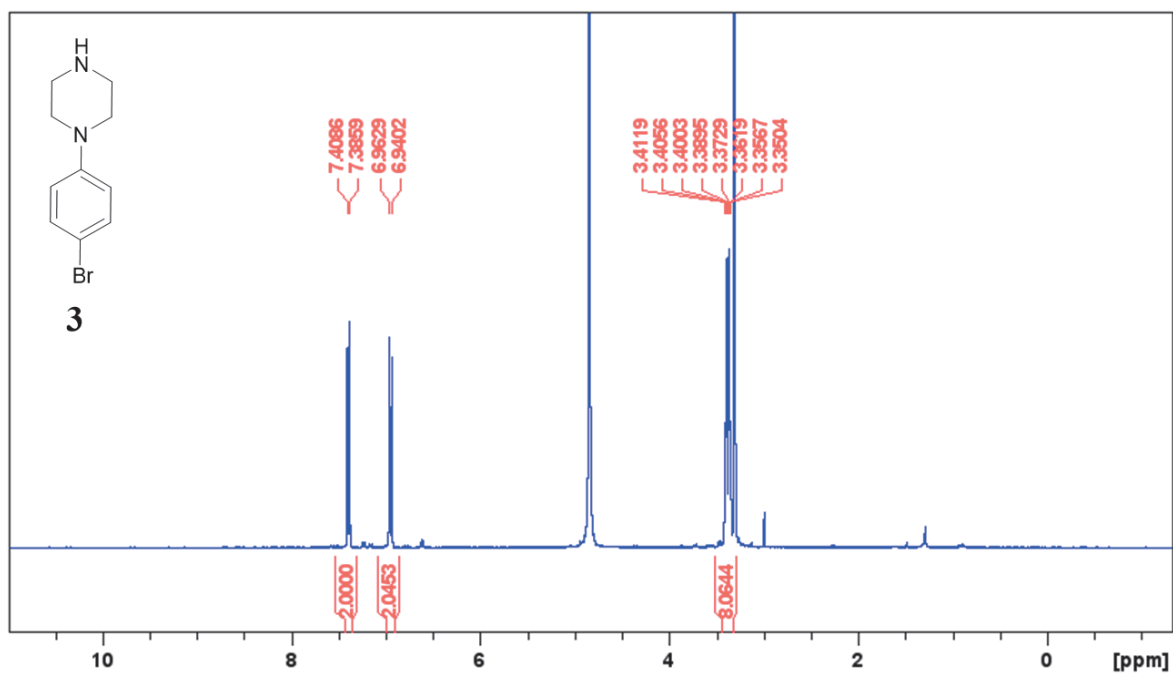


Figure 16. <sup>1</sup>H-NMR spectrum of compound 3 (CD<sub>3</sub>OD, 400 MHz).

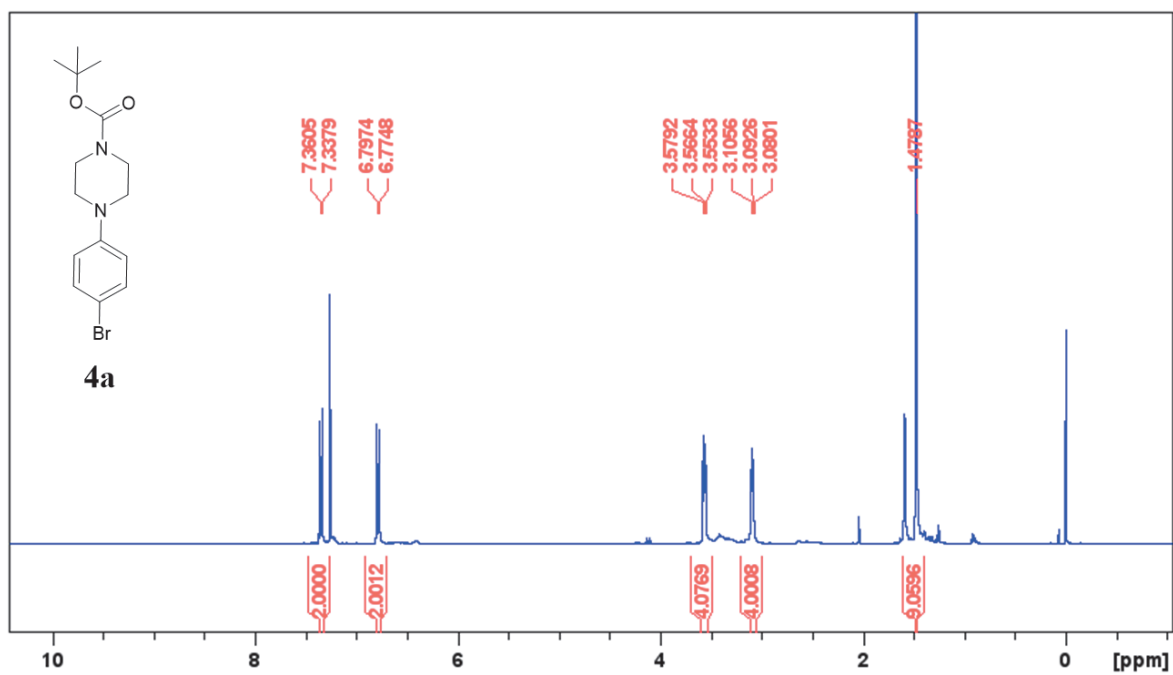


Figure 17. <sup>1</sup>H-NMR spectrum of compound 4a (CDCl<sub>3</sub>, 100 MHz).

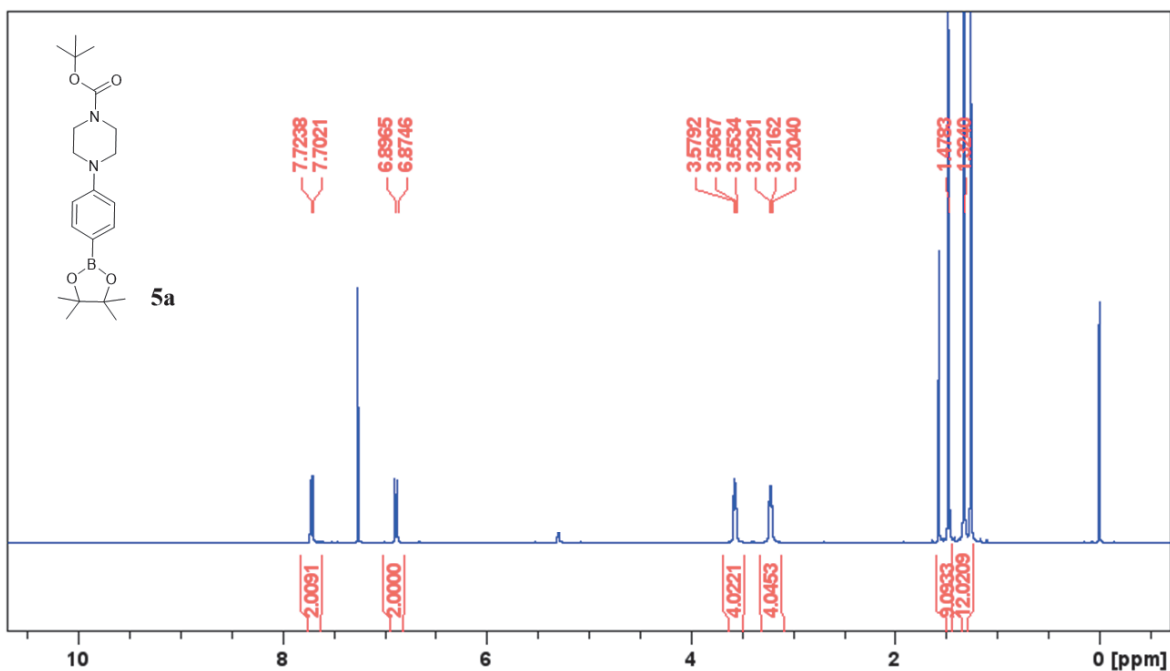


Figure 18.  $^1\text{H-NMR}$  spectrum of compound **5a** ( $\text{CDCl}_3$ , 400 MHz).

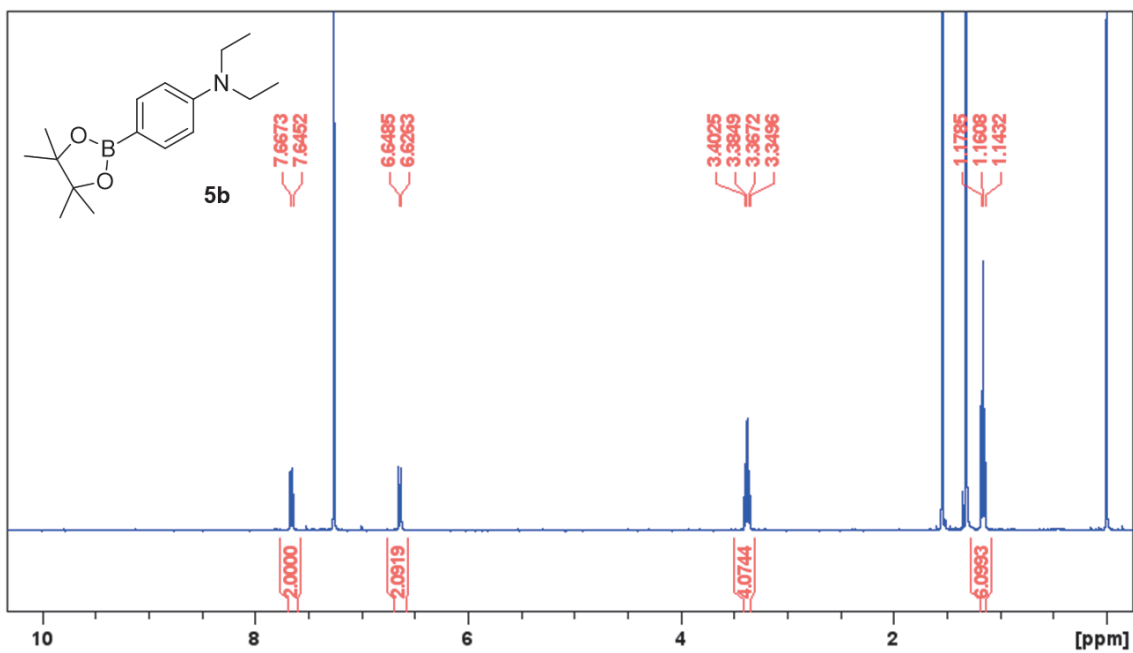


Figure S19.  $^1\text{H-NMR}$  spectrum of compound **5b** ( $\text{CDCl}_3$ , 400 MHz).

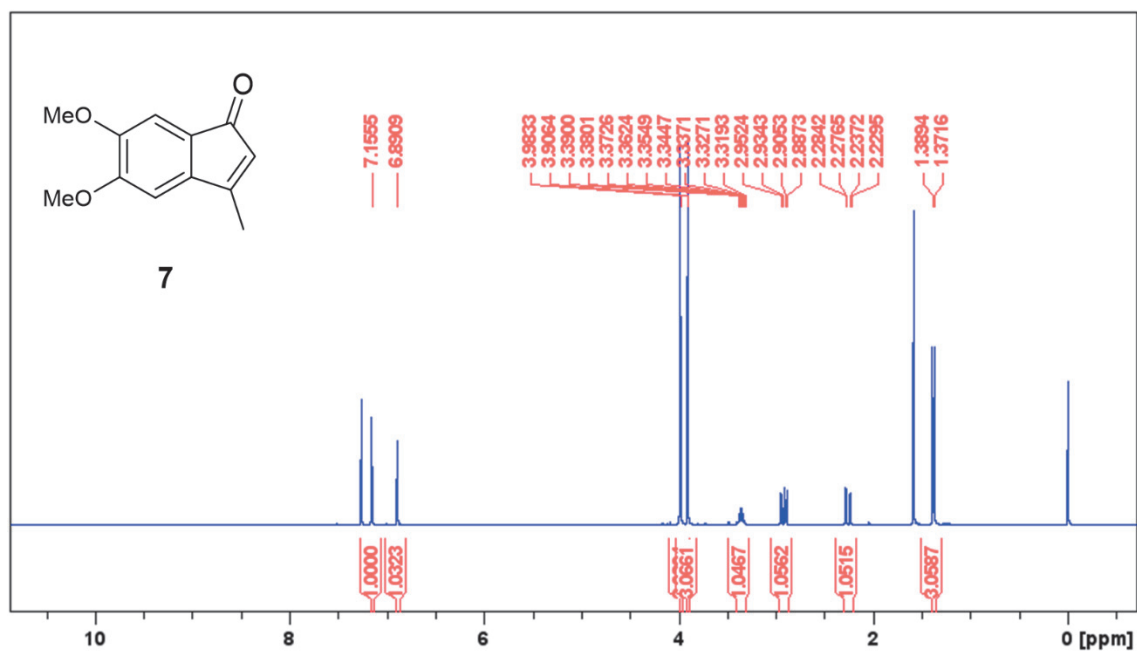


Figure 20.  $^1\text{H-NMR}$  spectrum of compound 7 ( $\text{CDCl}_3$ , 400 MHz).

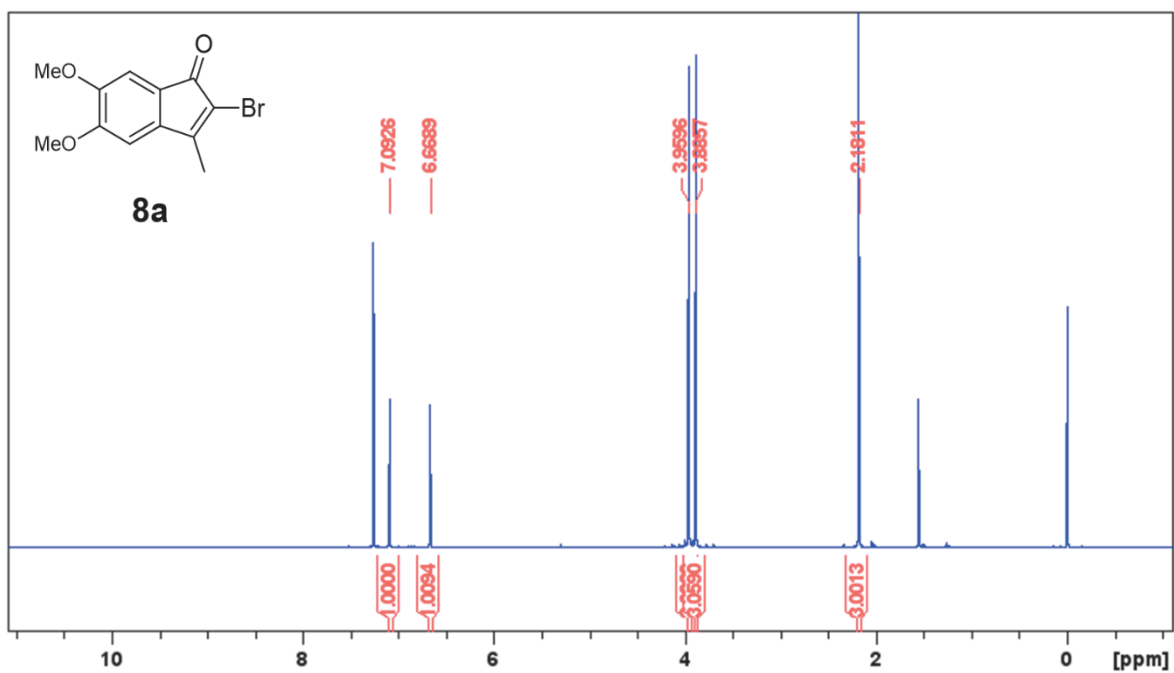


Figure 21.  $^1\text{H}$ -NMR spectrum of compound **8a** ( $\text{CDCl}_3$ , 400 MHz).

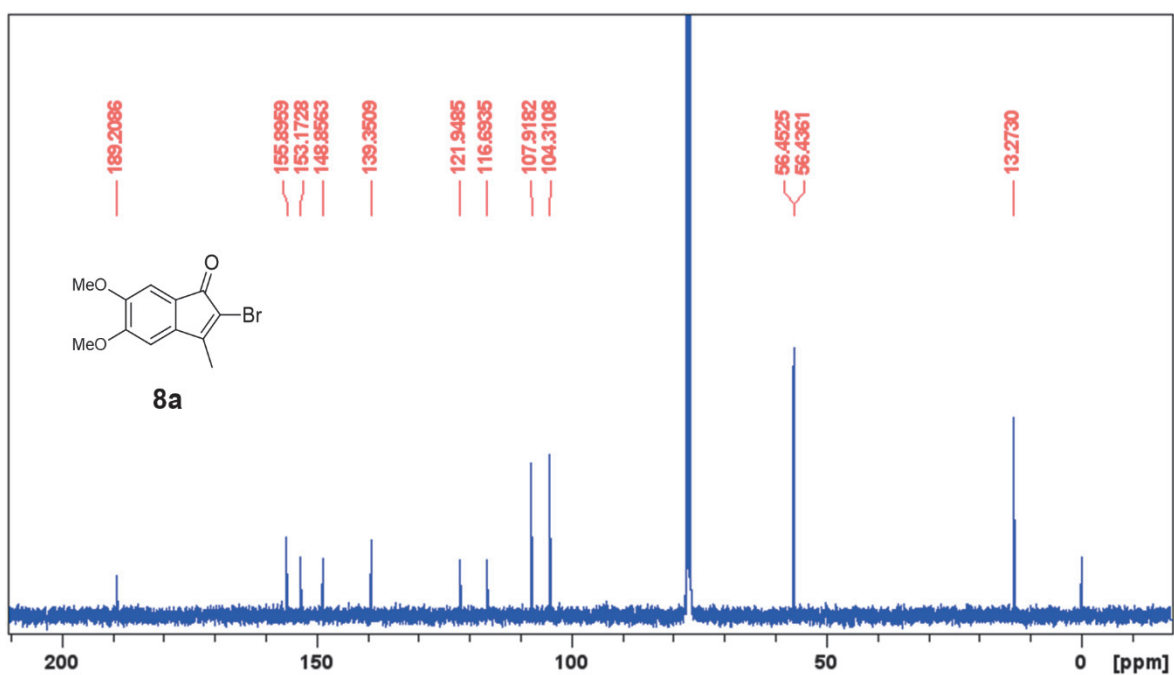


Figure 22.  $^{13}\text{C}\{^1\text{H}\}$ -NMR spectrum of compound **8a** ( $\text{CDCl}_3$ , 100 MHz).

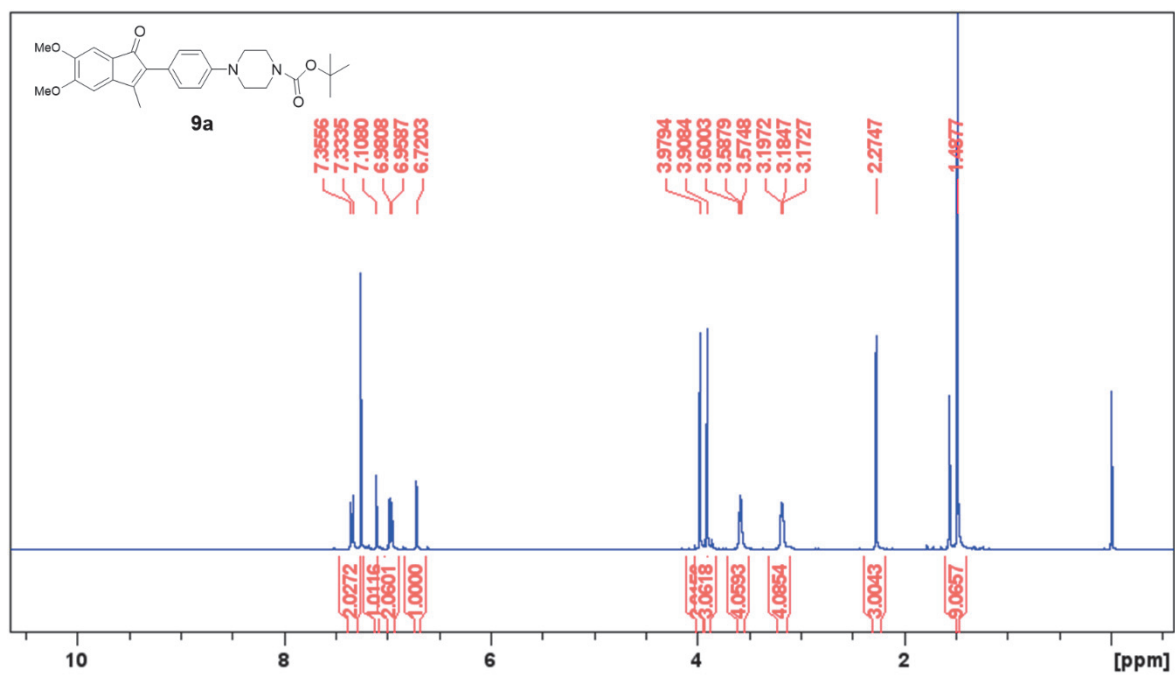


Figure 23.  $^1\text{H}$ -NMR spectrum of compound **9a** ( $\text{CDCl}_3$ , 400 MHz)

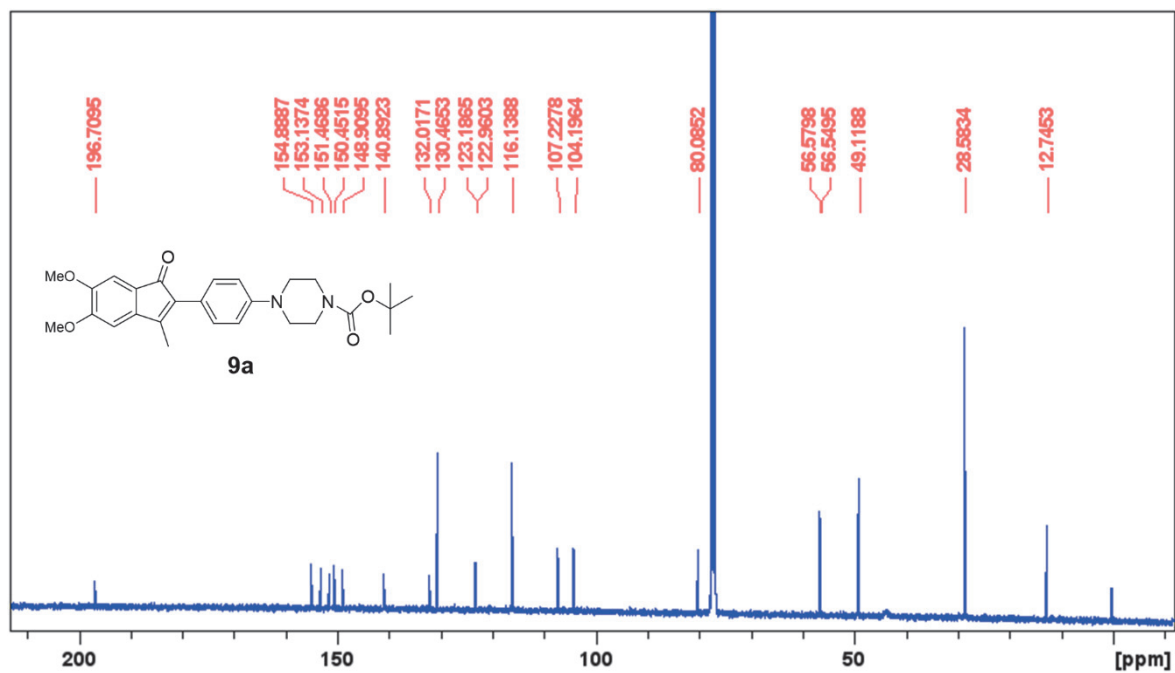


Figure 24.  $^{13}\text{C}\{^1\text{H}\}$ -NMR spectrum of compound **9a** ( $\text{CDCl}_3$ , 100 MHz).

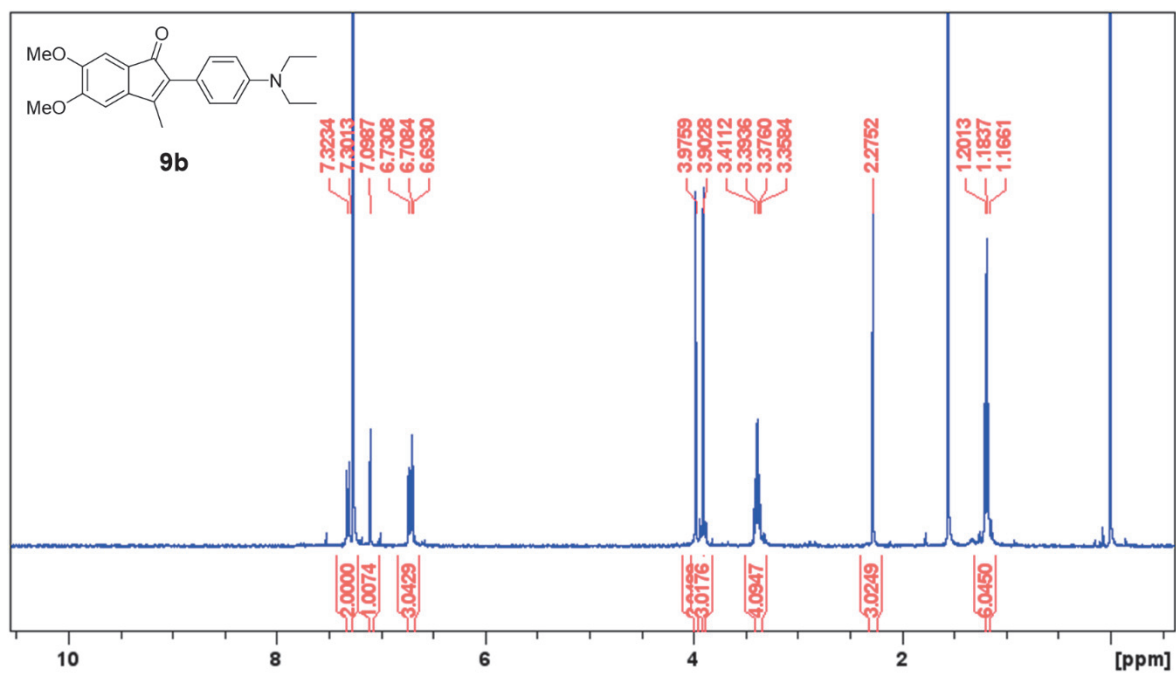


Figure 25.  $^1\text{H}$ -NMR spectrum of compound **9b** ( $\text{CDCl}_3$ , 400 MHz)

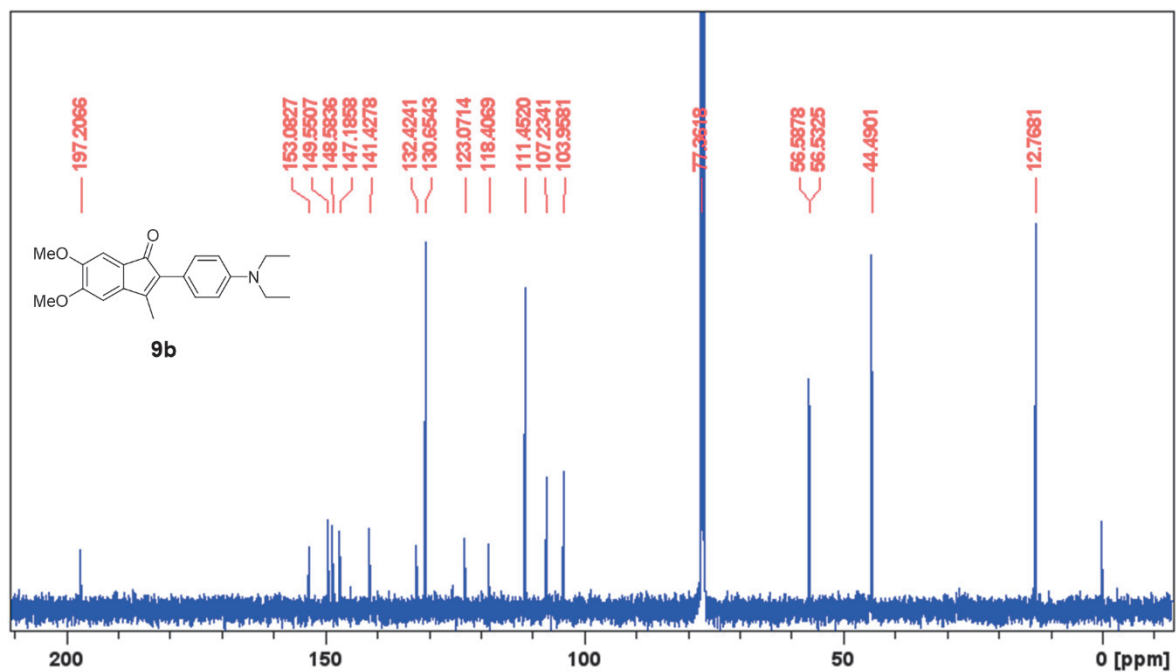


Figure 26.  $^{13}\text{C}\{^1\text{H}\}$ -NMR spectrum of compound **9b** ( $\text{CDCl}_3$ , 100 MHz).

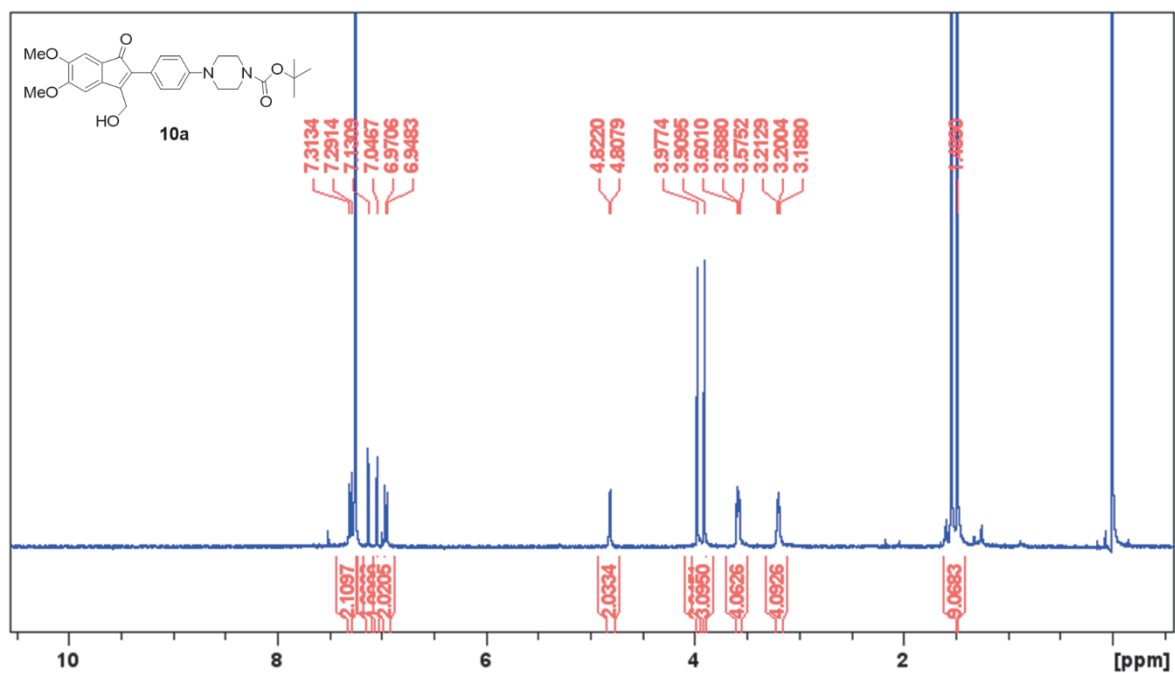


Figure 27. <sup>1</sup>H-NMR spectrum of compound **10a** (CDCl<sub>3</sub>, 400 MHz)

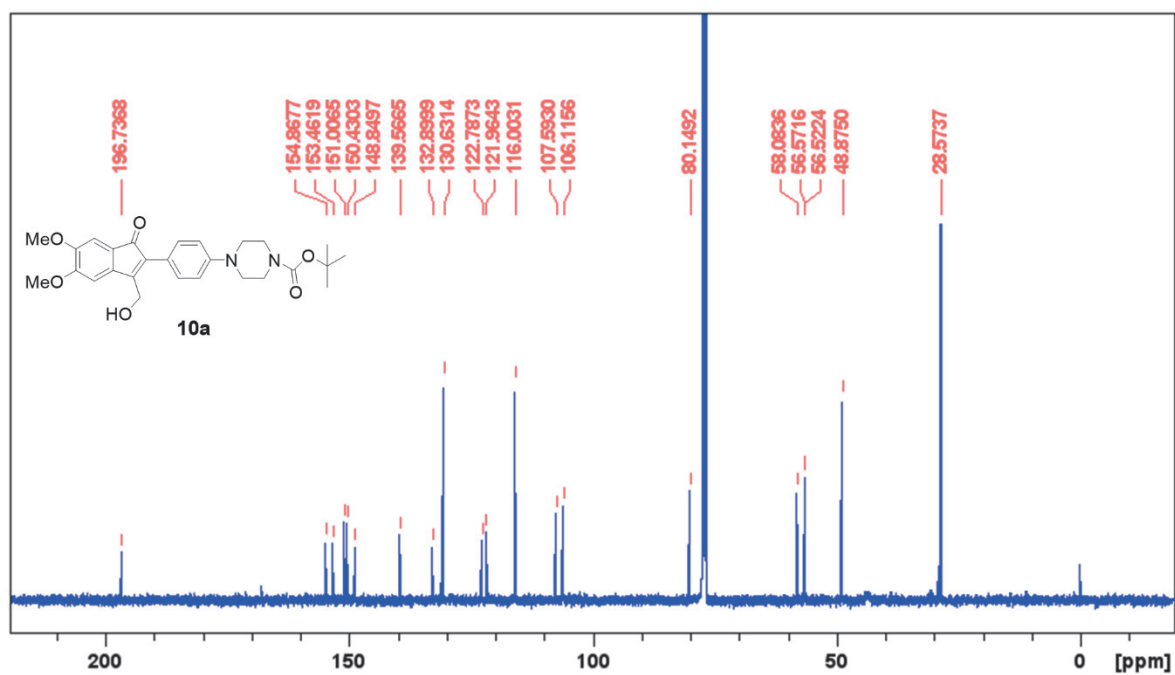


Figure 28. <sup>13</sup>C{<sup>1</sup>H}-NMR spectrum of compound **10a** (CDCl<sub>3</sub>, 100 MHz).

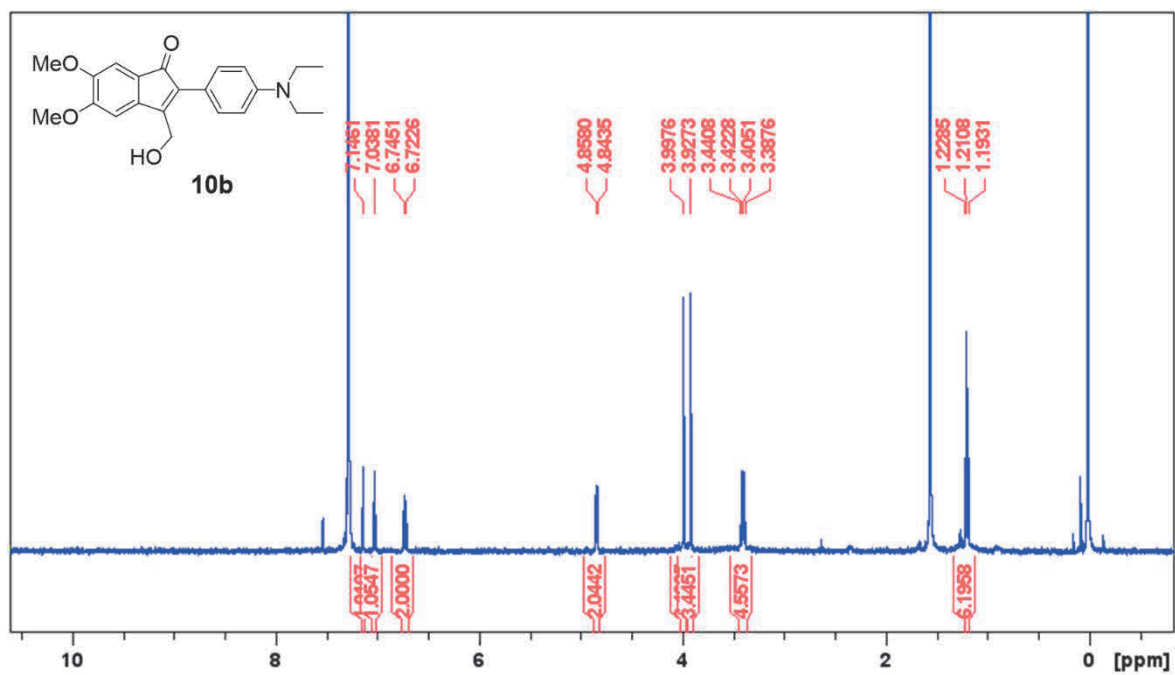


Figure 29.  $^1\text{H}$ -NMR spectrum of compound **10b** ( $\text{CDCl}_3$ , 400 MHz)

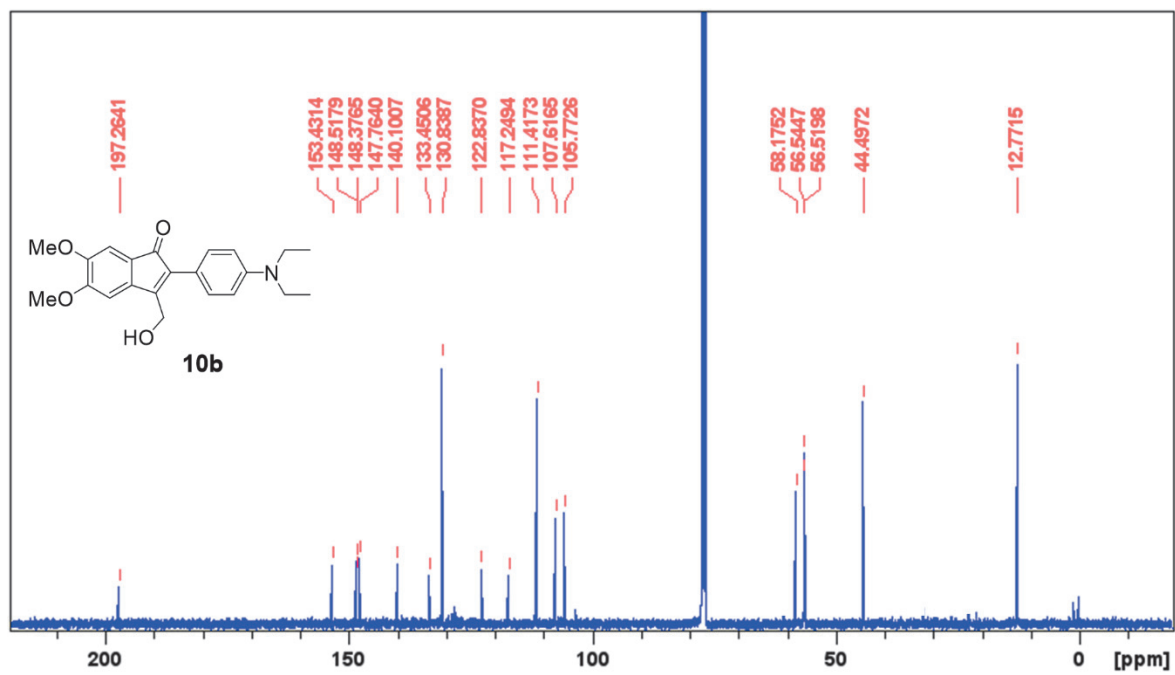


Figure 30.  $^{13}\text{C}\{^1\text{H}\}$ -NMR spectrum of compound **10b** ( $\text{CDCl}_3$ , 100 MHz).



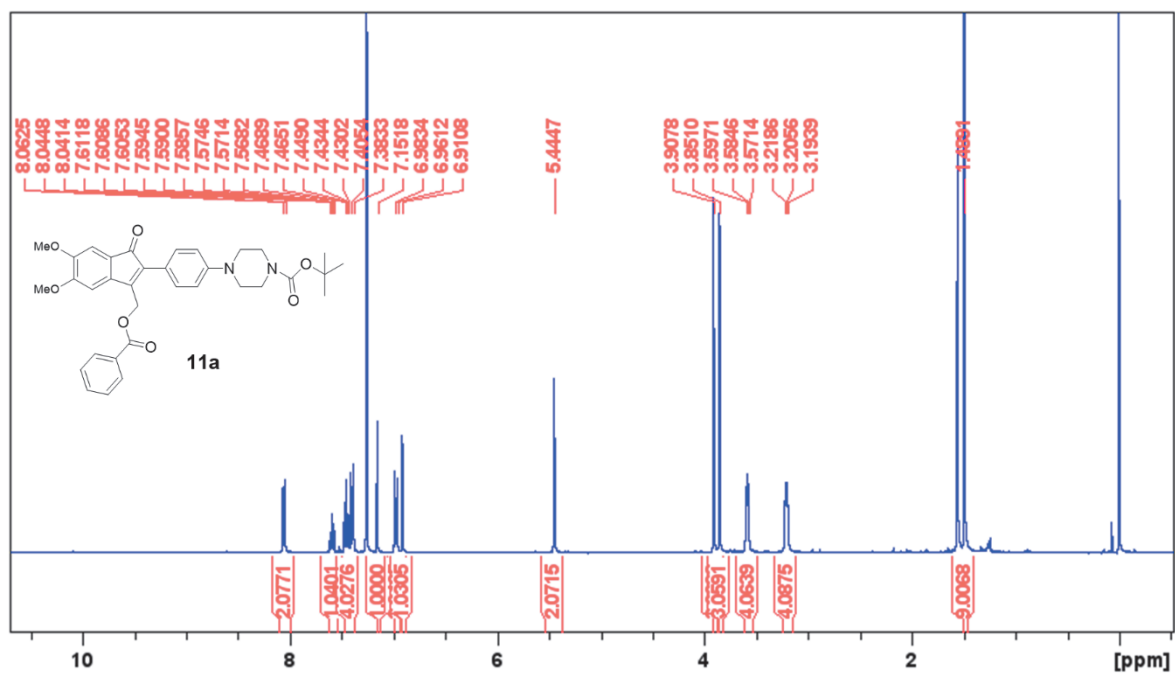


Figure 30.  $^1\text{H}$ -NMR spectrum of compound **11a** ( $\text{CDCl}_3$ , 400 MHz)

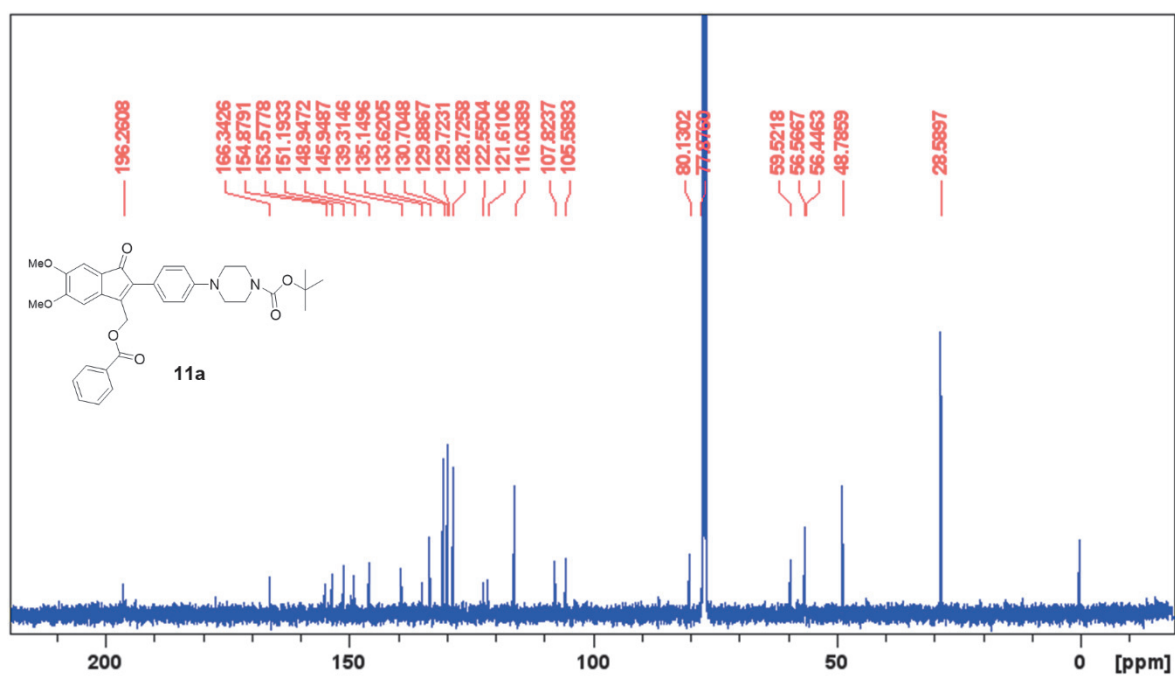


Figure 31.  $^{13}\text{C}\{^1\text{H}\}$ -NMR spectrum of compound **11a** ( $\text{CDCl}_3$ , 100 MHz).

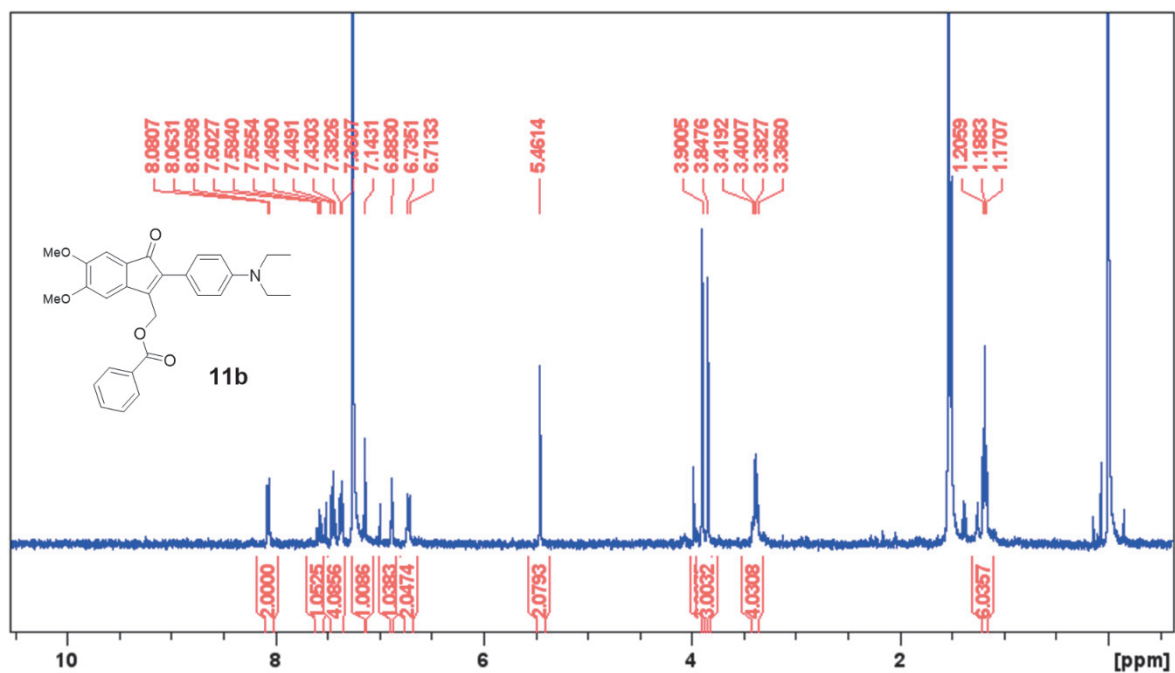


Figure 32.  $^1\text{H}$ -NMR spectrum of compound **11b** ( $\text{CDCl}_3$ , 400 MHz).

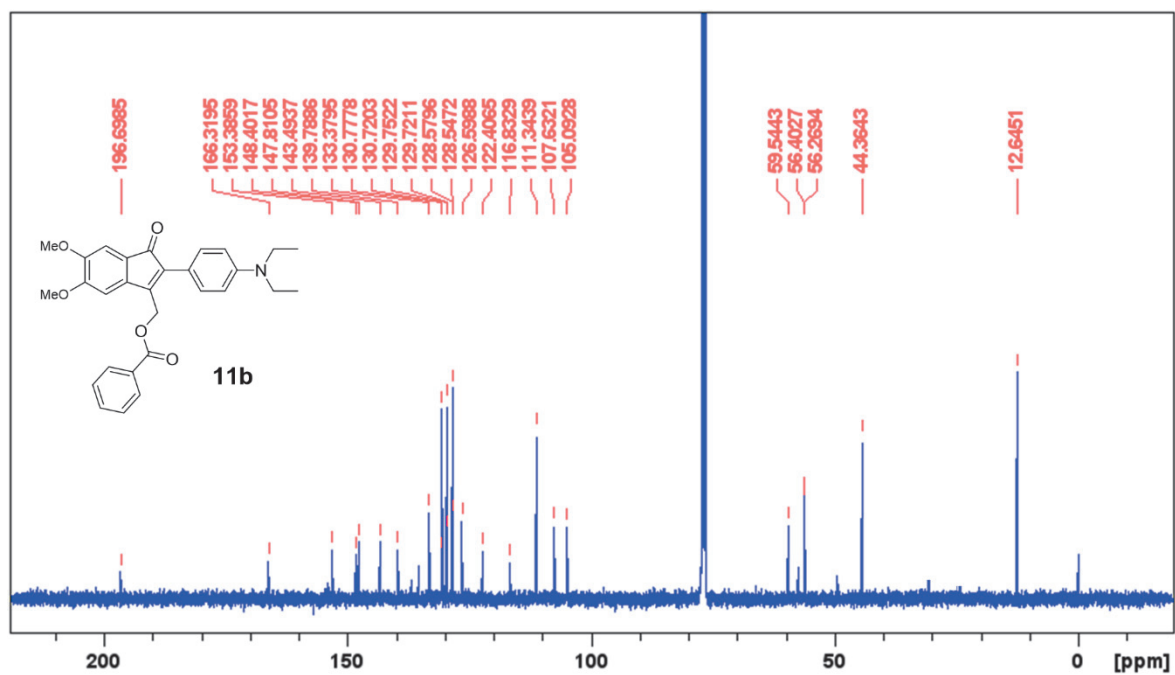


Figure 33.  $^{13}\text{C}\{^1\text{H}\}$ -NMR spectrum of compound **11b** ( $\text{CDCl}_3$ , 400 MHz).

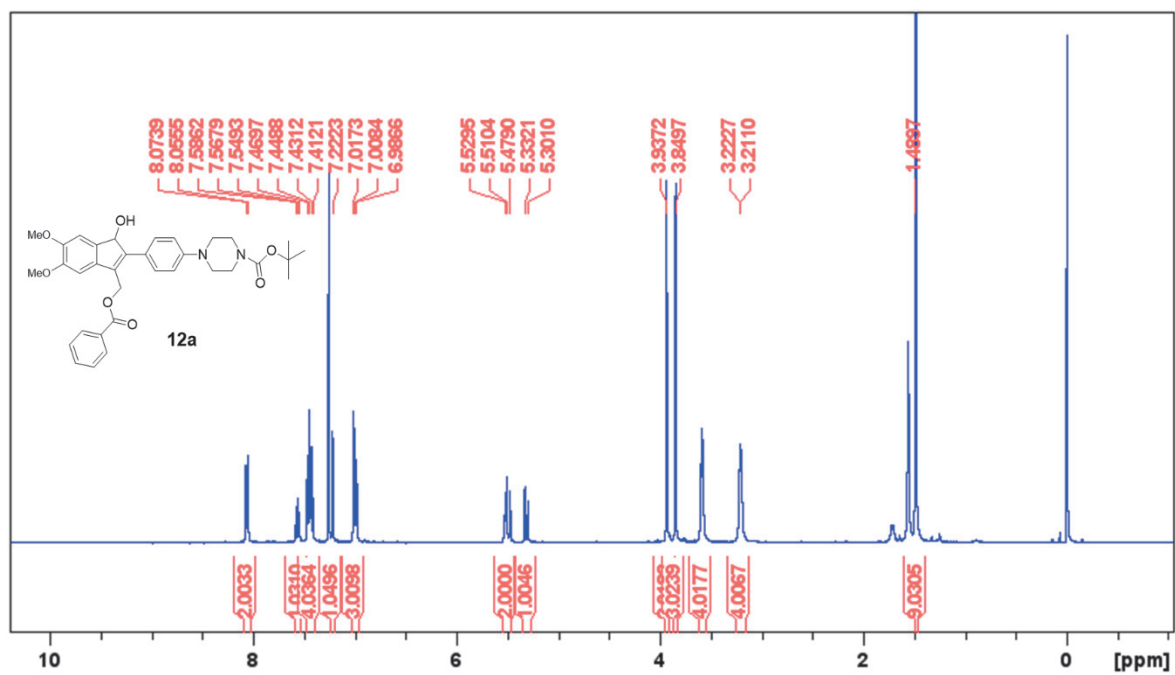


Figure 34.  $^1\text{H}$ -NMR spectrum of compound **12a** ( $\text{CDCl}_3$ , 400 MHz)

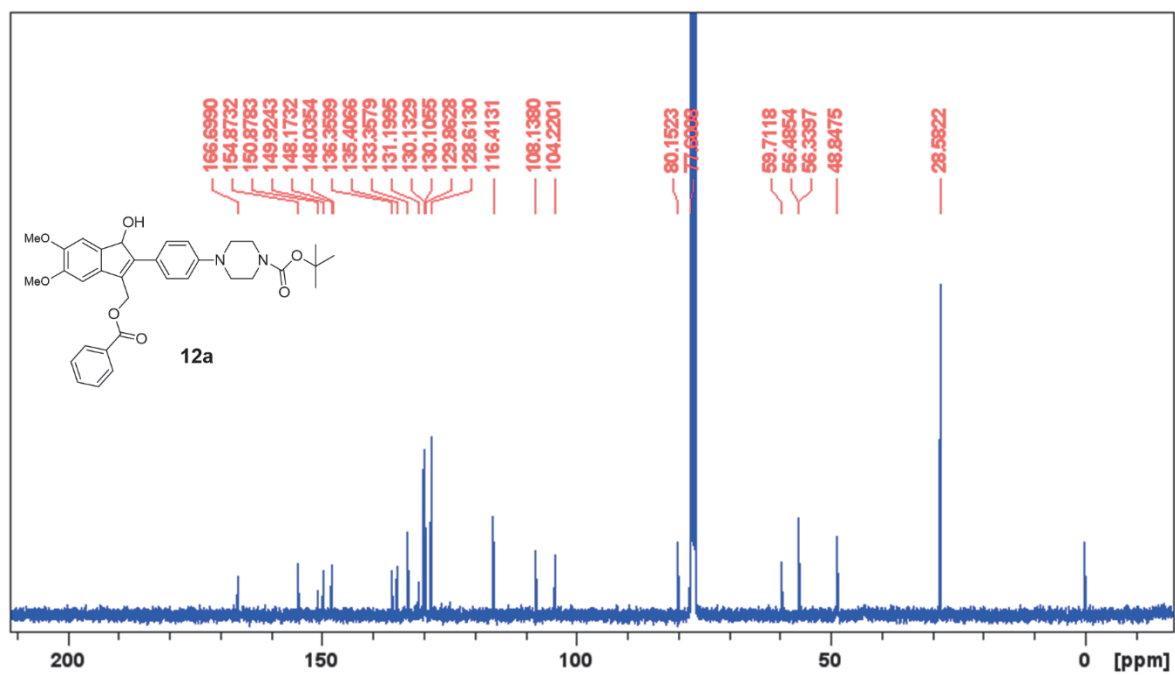


Figure 35.  $^{13}\text{C}\{^1\text{H}\}$ -NMR spectrum of compound **12a** ( $\text{CDCl}_3$ , 100 MHz).

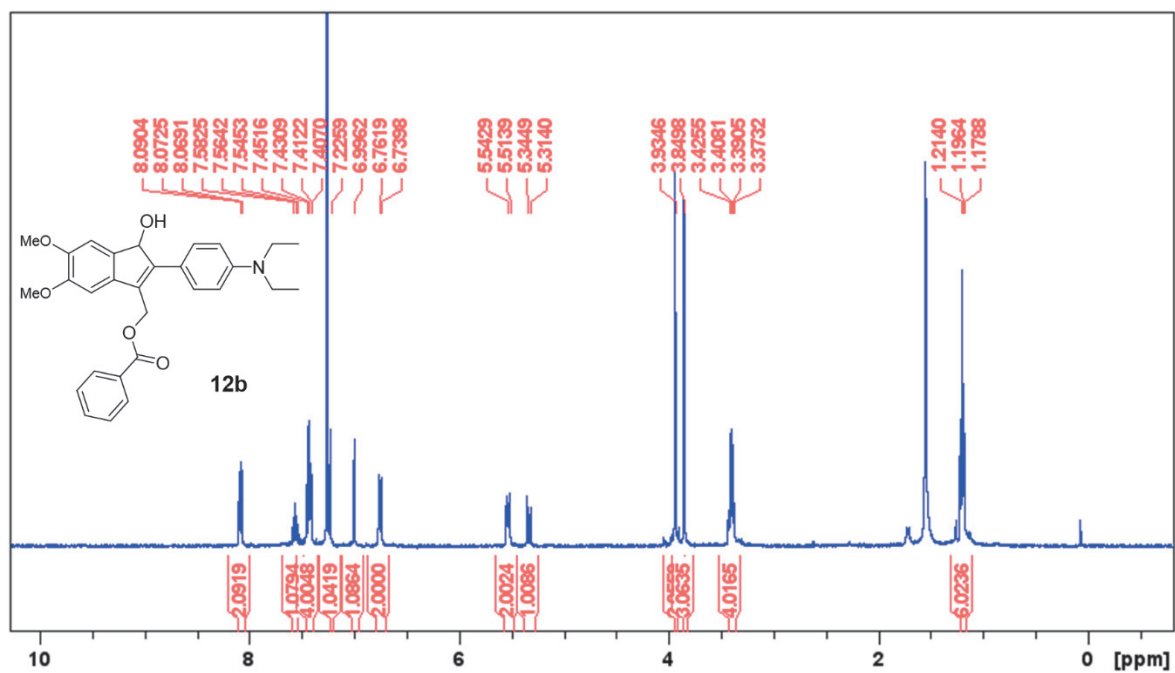


Figure 37.  $^1\text{H}$ -NMR spectrum of compound **12b** ( $\text{CDCl}_3$ , 400 MHz)

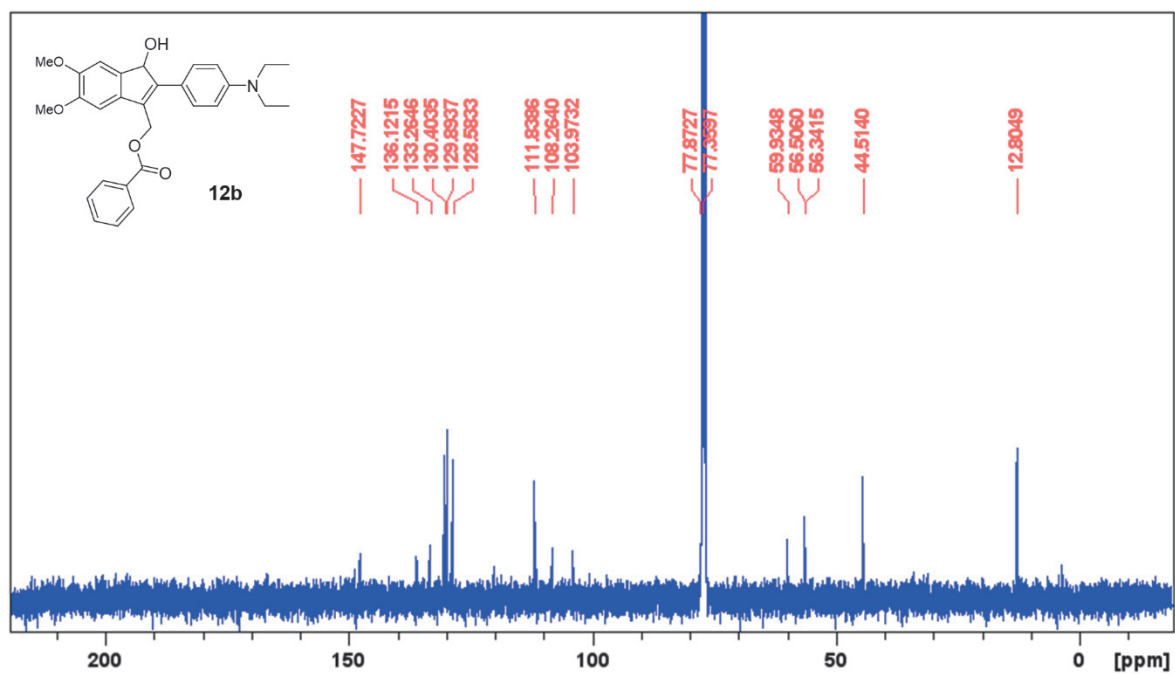


Figure S38.  $^{13}\text{C}\{^1\text{H}\}$ -NMR spectrum of compound **12b** ( $\text{CDCl}_3$ , 100 MHz).

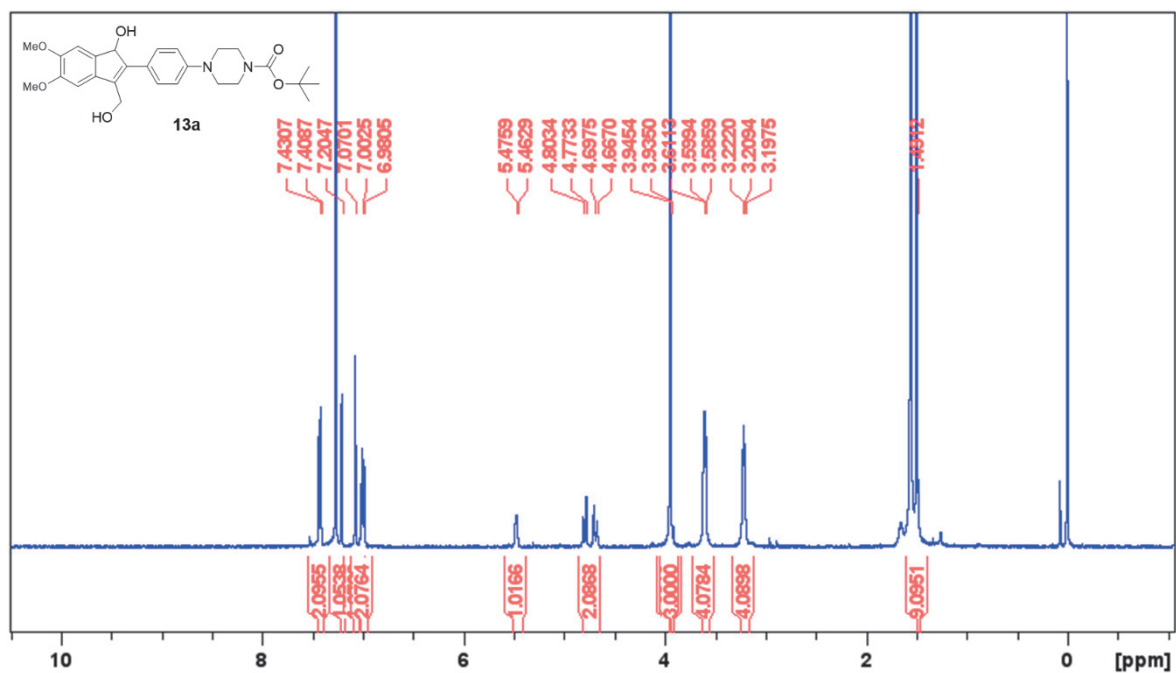


Figure 39.  $^1\text{H}$ -NMR spectrum of compound 13a ( $\text{CDCl}_3$ , 400 MHz)

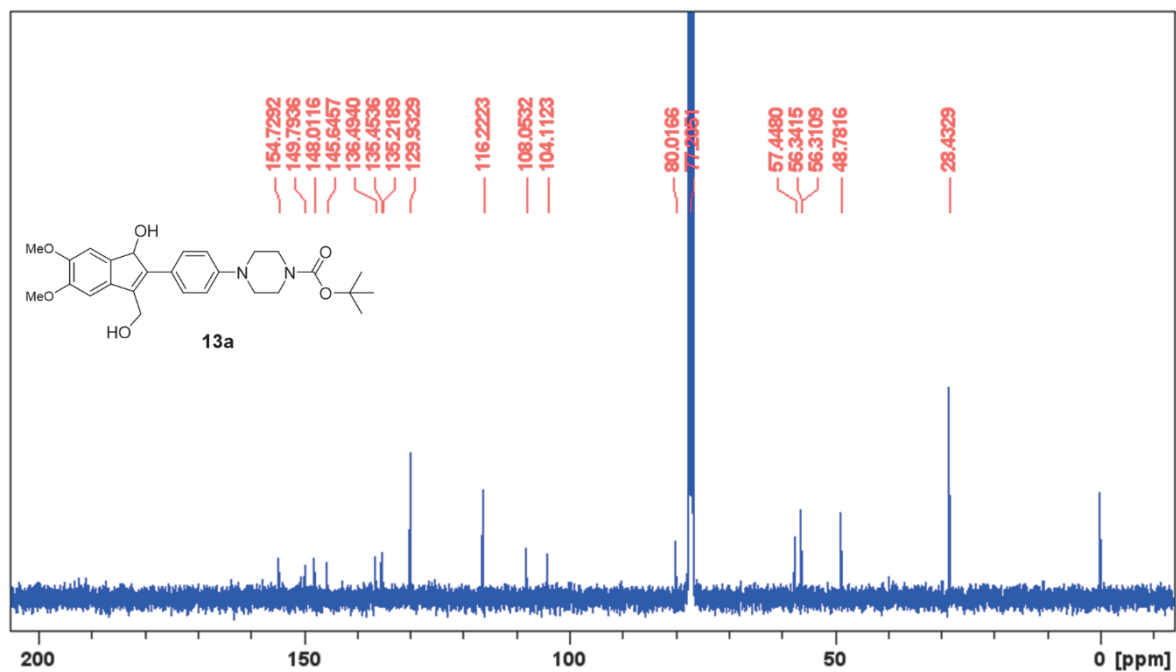


Figure 40.  $^{13}\text{C}\{^1\text{H}\}$ -NMR spectrum of compound 13a ( $\text{CDCl}_3$ , 100 MHz).

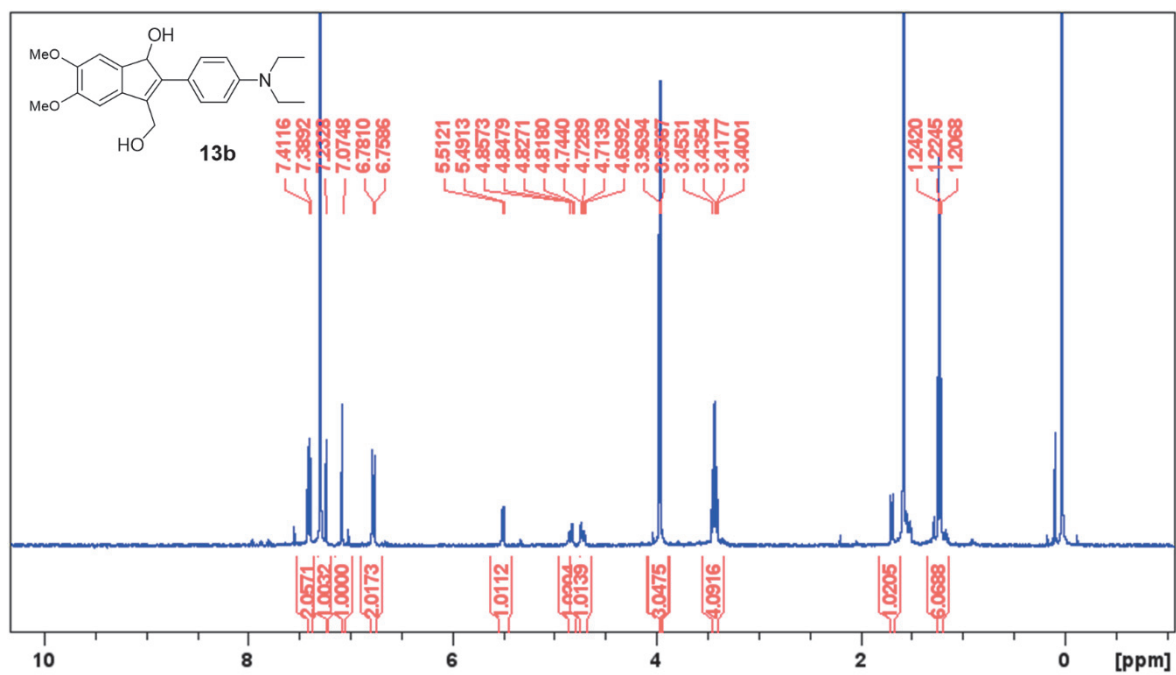


Figure 41.  $^1\text{H}$ -NMR spectrum of compound **13b** ( $\text{CDCl}_3$ , 400 MHz)

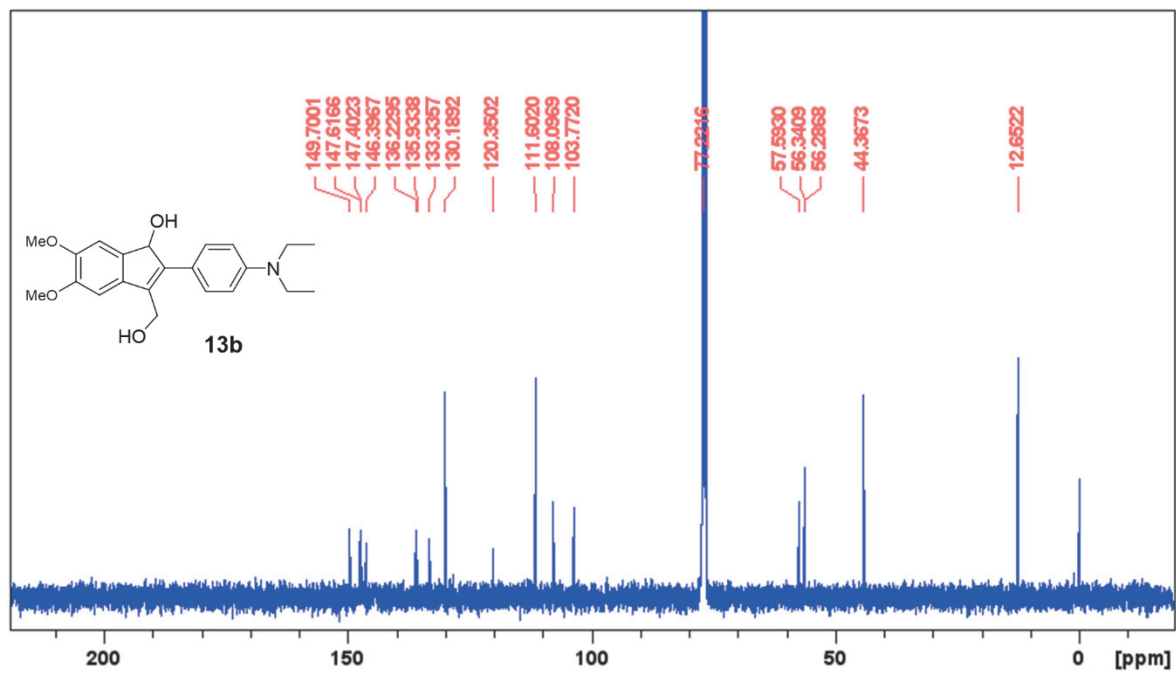


Figure 42.  $^{13}\text{C}\{^1\text{H}\}$ -NMR spectrum of compound **13b** ( $\text{CDCl}_3$ , 100 MHz).

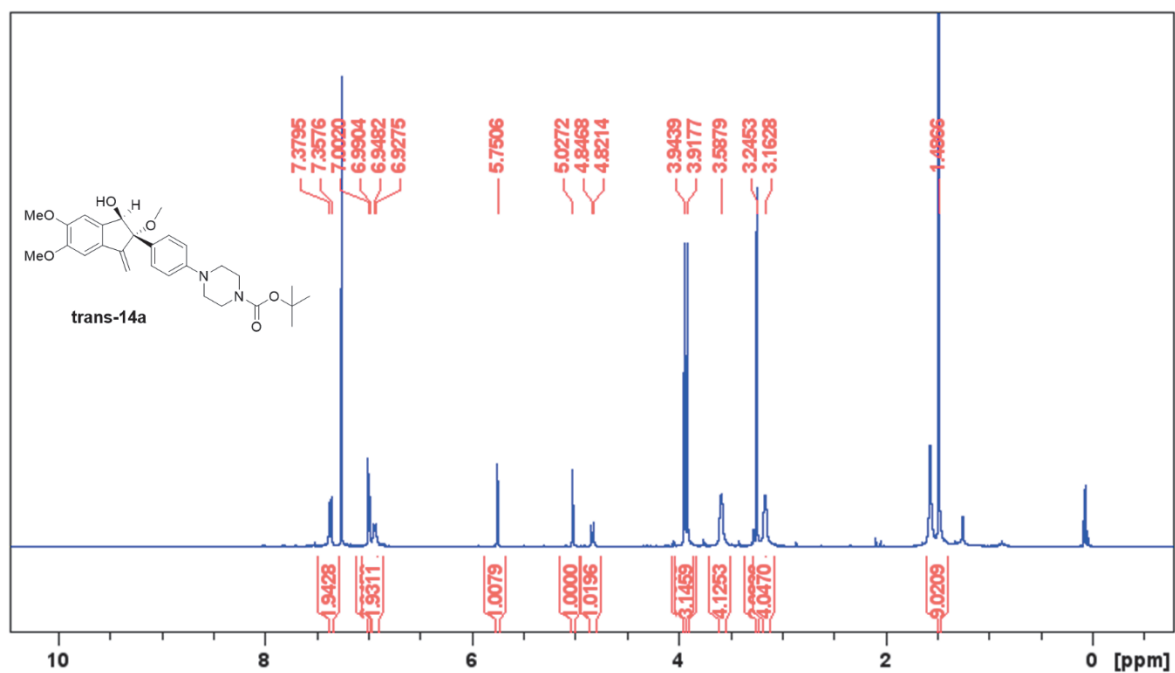


Figure 43. <sup>1</sup>H-NMR spectrum of compound **trans-14a** (CDCl<sub>3</sub>, 400 MHz)

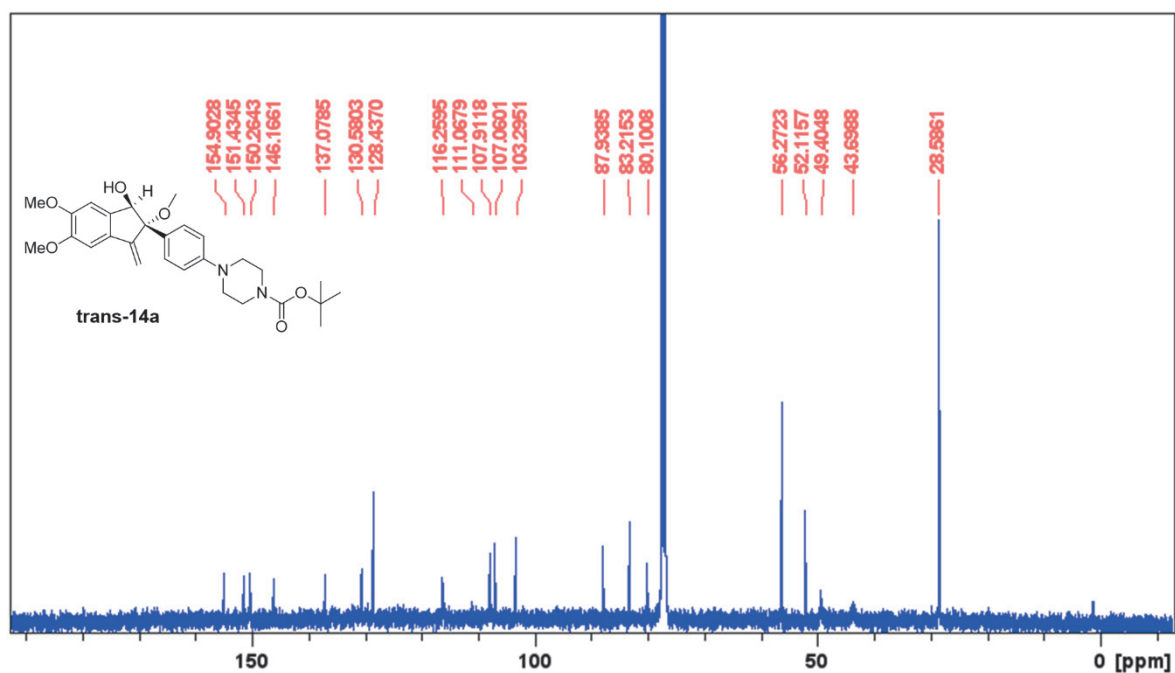


Figure 44. <sup>13</sup>C{<sup>1</sup>H}-NMR spectrum of compound **trans-14a** (CDCl<sub>3</sub>, 100 MHz).

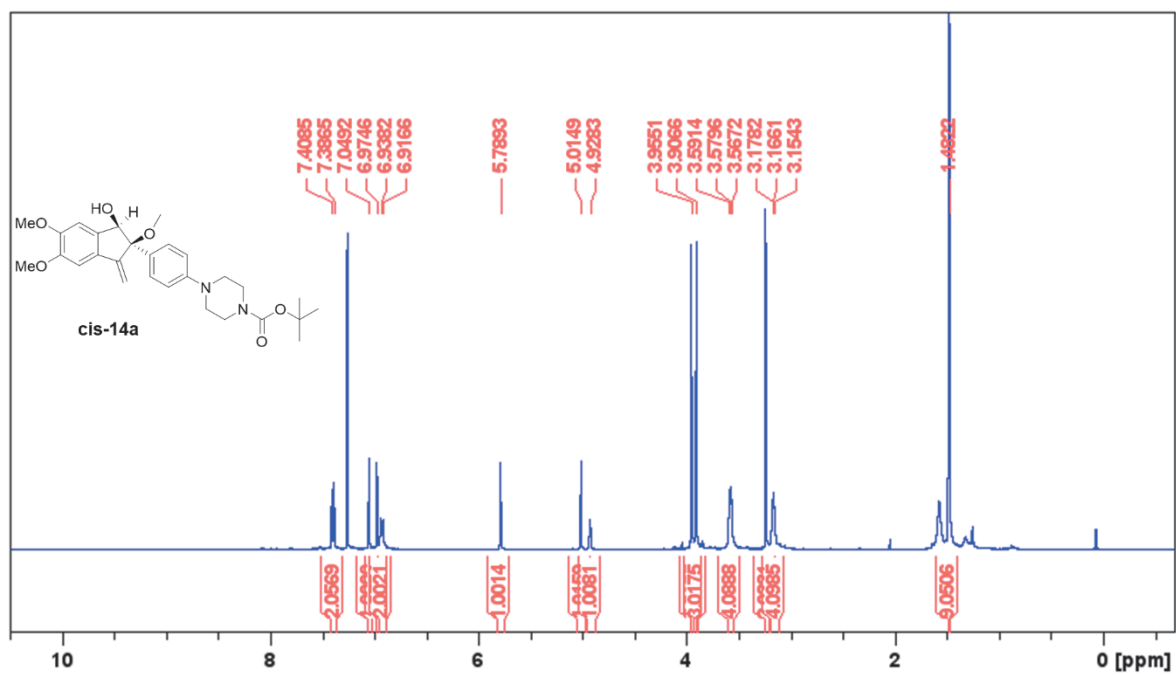


Figure 45.  $^1\text{H-NMR}$  spectrum of compound **cis-14a** ( $\text{CDCl}_3$ , 400 MHz).

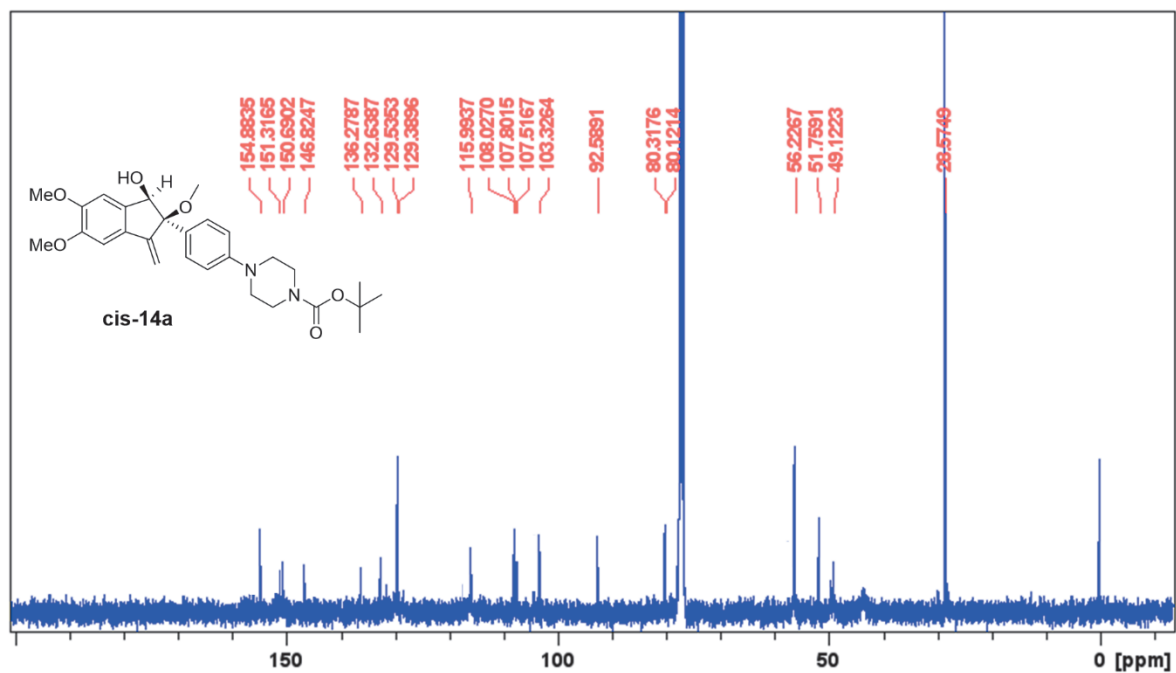


Figure 46.  $^{13}\text{C}\{^1\text{H}\}$ -NMR spectrum of compound **cis-14a** ( $\text{CDCl}_3$ , 400 MHz).



Computational of optimization of compound 12a

# opt freq rb3lyp/6-31g(d)

Symbolic Z-matrix:

Charge = 0 Multiplicity = 1

C	<b>-5.18094</b>	-0.56401	-0.5415
C	-7.43677	0.94806	-0.01279
C	-6.3803	-1.23636	-0.36946
C	-5.10788	0.80193	-0.58783
C	-6.21147	1.60171	-0.28352
C	-7.5273	-0.46716	-0.10196
H	-6.42569	-2.30397	-0.42629
H	-6.1325	2.66809	-0.25524
O	-8.59526	1.70573	0.35349
O	-8.78739	-1.11542	0.08609
C	-8.53722	3.00559	-0.22976
H	-7.65061	3.50622	0.09785
H	-9.39507	3.56728	0.07194
H	-8.52319	2.91756	-1.29485
C	-8.957	-1.46182	1.46455
H	-8.1737	-2.12638	1.76774
H	-9.90204	-1.94367	1.59382
H	-8.9221	-0.57608	2.06211
C	-3.67825	1.20153	-0.99775
C	-3.77031	-1.14987	-0.66918
C	-2.88923	-0.10292	-0.70464
H	-3.63722	1.42332	-2.04511
O	-3.19358	2.33812	-0.28296
H	-3.7436	3.0979	-0.49016
C	-1.50191	-0.18254	-0.48605
C	1.2005	-0.30427	0.08569
C	-0.71237	0.97494	-0.56725
C	-0.90702	-1.41105	-0.16754
C	0.42037	-1.47048	0.11823
C	0.61464	0.91649	-0.28496
H	-1.15611	1.9064	-0.84907
H	-1.50063	-2.3015	-0.14313
H	0.869	-2.40866	0.37201
H	1.2132	1.80289	-0.34093
N	2.50103	-0.35163	0.4158
C	3.32744	0.87512	0.3909

H	2.71033	1.72546	0.59664
H	3.80395	1.01468	-0.558
C	3.15071	-1.61822	0.82515
H	3.07146	-1.77408	1.88227
H	2.68974	-2.43815	0.31683
C	4.3595	0.69197	1.4935
H	3.81184	0.45497	2.38143
H	4.93353	1.58127	1.64774
C	4.61431	-1.49261	0.40996
H	4.61545	-1.2418	-0.62881
H	5.1504	-2.40845	0.56136
N	5.28653	-0.41841	1.17769
C	6.41008	0.0208	0.33402
O	7.07429	-0.90546	-0.53247
O	6.79266	1.22153	0.37652
C	8.41308	-0.45493	-0.7515
C	9.15438	-0.3582	0.59714
H	10.15654	-0.01979	0.43321
H	8.64357	0.33475	1.23182
H	9.17724	-1.32081	1.06397
C	8.37611	0.93332	-1.41112
H	9.37445	1.27595	-1.57805
H	7.85891	0.87273	-2.34584
H	7.86678	1.61771	-0.76476
C	9.15021	-1.44612	-1.67575
H	8.63744	-1.50963	-2.61258
H	10.1512	-1.10375	-1.84016
H	9.1752	-2.41231	-1.21716
C	-3.45978	-2.65912	-0.71525
H	-2.58723	-2.83552	-1.3096
H	-4.29461	-3.16976	-1.14637
O	-3.2314	-3.14833	0.60932
C	-3.10196	-4.57279	0.56469
O	-3.29132	-5.2562	1.60404
C	-2.74025	-5.26803	-0.76035
C	-2.54812	-4.49938	-1.91442
C	-2.60989	-6.66363	-0.81661
C	-2.243	-5.12346	-3.12884
H	-2.63649	-3.43396	-1.868
C	-2.30069	-7.28767	-2.03327
H	-2.7465	-7.25322	0.06697

C	-2.12193	-6.5177	-3.19077
H	-2.10227	-4.53473	-4.01032
H	-2.20156	-8.35324	-2.07895
H	-1.8932	-6.99415	-4.12115

C	0.446	-0.119	1.752
C	0.647	0.548	4.467
C	0.659	-1.128	2.675
C	0.336	1.208	2.177
C	0.433	1.557	3.519
C	0.78	-0.792	4.031
H	0.743	-2.165	2.368
H	0.338	2.603	3.786
O	0.71	0.772	5.819
O	0.97	-1.872	4.86
C	0.566	2.111	6.273
H	1.37	2.748	5.888
H	0.644	2.103	7.364
H	-0.418	2.514	6.013
C	2.019	-1.699	5.809
H	2.818	-1.042	5.446
H	2.461	-2.682	5.997
H	1.615	-1.335	6.758
C	0.094	2.097	0.997
C	0.304	-0.176	0.292
C	0.137	1.094	-0.141
H	-0.877	2.597	1.075
O	1.135	3.052	0.9
H	1.191	3.312	-0.034
C	0.348	-1.46	-0.468
H	0.218	-1.296	-1.543
H	1.313	-1.954	-0.302
O	-0.717	-2.298	-0.002
C	-0.054	1.531	-1.525
C	-0.388	2.437	-4.203
C	-1.186	2.261	-1.893
C	0.911	1.26	-2.498
C	0.741	1.702	-3.817
C	-1.347	2.701	-3.213
H	-1.97	2.478	-1.172
H	1.815	0.711	-2.243
H	1.528	1.478	-4.53
H	-2.259	3.232	-3.474

N	-0.595	2.897	-5.515
C	-0.701	4.365	-5.638
H	-1.389	4.778	-4.892
H	-1.15	4.623	-6.603
C	0.065	2.158	-6.603
H	1.115	2.458	-6.703
H	0.048	1.082	-6.386
C	0.646	5.064	-5.514
H	1.118	4.861	-4.547
H	0.515	6.148	-5.602
H	1.337	4.748	-6.301
C	-0.653	2.341	-7.933
H	-0.538	3.358	-8.318
H	-1.723	2.13	-7.837
H	-0.236	1.659	-8.682
C	-0.752	-3.521	-0.581
O	0.011	-3.925	-1.443
C	-1.868	-4.329	-0.018
C	-3.937	-5.931	0.978
C	-2.124	-5.586	-0.583
C	-2.655	-3.881	1.052
C	-3.686	-4.682	1.547
C	-3.157	-6.383	-0.085
H	-1.52	-5.949	-1.412
H	-2.474	-2.913	1.515
H	-4.293	-4.332	2.379
H	-3.352	-7.357	-0.527
H	-4.74	-6.553	1.366

Computational of optimization of compound 12b

# opt freq rb3lyp/6-31g(d)

Symbolic Z-matrix:

Charge = 0 Multiplicity = 1

C	0.446	-0.119	1.752
C	0.647	0.548	4.467
C	0.659	-1.128	2.675
C	0.336	1.208	2.177
C	0.433	1.557	3.519
C	0.78	-0.792	4.031
H	0.743	-2.165	2.368
H	0.338	2.603	3.786
O	0.71	0.772	5.819
O	0.97	-1.872	4.86
C	0.566	2.111	6.273

H	1.37	2.748	5.888
H	0.644	2.103	7.364
H	-0.418	2.514	6.013
C	2.019	-1.699	5.809
H	2.818	-1.042	5.446
H	2.461	-2.682	5.997
H	1.615	-1.335	6.758
C	0.094	2.097	0.997
C	0.304	-0.176	0.292
C	0.137	1.094	-0.141
H	-0.877	2.597	1.075
O	1.135	3.052	0.9
H	1.191	3.312	-0.034
C	0.348	-1.46	-0.468
H	0.218	-1.296	-1.543
H	1.313	-1.954	-0.302
O	-0.717	-2.298	-0.002
C	-0.054	1.531	-1.525
C	-0.388	2.437	-4.203
C	-1.186	2.261	-1.893
C	0.911	1.26	-2.498
C	0.741	1.702	-3.817
C	-1.347	2.701	-3.213
H	-1.97	2.478	-1.172
H	1.815	0.711	-2.243
H	1.528	1.478	-4.53
H	-2.259	3.232	-3.474
N	-0.595	2.897	-5.515
C	-0.701	4.365	-5.638
H	-1.389	4.778	-4.892
H	-1.15	4.623	-6.603
C	0.065	2.158	-6.603
H	1.115	2.458	-6.703
H	0.048	1.082	-6.386
C	0.646	5.064	-5.514
H	1.118	4.861	-4.547
H	0.515	6.148	-5.602
H	1.337	4.748	-6.301
C	-0.653	2.341	-7.933
H	-0.538	3.358	-8.318
H	-1.723	2.13	-7.837

H	-0.236	1.659	-8.682
C	-0.752	-3.521	-0.581
O	0.011	-3.925	-1.443
C	-1.868	-4.329	-0.018
C	-3.937	-5.931	0.978
C	-2.124	-5.586	-0.583
C	-2.655	-3.881	1.052
C	-3.686	-4.682	1.547
C	-3.157	-6.383	-0.085
H	-1.52	-5.949	-1.412
H	-2.474	-2.913	1.515
H	-4.293	-4.332	2.379
H	-3.352	-7.357	-0.527
H	-4.74	-6.553	1.366

Computational of optimization of cation form from compound **12a**

# opt freq rb3lyp/6-31g(d)

Symbolic Z-matrix:

Charge = 0 Multiplicity = 1

C	-2.57148	-0.85403	-0.20006
C	-4.95334	0.47652	0.30133
C	-3.69384	-1.61934	0.09747
C	-2.63873	0.5238	-0.3462
C	-3.80531	1.22173	-0.04256
C	-4.90564	-0.94195	0.34218
H	-3.63783	-2.68717	0.1454
H	-3.83319	2.29103	-0.07773
O	-6.17549	1.15436	0.60491
O	-6.09283	-1.68628	0.6354
C	-6.24748	2.36731	-0.14937
H	-5.41463	2.99158	0.0986
H	-7.15843	2.87857	0.08311
H	-6.22321	2.13918	-1.19463
C	-6.20568	-1.88422	2.04708
H	-5.35547	-2.42879	2.40065
H	-7.09666	-2.43771	2.25843
H	-6.25029	-0.93451	2.53842

C	-1.29878	1.1058	-0.86873
C	-1.12415	-1.3175	-0.38568
C	-0.30451	-0.04731	-0.6226
H	-1.37501	1.29313	-1.91938
O	-0.92331	2.32144	-0.21594
H	-1.58968	2.99161	-0.3821
C	-0.66152	-2.58933	-0.32661
H	0.38061	-2.78638	-0.46206
H	-1.34027	-3.39673	-0.14383
C	1.09298	0.05341	-0.61422
C	3.84237	0.25776	-0.64478
C	1.70042	1.28878	-0.86481
C	1.88232	-1.07814	-0.36151
C	3.23608	-0.97827	-0.37525
C	3.05042	1.38981	-0.88095
H	1.09691	2.153	-1.04563
H	1.41705	-2.01879	-0.15972
H	3.83834	-1.84163	-0.18283
H	3.51303	2.33466	-1.07574
N	5.17517	0.371	-0.68184
C	5.85768	1.58649	-0.94788
H	5.26667	2.31461	-1.4641
H	6.71747	1.36139	-1.54215
C	6.13252	-0.71514	-0.4282
H	5.71299	-1.41145	0.26781
H	6.35619	-1.22131	-1.34449
C	6.30011	2.0513	0.4106
H	5.50335	2.4836	0.97836
H	7.07468	2.77982	0.28947
C	7.46965	-0.08977	0.17407
H	7.72236	0.30973	-0.78547
H	7.70991	-1.08471	0.48485
N	6.7603	0.82507	1.10781
C	7.62454	1.24542	2.22081
O	9.02277	1.43963	1.99507
O	7.13507	1.43607	3.36519
C	9.2116	1.91094	0.65564
C	10.71098	2.14446	0.39628
H	10.84929	2.49705	-0.605
H	11.08256	2.87412	1.08539
H	11.24243	1.22652	0.52792

C	8.44848	3.23445	0.46632
H	8.58571	3.5858	-0.53547
H	7.40655	3.07431	0.64821
H	8.82296	3.96306	1.15411
C	8.67544	0.86349	-0.33774
H	7.63359	0.70013	-0.15697
H	8.8125	1.21875	-1.33812
H	9.20772	-0.05528	-0.20906

Computational of optimization of cation form from compound **12b**

# opt freq rb3lyp/6-31g(d)

Symbolic Z-matrix:

Charge = 0 Multiplicity = 1

C	-1.59658	-1.16929	-0.25936
C	-3.46842	-3.22189	0.10413
C	-2.93122	-0.95067	-0.61218
C	-1.21731	-2.4051	0.28153
C	-2.13007	-3.43359	0.46698
C	-3.86207	-1.97401	-0.4359
H	-3.27857	-0.00436	-1.01203
H	-1.80365	-4.38209	0.87796
O	-4.46266	-4.15074	0.24366
O	-5.18118	-1.72107	-0.736
C	-4.12715	-5.40644	0.81084
H	-3.38897	-5.9434	0.20034
H	-5.05653	-5.97844	0.84048
H	-3.73677	-5.29594	1.83116
C	-5.69413	-2.40318	-1.88124
H	-5.1177	-2.14645	-2.78053
H	-6.72376	-2.05784	-2.00292



H	-5.68669	-3.48857	-1.73939
C	0.25352	-2.36714	0.61212
C	-0.39975	-0.3141	-0.36674
C	0.68947	-0.99604	0.08343
H	0.37886	-2.37895	1.71162
O	0.9399	-3.47543	0.03867
H	1.89024	-3.29283	0.13041
C	-0.42806	1.08016	-0.90675
H	0.51737	1.60153	-0.74381
H	-0.63978	1.10357	-1.98315
C	2.10266	-0.61212	0.09877
C	4.89791	0.0946	0.15174
C	2.95429	-1.00566	1.15205
C	2.70881	0.10876	-0.94628
C	4.05524	0.45209	-0.92778
C	4.30106	-0.67113	1.18233
H	2.54621	-1.562	1.99268
H	2.12412	0.36939	-1.82361
H	4.45217	0.97939	-1.78558
H	4.8844	-0.99619	2.03517
N	6.23672	0.48845	0.20819
C	7.17557	-0.29355	1.01569
H	6.75827	-0.42071	2.01834
H	8.0766	0.30581	1.15734
C	6.77296	1.25769	-0.92039
H	6.83245	0.64159	-1.8348
H	6.05721	2.05831	-1.13201
C	7.5454	-1.65886	0.41918
H	6.65673	-2.28475	0.28774
H	8.24306	-2.18904	1.07817
H	8.02617	-1.54589	-0.55932
C	8.13105	1.91304	-0.66676
H	8.95045	1.19033	-0.60069
H	8.11906	2.51261	0.24986
H	8.35651	2.5823	-1.50394

## 2.5. References

- (1) J. H. Kaplan; A. P. Somlyo. Flash Photolysis of Caged Compounds: New Tools for Cellular Physiology. *TECHNIQUES* **1989**, *12* (2), 54–59.
- (2) Bochet, C. G. Photolabile Protecting Groups and Linkers. *Journal of the Chemical Society. Perkin Transactions 1*. 2002, pp 125–142.
- (3) Jakkampudi, S.; Abe, M. Caged Compounds for Two-Photon Uncaging. In *Reference Module in Chemistry, Molecular Sciences and Chemical Engineering*; Elsevier, 2018.
- (4) Sasaki, M.; Tran Bao Nguyen, L.; Yabumoto, S.; Nakagawa, T.; Abe, M. Structural Transformation of the 2-(p-Aminophenyl)-1-Hydroxyinden-3-Ylmethyl Chromophore as a Photoremovable Protecting Group. *ChemPhotoChem* **2020**, *4* (12), 5392–5398.
- (5) Abe, M.; Chitose, Y.; Jakkampudi, S.; Thuy, P. T. T.; Lin, Q.; Van, B. T.; Yamada, A.; Oyama, R.; Sasaki, M.; Katan, C. Design and Synthesis of Two-Photon Responsive Chromophores for Near-Infrared Light-Induced Uncaging Reactions. *Synthesis (Germany)*. Georg Thieme Verlag August 1, 2017, pp 3337–3346
- (6) Nguyen, L. T. B.; Abe, M. Development of Photoremovable Protecting Groups Responsive to Near-Infrared Two-Photon Excitation and Their Application to Drug Delivery Research. *Bulletin of the Chemical Society of Japan*. Chemical Society of Japan September 1, 2023, pp 899–906
- (7) Ge, Z.; Ji, Q.; Chen, C.; Liao, Q.; Wu, H.; Liu, X.; Huang, Y.; Yuan, L.; Liao, F. Synthesis and Biological Evaluation of Novel 3-Substituted Amino-4-Hydroxycoumarin Derivatives as Chitin Synthase Inhibitors and Antifungal Agents. *J Enzyme Inhib Med Chem* **2016**, *31* (2), 219–228.
- (8) Andersen, V. L.; Herth, M. M.; Lehel, S.; Knudsen, G. M.; Kristensen, J. L. Palladium-Mediated Conversion of Para-Aminoarylboronic Esters into Para-Aminoaryl-11C-Methanes. *Tetrahedron Lett* **2013**, *54* (3), 213–216.
- (9) Uetake, Y.; Niwa, T.; Hosoya, T. Rhodium-Catalyzed Ipso-Borylation of Alkylthioarenes via C-S Bond Cleavage. *Org Lett* **2016**, *18* (11), 2758–2761.
- (10) Xiong Cai; Haixiao Zhai; Changgeng Qian. Phosphoinositide 3-Kinase Inhibitors With A Zinc Binding Moiety. **2012**, 1–226.
- (11) Kraft, P.; Eichenberger, W. Conception, Characterization and Correlation of New Marine Odorants. *European J Org Chem* **2003**, No. 19, 3735–3743.

# **Chapter 3**

## **Summary**

## Summary

In this study, we aimed to develop a novel two-photon (2P) responsive photoremovable protecting group (PPG) for efficient release of functional groups using visible to near-infrared (NIR) light in the biological window. The newly designed PPG, 2-(p-aminophenyl)-5,6-dimethoxy-1-hydroxyinden-3-ylmethyl, demonstrated a two-photon cross-section of approximately 40–50 GM at approximately 700 nm, with an uncaging efficiency of approximately 30 GM at approximately 700 nm and a quantum yield exceeding 0.7. Visible to NIR-2P responsive caged-compounds **12a** and **12b** were synthesized, showing high chemical yields (92% and 94%) and quantum yields (0.73 and 0.74) for benzoic acid release, respectively. Proposed photoreaction mechanisms were elucidated, emphasizing a carbocation B2 as a key intermediate. The calculated 2P uncaging efficiencies of 36 and 30 GM for compounds **12a** and **12b** suggest their promise for future biological experiments. This study contributes a new 2P responsive chromophore, improving understanding of photo uncaging mechanisms and advancing the development of tools for biological research, with potential implications for therapeutic and diagnostic applications.

# **Acknowledgements**

## Acknowledgements

First words, the author would like to express sincere thanks to Professor Dr. Manabu Abe for the continuous support of the author's PhD to study and research, with his devotion, enthusiasm, and knowledge. His supervision helped the author in research, writing publication and this thesis, also guide the life of author in Japan.

The author would like to thank the INOAC group and the Next-Generation Fellowship in Hiroshima University for providing the author's PhD scholarship.

The next, the author is also grateful to Dr. Ryukichi Takagi and Dr. Sayaka Hatano for their time, suggestion, and encouragement during the research study. In particular, the author would like to thank all the Reaction Organic Chemistry lab members.

The author also thanks Ms. Tomoko Amimoto from N-BARD, Hiroshima University for helping the author with HRMS measurement.

Last but not least, the author would like to thank family: the author's parents Ms. Nguyen Dang Lan and Mrs. Dang Thi Tuyet Lan and all family members for their unconditional love, caring sacrifices. Also, to my friends thanks for their support of the author's life.



# Publications



## List of publications

1. Development of a Two-Photon-Responsive Chromophore, 2-(*p*-Aminophenyl)-5,6-dimethoxy-1-(hydroxyinden-3-yl)methyl Derivative, as a Photoremovable Protecting Group

Tuan Phong Nguyen, Hai Dang Nguyen, and Manabu Abe

The Journal of Organic Chemistry, American Chemical Society, 2024.

<https://doi.org/10.1021/acs.joc.3c02943>